

Aus dem Institut für Immunologie  
im Biomedizinischen Zentrum München  
der Ludwig-Maximilians-Universität München  
Direktor: Prof. Dr. Thomas Brocker

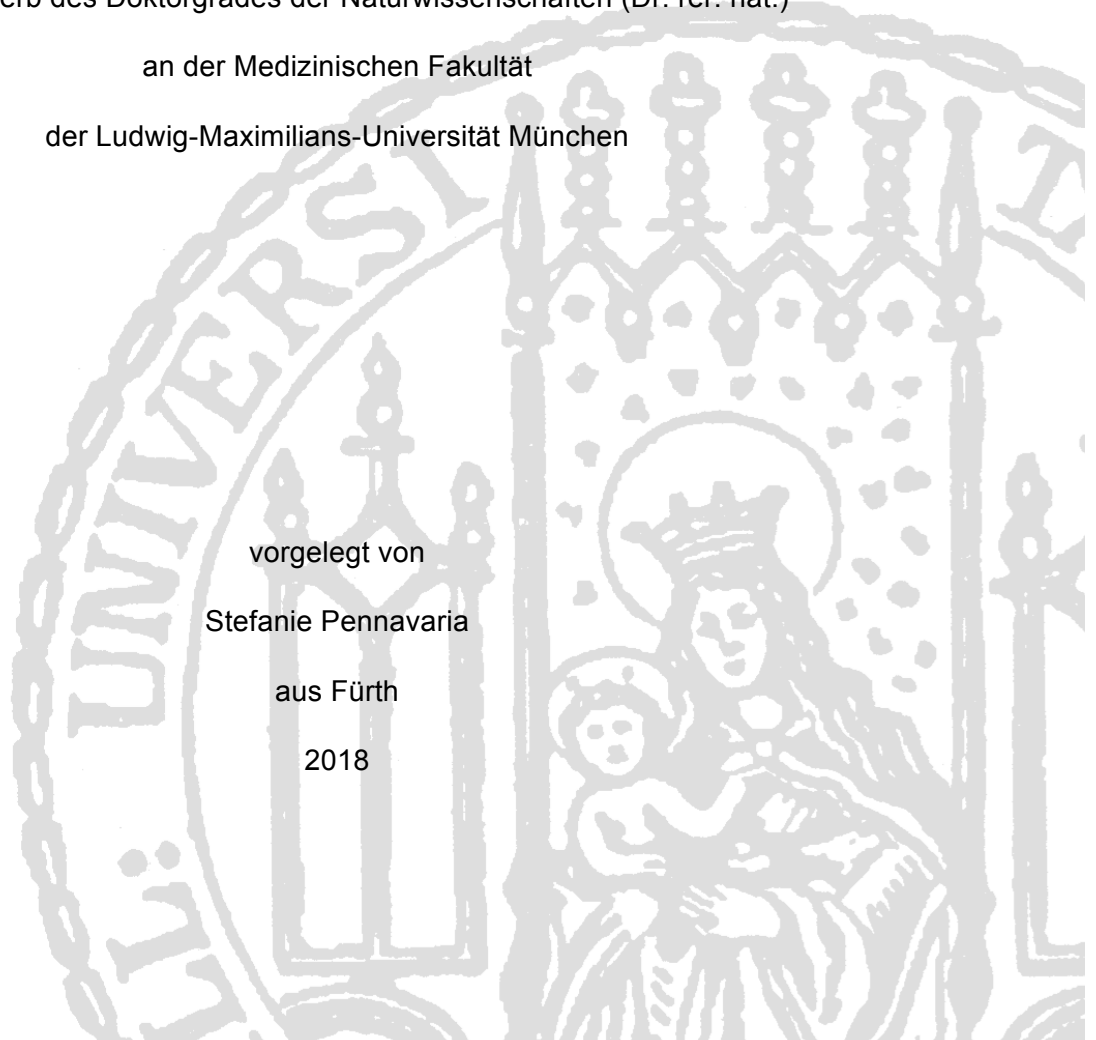
# **mTORC1-dependent RNA synthesis in proliferating T cells**

Dissertation

zum Erwerb des Doktorgrades der Naturwissenschaften (Dr. rer. nat.)

an der Medizinischen Fakultät  
der Ludwig-Maximilians-Universität München

vorgelegt von  
Stefanie Pennavaria  
aus Fürth  
2018



**Gedruckt mit Genehmigung der Medizinischen Fakultät der Ludwig-Maximilians-Universität München**

Betreuer: PD Dr. Reinhard Obst

Zweitgutachter: PD Dr. Klaus Dornmair

Dekan: Prof. Dr. med. dent. Reinhard Hickel

Tag der mündlichen Prüfung: 11.07.2019

## **Eidesstattliche Versicherung**

Name, Vorname: Stefanie Pennavaria

Ich erkläre hiermit an Eides statt, dass ich die vorliegende Dissertation mit dem Titel „mTORC1-dependent RNA synthesis in proliferating T cells“ selbständig verfasst, mich außer der angegebenen keiner weiteren Hilfsmittel bedient und alle Erkenntnisse, die aus dem Schrifttum ganz oder annähernd übernommen sind, als solche kenntlich gemacht und nach ihrer Herkunft unter Bezeichnung der Fundstelle einzeln nachgewiesen habe.

Ich erkläre des Weiteren, dass die hier vorgelegte Dissertation nicht in gleicher oder in ähnlicher Form bei einer anderen Stelle zur Erlangung eines akademischen Grades eingereicht wurde.

Ort, Datum: Stein, den 01.08.2019

Unterschrift Doktorandin: Stefanie Pennavaria

# Table of Content

<b>Table of Content</b>	<b>i</b>
<b>A Abstract</b>	<b>1</b>
<b>1 Abstract</b>	<b>1</b>
<b>2 Zusammenfassung</b>	<b>3</b>
<b>B Introduction</b>	<b>5</b>
<b>1 T cells in the context of immune response</b>	<b>5</b>
1.1 T cell development	5
1.2 Antigen recognition by the T cell receptor	6
1.3 T cell receptor signaling	7
1.4 T cell effector function	8
1.5 T cell memory formation and causes of exhaustion	9
<b>2 Metabolic demands of T cells</b>	<b>10</b>
<b>3 The mechanistic target of rapamycin, mTOR</b>	<b>11</b>
3.1 The composition of mTORC1 and mTORC2	12
3.2 Downstream targets of mTORC1	12
3.3 Upstream activators of mTORC1	14
3.4 mTORC1 in T cells	15
<b>4 Cell cycle in T cells</b>	<b>18</b>
<b>5 RNA expression in T cells</b>	<b>19</b>
<b>6 The nucleolus</b>	<b>20</b>
<b>7 Aims of this thesis</b>	<b>20</b>
<b>C Material and Methods</b>	<b>22</b>
<b>1 Material</b>	<b>22</b>
1.1 Chemicals and Solutions	22
1.2 Buffers and Media	23
1.3 Oligonucleotides	26
1.4 Antibodies	27
1.5 Cytokines	28
1.6 Enzymes	29

1.7 Consumables	29
1.8 Kits	30
1.9 Laboratory Equipment	30
1.10 Software	31
<b>2 Methods</b>	<b>32</b>
2.1. Mice	32
2.1.1 Wildtype mice	33
2.1.2 Congenic marker	33
2.1.3 TCR transgenic mice	33
2.1.4 TCR signaling reporter mice	34
2.1.5 T cell specific mTORC1/2- deficient mice	34
2.1.6 Bm1 and Bm12 mice	34
2.1.7 RAG-deficient mice	35
2.1.8 Double-transgenic mice	35
2.1.9 R26-rtTA-M2 mice	36
2.2 Mice Typing	37
2.2.1 Tissue digestion	37
2.2.2 Polymerase Chain Reaction	37
2.2.3 Gel electrophoresis	37
2.3 Cell extraction from mouse organs	38
2.4 Intra peritoneal injection of anti-CD40	38
2.5 CFSE/CTV labeling of naïve T cells	38
2.6 Adoptive T cell transfer	38
2.7 Doxycycline treatment	39
2.8 Immunization	39
2.8.1 Immunization with MVA-Ova	39
2.8.2 Immunization with MHV-68_OVA	39
2.9 Magnetic purification of CD4 <sup>+</sup> and CD8 <sup>+</sup> T cells	39
2.10 Stimulation with anti-CD3 and anti-CD28	40
2.11 Stimulation with PMA and ionomycin	40
2.12 Inhibitor treatment	41
2.13 Cell preparation for flow cytometry	41

2.13.1 Antibody staining	41
2.13.2 Fixation with 4% PFA	42
2.13.3 Permeabilization with Perm III Buffer	42
2.13.4 Intracellular antibody staining for phospho-proteins	42
2.13.5 RNA and DNA staining with Pyronin Y and DAPI	42
2.13.6 Intracellular cytokine staining	43
2.13.7 Visualization of translational activity	43
2.14 RNase digestion of fixed and permeabilized cells.	45
2.15 Total RNA Sequencing	45
2.15.1 Cell sorting	45
2.15.2 Trizol treatment	45
2.15.3 RNA Preparation	45
2.15.4 cDNA synthesis	45
2.15.5 Pool generation and size fractionation	47
2.15.6 Description of the cDNA	47
2.15.7 Illumina sequencing	47
2.15.8 RNA sequencing analysis	47
2.16 <i>In vivo</i> killing assay	48
2.17 Statistic analysis	48
<b>D Results</b>	<b>49</b>
<b>I mTORC1-dependent RNA synthesis in proliferating T cells</b>	<b>49</b>
<b>1 mTORC1-dependent physiological changes upon TCR stimulation</b>	<b>49</b>
1.1 The phosphorylation of S6 in stimulated T cells is mTORC1-dependent	49
1.2 T cell blast formation is delayed in mTORC1-deficient T cells	50
<b>2 Clonal expansion and survival of T-Rptor<sup>-/-</sup> cells <i>in vivo</i></b>	<b>52</b>
2.1 Impaired GvH response of T-Rptor <sup>-/-</sup>	53
2.2 T-Rptor <sup>-/-</sup> cells proliferate slower and accumulate less in response to antigen	54
2.3 T-Rptor <sup>-/-</sup> OT-I T cells expand less in response to transient TCR stimulation	56

2.4 T-Rptor <sup>-/-</sup> cells expand and persist less in response to an infection with MVA-OVA	57
2.5 Lymphopenic-driven expansion is diminished in T-Rptor <sup>-/-</sup> cells	58
<b>3 rRNA expression limits T cell proliferation</b>	<b>59</b>
3.1 The expression of RNA Polymerase I subunits is mTORC1-dependent	59
3.2 TCR induced expression of total and ribosomal RNA is mTORC1 dependent -quantity versus specificity	60
3.3 Visualization of RNA synthesis by flow cytometry	62
3.4 RNA expression in T cells correlates with cell cycle entry – kinetics	64
3.5 RNA expression in activated T-WT versus T-Rptor <sup>-/-</sup> and T-Rictor <sup>-/-</sup> cells	66
3.6 Differential translational activity in mTORC1-deficient T cells	67
3.7 Drug-induced inhibition of RNA Polymerase I reduces the expression of RNA and limits cell cycle entry in vitro	69
<b>4 Persistent RNA synthesis is required for T cell proliferation</b>	<b>71</b>
<b>5 T-Rptor<sup>-/-</sup> cells show a lower cell cycle progression with changed cell abundance in G<sub>0</sub>- and S-phase</b>	<b>73</b>
<b>II Development of a mouse system to investigate CD8<sup>+</sup> T cell development upon acute and chronic antigen presentation under sterile conditions</b>	<b>75</b>
<b>1 Improved performance of iOVA by the Tet-repressor KRAB</b>	<b>75</b>
<b>2 Effector T cell generation in iOVA-KRAB mice</b>	<b>78</b>
<b>3 Persistent antigen-exposure compromises memory formation in OT-I T cells</b>	<b>79</b>
<b>4 Establishment of an antigen-inducible latent virus in mice</b>	<b>82</b>
<b>E Discussion</b>	<b>85</b>
<b>1 TCR signaling increases mTORC1 activity</b>	<b>85</b>
<b>2 Cell size increase is delayed in T-Rptor<sup>-/-</sup> cells</b>	<b>86</b>
<b>3 Proliferation of T-Rptor<sup>-/-</sup> cells is compromised <i>in vivo</i></b>	<b>87</b>
<b>4 RNA Polymerase I-induced rRNA expression can be linked with T cell proliferation</b>	<b>91</b>

4.1 mTORC1 controls RNA Polymerase I expression	91
4.2 mTORC1 is necessary for global RNA upregulation	92
4.3 T cell proliferation can be linked to RNA synthesis	93
<b>5 Differences between CD4<sup>+</sup> and CD8<sup>+</sup> T cells</b>	<b>96</b>
<b>6 Role of mTORC2 on RNA synthesis, stability and T cell proliferation</b>	<b>97</b>
<b>7 Technical challenges and benefits</b>	<b>97</b>
7.1 Pyronin Y in flow cytometry	97
7.2 mTORC1 signaling inhibitors	98
<b>8 KRAB in a tet-inducible system</b>	<b>100</b>
<b>9 Outlook</b>	<b>102</b>
<b>F Abbreviations</b>	<b>103</b>
<b>G Literature</b>	<b>107</b>
<b>H Acknowledgments</b>	<b>130</b>
<b>I Appendix</b>	<b>131</b>
<b>I Gating strategies</b>	<b>131</b>
<b>II MHV-68_OVA</b>	<b>136</b>

## A Abstract

### 1 Abstract

When a T cell gets activated by antigen, 1-100 cells per one million T cells give rise to a population of antigen-specific effector cells within a few days. The T cells proliferate vigorously and induce many physiological changes to fully develop an effector phenotype. Two complexes formed by the mammalian/mechanistic target of rapamycin, mTORC1 and mTORC2 have been found to be in the center of integrating external signals and translating them into cellular changes on the level of transcription, translation and cell growth.

Even though it is known that both RNA Polymerase I and T cell proliferation are regulated by mTORC1 a direct correlation between ribosomal RNA synthesis and proliferation has not been investigated so far.

This study asked whether TCR signaling induces mTORC1-dependent ribosomal RNA synthesis and thus proliferation in primary T cells. Therefore, *in vitro* and *in vivo* studies were performed comparing mTORC1 sufficient with deficient T cells, showing a TCR induced activation of mTORC1-signaling being highly reduced in mTORC1 deficient T cells. This resulted in less proliferation of polyclonal and TCR transgenic mTORC1 deficient T cells in graft-versus-host responses, a lower response upon transient TCR stimuli and lower cell expansion early and late upon a viral infection with the modified Vaccinia Ankara virus expressing ovalbumin (MVA-OVA). Furthermore, homeostatic survival and lymphopenic proliferation was reduced in the absence of mTORC1.

*In vitro* applications with a specific inhibitor of RNA Polymerase I, quarfloxin, demonstrated that T cell proliferation requires *de novo* synthesis of ribosomal RNA at both the initial transition from G<sub>0</sub> to G<sub>1</sub> and the transition from G<sub>1</sub> to S phase cell cycle checkpoint of the consecutive divisions. Total RNA sequencing and directly assessing relative RNA expression by flow cytometry with the dye Pyronin Y revealed that mTORC1-signaling is essential for ribosomal as well as global RNA expression in primary T cells.

Our data indicate a major role of ribosomal RNA for the clonal expansion of T cells. RNA Polymerase I is being seen as a potential target in cancer therapy. However, its inhibition may have side effects that may cause a transient immunodeficiency.

## **A Abstract**

Based on previously published data in Rabenstein et al., 2014, in a second project a transcriptional repressor, the Krüppel associated box (KRAB) domain, was tested in iOVA mice and mice infected with MHV-68\_OVA. Since the KRAB domain was fused to the DNA-binding domain of the tet-repressor a negative regulation of the expression of genes under the control of the tet-operator was detected. In kinetic studies as well as functional analysis of antigen-exposed OT-I T cells we showed that the repressing function of the KRAB domain did improve the leaky expression of K<sup>b</sup>/OVA<sub>257-264</sub> under the control of the tet-operator in iOVA mice.

### 2 Zusammenfassung

Wenn eine T-Zelle durch fremdes Antigen aktiviert wird, sind es lediglich wenige hundert Zellen unter Millionen aus denen sich eine große Population antigenspezifischer Effektorzellen bildet. Dieser Prozess dauert nur wenige Tage und erfordert deshalb eine schnelle Expansion und physiologische Anpassung der T-Zellen. Zwei Proteinkomplexe, in deren Zentrum sich das mammalian/mechanistic target of Rapamycin (mTOR) befindet, mTORC1 und mTORC2, spielen eine tragende Rolle bei der Integration und Übersetzung von externen Signalen. Während einer Infektion werden diese in zelluläre Prozesse der Transkription, Translation und Wachstum umgewandelt.

Obwohl bekannt ist, dass sowohl die Aktivität der RNA Polymerase I als auch T-Zell Proliferation von mTORC1 reguliert wird, wurde der Zusammenhang ribosomaler RNA-Synthese mit Proliferation bislang nicht untersucht.

Ziel dieser Studie ist es, den Zusammenhang von T-Zellrezeptor-induzierter und mTORC1-abhängiger ribosomaler RNA-Synthese mit der Proliferation von primären T-Zellen zu untersuchen.

In diesem Zusammenhang wurden Experimente sowohl *in vitro* als auch *in vivo* mit T-Zellen aus mTORC1-defizienten und Kontroll-Tieren durchgeführt. Diese zeigten eine geringere Zellteilung von adoptiv transferierten mTORC1-defizienten polyklonalen und TCR transgenen T-Zellen in Graft-versus-Host Reaktionen auf. Zudem konnte eine geringere Reaktion auf transiente TCR-Stimuli und eine reduzierte Zellexpansion als Antwort auf eine Infektion mit dem Virus MVA-OVA (Modified Vaccinia Ankara Virus, welches Ovalbumin exprimiert) zu frühen und späten Zeitpunkten festgestellt werden. Auch war das homöostatische Überleben und die Proliferation unter lymphopenischen Bedingungen in diesen Zellen stark reduziert.

Eine *in vitro* Behandlung von Wildtyp-T-Zellen mit Quarfloxin, einem Inhibitor gegen die Aktivität der RNA Polymerase I, konnte aufzeigen, dass proliferierende T-Zellen stark von einer kontinuierlichen Synthese ribosomaler DNA abhängig sind, sowohl beim anfänglichen Übergang von G<sub>0</sub> zu G<sub>1</sub> als auch beim Übergang von G<sub>1</sub> zur S-Phase der darauffolgenden Zellteilungen. Anhand von Sequenzierungsdaten von Gesamt-RNA, und der direkten Visualisierung der relativen RNA-Expression mittels Durchflusszytometrie anhand des Farbstoffs Pyronin Y, konnte ein direkter Zusammenhang zwischen mTORC1-Aktivität und ribosomaler wie auch globaler RNA-Expression, ermittelt werden.

## **A Abstract**

Unsere Daten deuten auf eine tragende Rolle der ribosomalen RNA bei der klonalen Expansion von T-Zellen hin, wobei die RNA-Polymerase I selbst bereits als potenzielles Ziel in der Krebstherapie untersucht wird. Mögliche Nebenwirkungen wie zum Beispiel vorübergehende Immundefekte können hierbei jedoch nicht ausgeschlossen werden.

Ausgehend von einer im Jahr 2014 publizierten Studie von Rabenstein et al., wurde in einem weiteren Projekt die Auswirkungen des tet-Repressors KRAB (Krüppel-associated box) auf die Genexpression von OVA<sub>257-264</sub> in iOVA Mäusen bzw. MHV-68\_OVA infizierten Mäusen untersucht. Da die KRAB-Domäne mit der DNA-Bindedomäne des Tet-Repressors fusioniert war, konnte eine negative Regulation der unter dem Tet-Operator exprimierten Gene detektiert werden. In Experimenten hinsichtlich der Kinetik von Antigen-Expression sowie funktionelle Analysen von Antigen-stimulierten OT-I T-Zellen konnte im Rahmen dieser Arbeit eine Verbesserung der Expressionskontrolle des Peptids OVA<sub>257-264</sub> gezeigt werden.

## B Introduction

### 1 T cells in the context of immune response

In order to fight pathogens, vertebrates have developed two conceptual systems to generate a successful host-pathogen defense – innate and adaptive immunity.

Whereas innate immune cells show a broad spectrum of recognition mediated via pattern recognition receptors (PRRs), cells of the adaptive immune system have high antigen specificity, inducing a humoral, antibody-mediated and cellular T and B lymphocyte response.

T cell progenitors originate from the bone marrow and mature in the thymus into single positive CD4<sup>+</sup> and CD8<sup>+</sup> T cells with distinct effector functions. While CD4<sup>+</sup> T cells can develop into several subsets with distinct T helper cell characteristics (e.g. Th1, Th2, Th17, Treg, etc.), CD8<sup>+</sup> T cells show a lower level of plasticity and mainly develop a cytotoxic function, killing pathogen-infected or neoplastic cells.

For CD8<sup>+</sup> T cells, precursor frequencies between 1 and 100 cells per 10<sup>6</sup> cells were found, whereas the numbers for CD4<sup>+</sup> T cells were around five times lower (Jenkins & Moon, 2012; Nelson *et al.*, 2015; Obst, 2015). These few antigen-specific T cells expand vigorously upon T cell receptor ligation and develop an effector function, which enables the clearance of a pathogen within days. What follows is a contraction of clones where around 90% of all antigen-specific T cells die. The few survivors remain as memory T cells and provide protection in case of a secondary infection with the same pathogen (Kaech & Cui, 2012; Masopust & Schenkel, 2013).

#### 1.1 T cell development

T cells develop in the thymus. Lymphoid progenitor cells leave the bone marrow and migrate into the cortex of the thymus via blood vessels, expressing neither CD4 nor CD8 on their surface. These cells are called double negative (DN) thymocytes. DN thymocytes can be further distinguished by the expression of CD44 and CD25 on their surface. DN1 thymocytes are CD44<sup>+</sup> and CD25<sup>-</sup>. Upon expression of CD25 and downregulation of CD44, DN1 thymocytes develop into DN3 cells, passing the DN2 (CD44<sup>+</sup>, CD25<sup>+</sup>) state. In DN3 cells, a RAG1- and RAG2-dependent rearrangement of the TCR $\beta$ -chain takes place. The successful TCR $\beta$  rearrangement, expression and pairing with the pT $\alpha$ -chain induces the DN4 stage, including the formation of the pre-TCR in complex with CD3 molecules. The signaling via the pre-TCR induces cell survival and proliferation. With the fixation of the  $\beta$ -chain locus of the TCR, CD4 and

## B Introduction

CD8 molecules are getting upregulated on the surface of the cell defining them as double positive. DP cells rearrange the TCR $\alpha$ -chain loci to build the  $\alpha\beta$ -TCR. They subsequently interact with self-peptide major histocompatibility complex (MHC)-encoded proteins on thymus-specific antigen-presenting cells, the cortical thymus epithelial cells (cTECs). Those cells that bind self-peptide MHC with an appropriate affinity get positively selected and enter the medulla of the thymus. Cells that bind with a weak or no affinity die of apoptosis (around 85%). In the medulla, cells undergo negative selection induced by the interaction with self-peptide MHC on medullar TECs (mTECs) or other antigen presenting cells (APCs) such as dendritic cells, B cells and macrophages (M $\Phi$ ). DP cells that interact too strong with self-peptide MHC undergo further differentiation or apoptosis, those that survive develop into naïve single positive CD4<sup>+</sup> or CD8<sup>+</sup> T cell, depending to which MHC class the T cell binds (Starr *et al.*, 2003).

Most of the T cells in the thymus give rise to  $\alpha\beta$  T cells. Nevertheless, 5% develop into  $\gamma\delta$  T cells, mainly located in the skin and mucosal tissue (Jameson *et al.*, 2002). This thesis focuses on  $\alpha\beta$  T cells.

### 1.2 Antigen recognition by the T cell receptor

Antigen recognition by T cells is a prerequisite for a successful immune response. It induces a cascade of biophysical, biochemical and genetic reactions that enables proliferation and thus the clonal expansion of antigen specific T cells. The cell cycle of proliferating T cells is perhaps among the fastest cell divisions in adult mammals (Mayya & Dustin, 2016; Obst, 2015).

T cells recognize pathogen-derived antigens in the context of MHC polymorphic proteins expressed on the surface of antigen presenting cells via their T cell receptor. The MHC genes are organized in a multigenic region called H-2 in mice and Human Leucocyte Antigen (HLA) in humans. CD4<sup>+</sup> T cells recognize peptides bound to MHC class II (MHC-II) proteins (H-2A, H-2E in mice and HLA-DP, -DM, -DOA, -DOB, -DQ and -DR in humans), CD8<sup>+</sup> T cells respond to peptides in the context of MHC class I (MHC-I) proteins (H-2D, H-2K and in some strains H-2L in mice; HLA-A, -B and -C in humans).

MHC-I and -II are structurally different and peptide loading is mediated via different mechanisms.

MHC-I is loaded with peptides from cytosolic proteins e.g. from viral origin, which are degraded by the proteasome, transported into the endoplasmatic reticulum (ER) and loaded on MHC-I by TAP. Peptides associated with MHC-II originate from extracellular

## B Introduction

proteins internalized by an APC by endo-, pino- or phagocytosis. Internalized proteins are enzymatically processed in the lysosome and loaded on MHC-II in late endosomes, in exchange of CLIP (class II-associated invariant chain peptide), which is removed from the peptide-binding groove of MHC-II. Whereas MHC-I is expressed on the surface of all nucleated cells, MHC-II can only be found on B cells, macrophages/monocytes and dendritic cells (Wieczorek *et al.*, 2017).

### 1.3 T cell receptor signaling

The interaction between the TCR and cognate peptide MHC (pMHC) complexes on an APC induces the activation of a mature T cell. It requires a stable contact that has to last for ~24 hours. It allows the T cell to stop migrating and thus to proliferate at the site of infection (Bousso & Robey, 2003; Mempel *et al.*, 2004).

The TCR is a heterodimer, consisting of a TCR $\alpha$ - and  $\beta$ -chain. It associates with the CD3 complex that is formed with one  $\delta$ -chain, one  $\gamma$ -chain, two  $\epsilon$ -chains and two  $\zeta$ -chains. The intracellular located immunoreceptor tyrosine based activating motifs (ITAMs) of the  $\epsilon$ - and  $\zeta$ -chains are phosphorylated upon TCR ligation.

Upon T cell receptor stimulation, a cascade of signals is induced. An early event is the recruitment of LCK (SRC family kinase) to the cytosolic domain of CD4 and CD8, which are associated with the TCR. LCK phosphorylates the  $\zeta$ -chain of the TCR and thus allows ZAP70 to bind. In turn, ZAP70 phosphorylates LAT, which recruits multiple adaptor and effector molecules to the TCR and thereby induces three major signaling pathways. First, the  $\text{Ca}^{2+}$ -Calcineurin dependent pathway, which leads to a translocation of NFAT into the nucleus, second, the mitogen-activated protein kinase (MAPK)-pathway that activates the transcription factors Fos, Jun and AP-1 and third, the NF $\kappa$ B signaling pathway. In combination with co-stimulation, T cell proliferation, differentiation and effector cell generation is induced (Gaud *et al.*, 2018).

One of these co-stimulatory signaling molecules is CD28, expressed on the surface of T cells. If bound by CD80 or CD83 expressed by an APC, it induces PI3K, which in turn can phosphorylate PIP3. PIP3 activates PDK1, which phosphorylates Akt on threonine 308. Akt phosphorylates TSC2 and thus induces the release of TSC2 from TSC1, which in complex negatively regulate RHEB. The release of RHEB allows it to bind and activate mTORC1 (Inoki *et al.*, 2003a; Pollizzi & Powell, 2015; Tee *et al.*, 2003; Zoncu *et al.*, 2011). Whether Akt is the only kinase upstream of mTORC1 or if there are additional pathways inducing it is yet unknown (Finlay *et al.*, 2012).

## B Introduction

### 1.4 T cell effector function

Upon infection, CD4<sup>+</sup> and CD8<sup>+</sup> T cells become activated in secondary lymphoid organs by APCs within days. Both cell types start to proliferate vigorously and show highly distinguishable effector functions. Whereas CD8<sup>+</sup> T cells develop into cytotoxic T lymphocytes (CTLs), CD4<sup>+</sup> T cells can differentiate into several distinct T helper (Th) cell types. The expression of well-defined key transcription factors and cytokines induces the development into different subpopulations of the CD4<sup>+</sup> Th cell compartment (O'Shea & Paul, 2010).

Th1 and Th2 cells were the first subsets defined by Mosmann and colleagues in 1986 (Mosmann & Coffman, 1989). Th1 cells are induced by the expression of the transcription factor T-bet and the cytokine IFN $\gamma$ . As main producers of IFN $\gamma$ , they induce an effective destruction of microbial pathogens by (a) phagocytic cells such as macrophages, (b) the cytotoxicity of NK cells and (c) the production of Immunoglobulin (Ig) G by B cells. Furthermore, the expression of IL-2 increases the number of effector T cells by inducing proliferation (Pipkin *et al.*, 2010; Schroder *et al.*, 2004).

Th2 cell differentiation occurs in the presence of IL-4 that triggers the expression of the transcription factor GATA-3 (Nair *et al.*, 2006). Th2 cells mediate the immune response against parasites at epithelial barriers and mucosal tissue by recruiting mast cells or inducing a class switch to IgE in B cells (Abbas *et al.*, 1996; Grogan *et al.*, 2001).

Over one decade later, two additional subpopulations of CD4<sup>+</sup> T cells were described, regulatory T cells (Tregs) and Th17 cells (Aggarwal *et al.*, 2003; Sakaguchi, 2000). Th17 cells show a characteristic production of IL-17A, IL-17E, IL-22 and IL-21. Not only do they promote protective immunity against extracellular bacteria and fungi at mucosal surfaces, but are also involved in autoimmunity and inflammatory disease. They are induced by IL-6 and/or IL-21 and express the transcription factor Ror $\gamma$ T. (Lee *et al.*, 2009; Miossec *et al.*, 2009).

Tregs are important to maintain central tolerance by producing IL-10 and TGF $\beta$  (von Boehmer, 2005). They are characterized by the expression of the transcription factor FoxP3 and CD25, the high affinity IL-2R $\alpha$ -chain. They very strongly rely on IL-2 and TGF $\beta$  signaling (Josefowicz & Rudensky, 2009; Sakaguchi *et al.*, 2008).

More recently, T follicular helper (Tfh) cells were described as CD4<sup>+</sup> T cells expressing CXCR5 and ICOS on their surface. Their key transcription factor is Bcl6. They produce high amounts of IL-21 and are involved in promoting germinal center responses and B cell class switching (Crotty, 2014; Vinuesa *et al.*, 2016).

## B Introduction

CD8<sup>+</sup> T cells show a lower variety and plasticity regarding their cell fate decision. Nevertheless, two different populations can be observed upon activation: The short-lived effector cells (SLECs) and memory precursor effector cells (MPECs). SLECs give rise to cells mainly carrying a cytotoxic function directly eliminating virus infected or neoplastic cells and are not very long lasting, whereas MPECs serve as precursors for long-lasting memory cells, beside their function as effector cells. Upon TCR stimulation CTLs start to produce IFN $\gamma$  as well as perforin, IL-2 and granzymes (Cruz-Guilloty *et al.*, 2009; Joshi *et al.*, 2007).

### 1.5 T cell memory formation and causes of exhaustion

Upon the clearance of a pathogen, T cells enter a phase in which more than 90% of the effector T cells generated during clonal expansion die, the phase of clonal contraction. Those that survive can remain for months or even years, defined as memory T cells (Badovinac *et al.*, 2002). They are characterized by a rapid secondary response to pathogens with a high proliferative capacity. Both CD4<sup>+</sup> and CD8<sup>+</sup> memory T cells rely on the presence of IL-7 for long-term maintenance. Furthermore, IL-15 is described as being essential for CD8<sup>+</sup> memory T cell sustainability (Jameson, 2002; Kaech & Cui, 2012; McKinstry *et al.*, 2012).

In chronic infections and in cancer, specific T cells lose their effector function and fail to differentiate into functional memory cells due to exhaustion (Wherry *et al.*, 2007). This term is used for the progressive and hierarchical loss of effector function, a sustained upregulation and co-expression of multiple inhibitory receptors, an altered expression and use of key transcription factors, metabolic derangements and a failure to transit into quiescence (Doering *et al.*, 2012; Schietinger & Greenberg, 2014; Wherry, 2011). Exhausted T cells were described in mice and humans (Gallimore *et al.*, 1998; Schietinger & Greenberg, 2014; Wherry *et al.*, 2003; Zajac *et al.*, 1998). They show a differential expression pattern of surface markers such as PD-1, KLRG-1, CD44, Ly6C, CD122 and CD127 as well as the transcription factors EOMES and T-bet (Paley *et al.*, 2012; Wherry *et al.*, 2007). Furthermore, they have a unique transcriptomic and epigenetic footprint by which they can be differentiated from effector or memory T cells (Crawford *et al.*, 2014; Doering *et al.*, 2012; Wherry *et al.*, 2007; Youngblood *et al.*, 2011; Zhang *et al.*, 2014a).

In the past decade, CD8<sup>+</sup> T cell exhaustion was extensively studied in chronic infections such as LCMV clone 13 in numerous mouse models, but also in pathogen-free animals. Chronic antigen exposure was found to be the central cause for T cell exhaustion (Han *et al.*, 2010; Wherry *et al.*, 2003). It was shown that exhausted T cells

## B Introduction

very much rely on antigen persistence with a faster turnover than T memory cells (Shin *et al.*, 2007).

Persistent antigen presentation can induce several mechanisms interfering with the functionality of a T cell. Among these is the expression of inhibitory receptors on the surface of a T cell and the desensitization of co-stimulatory pathways. Inhibitory receptors were originally described as negative regulators to prevent from autoreactivity and immunopathology (Sharpe *et al.*, 2007). An increased expression was also detected in exhausted T cells. Center of several studies became the inhibitory receptor PD-1 (Araki *et al.*, 2013; Odorizzi & Wherry, 2012). It is very often co-expressed with other inhibitory receptors such as LAG-3, 2B4, CD160, TIM3 and CTLA-4 (Blackburn *et al.*, 2009). Combined therapies interfering with their signaling pathway by monoclonal antibodies were found to have promising effects on tumor control (Wolchok *et al.*, 2013).

Furthermore, soluble mediators such as IL-10, TGF $\beta$ , Type I interferons and IL-6 can drive and promote exhaustion (Wherry & Kurachi, 2015). Source of such mediators can be regulatory T cells (Veiga-Parga *et al.*, 2013). On the other hand a general loss of CD4<sup>+</sup> T helper cells can lead to an even more severe exhaustion phenotype in CD8<sup>+</sup> T cells (Matloubian *et al.*, 1994).

In 2014, Crawford, Wherry and others were able to describe T cell exhaustion in CD4<sup>+</sup> T cells. They defined CD4<sup>+</sup> exhausted T cells as a subset not only distinct from CD4<sup>+</sup> T effector and memory cells, but also CD8<sup>+</sup> exhausted T cell. Nevertheless, some common features such as the expression of inhibitory receptors are shared (Brooks *et al.*, 2010; Crawford *et al.*, 2014; Han *et al.*, 2010).

The mechanisms responsible for the shift from memory precursor into exhaustion precursor cells were in the focus of more recent studies, showing a high plasticity among exhausted T cells (Hashimoto *et al.*, 2018; Im *et al.*, 2016; Utzschneider *et al.*, 2016; Wu *et al.*, 2016).

## 2 Metabolic demands of T cells

During T cell development, the metabolic requirements and availabilities of nutrients change drastically. Thus, metabolic pathways have to be engaged or suppressed in order to guide activation and differentiation. The two main pathways that supply adenosine triphosphate (ATP) within a cell are glycolysis and oxidative phosphorylation (OXPHOS). They are accompanied by fatty acid oxidation (FAO) and glutaminolysis (Geltink *et al.*, 2018).

## B Introduction

Naïve T cells show very low glucose utilization and mainly rely on OXPHOS as their energy source. Upon encountering their cognate antigen on an APC, TCR signaling induces a metabolic switch from OXPHOS to glycolysis for ATP production in T effector cells. Nevertheless mitochondrial metabolism is still active to produce calcium-dependent reactive oxygen species (ROS), which is essential for T cell activation. Although anaerobic glycolysis is less efficient in generating ATP than OXPHOS, a switch into this metabolic pathway allows lipids and other amino acids to be redirected into the generation of biomass to support cell division (Gerriets & Rathmell, 2012; Jones & Thompson, 2007).

Unlike T effector cells, Treg and Tmem cells show a downregulation of glycolysis and more rely on FAO and OXPHOS (Gerriets & Rathmell, 2012). Th17 cells use *de novo* FAO as energy source (Berod *et al.*, 2014).

The serine/threonine protein kinase mammalian/mechanistic target of rapamycin, short mTOR is a central molecule that mediates physiological changes dependent on metabolic changes in a cell (Geltink *et al.*, 2018).

### 3 The mechanistic target of rapamycin, mTOR

The mTOR homolog TOR (Target of rapamycin) was first discovered in yeast by Heitman, Moova and Hall in 1991 (Heitman *et al.*, 1991). Its name originates from the fungal toxin rapamycin, an antifungal, antibiotic product by *Streptomyces hygroscopicus* that was found to block the transition from G<sub>1</sub> to S phase in fungi (Singh *et al.*, 1979).

TOR was described as being the functional target of FKBP12-bound rapamycin (Cafferkey *et al.*, 1993; Koltin *et al.*, 1991). Two complexes formed by TOR, TORC1 (TOR1, TOR2, KOG1, LST8) and TORC2 (TOR2, AVO1, AVO2, AVO3, LST8) were described, with homologues in mammalian cell lines (Loewith *et al.*, 2002). Their differential sensitivity to rapamycin, with only TORC1 being sensitive to this toxin, revealed the essential contribution of TORC1 to G<sub>1</sub> progression and cell growth (Barbet *et al.*, 1996; Helliwell *et al.*, 1994; Kunz *et al.*, 1993; Loewith *et al.*, 2002).

The mammalian target of rapamycin (mTOR) was described in mammalian cell lines in two independent studies. Like TOR in yeast, it is sensitive to FKBP12-rapamycin (Brown *et al.*, 1994; Sabatini *et al.*, 1994; Sabers *et al.*, 1995). The application of rapamycin in experiments performed in mammalian cell lines allowed for the identification of mTOR signaling components. Thus, it was shown that, like in yeast, mTOR is part of two distinct protein complexes, mTORC1 and mTORC2. Both

## B Introduction

complexes have distinct activation signals, molecular targets and functions in mammal cells (Hara *et al.*, 2002; Sarbassov *et al.*, 2004).

### 3.1 The composition of mTORC1 and mTORC2

Besides several common components such as the scaffolding protein mLST8, the regulatory subunit DEPTOR and the Tti1/Tel2 complex, which is necessary for the assembly and stability, each complex also contains distinct components. mTORC1 is defined by being associated with the scaffolding protein Raptor as well as the negative regulator PRAS40, which is released upon growth factor receptor signaling. Rictor and mSin1 are mTORC2 specific components. Rictor mainly mediates mTORC2 assembly, stability, substrate identification and localization; mSin1 acts as negative regulator of the mTORC2 kinase activity until PI3K signaling induces the recruitment of mSin1 to the plasma membrane and release from mTORC2 (Aylett *et al.*, 2016; Sarbassov *et al.*, 2004; Yang & Chi, 2013) (Fig. B1 A). T cells with deletions of the Rictor and Raptor genes were used in this thesis.

### 3.2 Downstream targets of mTORC1

Cell growth and division is accompanied by an increased glucose metabolism and synthesis of proteins, lipids and nucleotides but also by the suppression of catabolic pathways such as protein turnover and autophagy. mTORC1 is central to processes coordinating anabolism and catabolism in proliferating cells (Saxton & Sabatini, 2017) (Fig. B1 B).

Among others, the two molecules S6K1 and 4E-BP1 have been described as direct targets of mTORC1. Their phosphorylation at Threonine-389 (S6K1) and Threonine-36/45 (4E-BP1) and thus activation is sensitive to inhibition by rapamycin (Brown *et al.*, 1995; Burnett *et al.*, 1998; Hara *et al.*, 2002; Kim *et al.*, 2002).

Protein synthesis is mainly regulated via these two molecules. Their activity shapes the binding of translation elongation factors to 5' TOP mRNA, including mostly genes related to protein synthesis (Saxton & Sabatini, 2017). S6K1 can phosphorylate substrates that can either promote or inhibit mRNA translation, therefore inducing their activation and degradation, respectively. The positive regulator of 5' cap binding eIF4F complex, eIF4B can be activated by S6K1 (Holz *et al.*, 2005). In contrast, the degradation of PDCD4, an inhibitor of this complex, can be facilitated by S6K1 (Dorrello *et al.*, 2006). The negative regulator of translation, 4E-BP1 is directly phosphorylated by mTORC1 and thus dissociates from the eIF4E complex. This allows the translation of 5' cap-dependent mRNA (Brunn *et al.*, 1997; Gingras *et al.*, 1999).

## B Introduction

The translational activity relies on the synthesis and activity of ribosomes. mTORC1 can regulate ribosome synthesis via its downstream targets TIF-IA (also known as Rrn3) and Ubf. These RNA Polymerase I specific transcription factors play major roles controlling the transcriptional and translational machinery by regulating the transcription of ribosomal ribonucleic acid (rRNA) (Claypool *et al.*, 2004; Hannan *et al.*, 2003; Mayer *et al.*, 2004). Upon inhibition of Akt or mTOR in T cells, the binding capacity of RNA Polymerase I as well as the processing of pre-rRNA were found to be limited, which led to reduced rRNA synthesis and ribosome biogenesis (Chan *et al.*, 2011).

Nucleotide synthesis is crucial for DNA replication and ribosome synthesis and therefore growth and proliferation of a cell. mTORC1 induces the expression and activation of key components of the purine and pyrimidine synthesis (Ben-Sahra *et al.*, 2016; Robitaille *et al.*, 2013).

Fatty acid and cholesterol biosynthesis is regulated via the sterol responsive element binding protein (SREBP) (Porstmann *et al.*, 2008). mTORC1 phosphorylates Lipin1, a negative regulator of SREBP (Duvel *et al.*, 2010; Peterson *et al.*, 2009). Furthermore, mTORC1 can induce an increased translation of the transcription factor HIF1a, which drives the expression of glycolytic transporters and enzymes (Duvel *et al.*, 2010; Powell *et al.*, 2012).

Another function of mTORC1 is the negative regulation of protein degradation by autophagy and ubiquitination. Under conditions where nutrients are available, mTORC1 phosphorylates ULK1 and thus prevents its binding to a complex driving the autophagosome formation, thereby inhibiting it (Kim *et al.*, 2011). Moreover, mTORC1 phosphorylates the transcription factor EB (TFEB), which in turn blocks the translocation of TFEB to the nucleus and the induction of genes, necessary for the autophagy machinery and lysosomal biogenesis (Martina *et al.*, 2012; Roczniak-Ferguson *et al.*, 2012; Settembre *et al.*, 2011; Settembre *et al.*, 2012).

It was recently demonstrated that proteasome-dependent proteolysis is associated with mTORC1 activity. When mTORC1 is inhibited for a limited time frame, global protein-ubiquitination and the expression of proteasomal chaperones are increased (Rousseau & Bertolotti, 2016; Zhao *et al.*, 2015). However, an increase of proteasomal activity was also detected in cells with hyperactivated mTORC1 activity, indicating different outcomes of acute versus prolonged inhibition of the mTORC1 signaling pathways (Zhang *et al.*, 2014b) (Fig B1 C).

## B Introduction

### 3.3 Upstream activators of mTORC1

A shift from catabolism in the direction of anabolism can be induced by a series of growth-promoting, endocrine signals. They are related to the stress and energy status of a cell and to the availability of oxygen and amino acids (Ananieva *et al.*, 2014; Laplante & Sabatini, 2012; Saxton & Sabatini, 2017; Zoncu *et al.*, 2011).

mTORC1 is described as downstream mediator of several growth factors via the Tuberous Sclerosis Complex (TSC), a negative regulator of mTOR (Saxton & Sabatini, 2017). TSC functions as GTPase activating protein (GAP). Upstream signaling by several growth factors induces the dissociation of TSC from the GTPase Rheb, which allows an interaction of Rheb with mTORC1 and thus activates the Serin/Threonine kinase activity of mTORC1. Such upstream signals can be insulin or insulin-like growth factor-1, Ras, Wnt and TNF $\alpha$ , which induce either PI3K or AMPK dependent signaling and thus phosphorylation of the heterodimeric subunits of TSC, TSC1 or TSC2 (Garami *et al.*, 2003; Inoki *et al.*, 2003a; Inoki *et al.*, 2003b; Long *et al.*, 2005; Manning *et al.*, 2002; Menon *et al.*, 2014; Sancak *et al.*, 2010; Sancak *et al.*, 2008; Tee *et al.*, 2003).

Furthermore, mTORC1 can respond to signals interfering with cell growth such as low ATP levels, hypoxia, DNA damage responses and glucose deprivation. Low ATP levels and glucose deprivation regulate mTORC1 via two different mechanisms: through inhibition of the Rag GTPase and activation of AMPK (Efeyan *et al.*, 2013; Gwinn *et al.*, 2008; Inoki *et al.*, 2003b; Kalender *et al.*, 2010; Shaw *et al.*, 2004). In addition, AMPK activation and thus mTORC1 inhibition can be induced by hypoxia and DNA damage-responses (Brugarolas *et al.*, 2004; Feng *et al.*, 2007).

Amino acids are essential building blocks for proteins and energy source of several metabolic pathways (Saxton & Sabatini, 2017). Changes in amino acid provision can be sensed by mTORC1-mediated mechanisms, if mTORC1 is translocated to the cytosolic side of the lysosome. It was demonstrated that the role of mTORC1 on lysosomal function relies on PI3K signaling induced by insulin on the one hand and the availability of amino acids on the other hand. If the amino acid arginine gets transported into the lysosome by SLC38A9, mTORC1 can bind to the Rag GTPases RagC and D, located in the lysosome in a complex formed with RagA/B and the guanine nucleotide exchange factor (GEF) Ragulator (Wang *et al.*, 2015). Furthermore, mTORC1 induces the phosphorylation of the transcription factor EB (TFEB), which in turn blocks the translocation of TFEB to the nucleus and the induction of genes,

## B Introduction

necessary for autophagy in the lysosome (Settembre *et al.*, 2011; Settembre *et al.*, 2012).

Several negative and positive regulators of mTORC1 were defined in studies addressing the role of mTORC1 on lysosomal function. PRAS40 binds to mTORC1 if not phosphorylated by Akt/PKB and inhibits the phosphorylation of S6K1 and cell growth (Sancak *et al.*, 2007). In addition FLCN-FNIP complex was described to bind to RagC/D in starved cells and thus blocks the binding of mTORC1 to RagC/D (Tsun *et al.*, 2013). GATOR1 and GATOR2 were found to have opposite effects on mTORC1 with GATOR1 functioning as GTPase activating protein (GAP) for RagA and hence as negative regulator of mTORC1 (Bar-Peled *et al.*, 2013). GATOR2 activates mTORC1 and is recruited by KICSTOR and regulated by CASTOR1 and Sestrin2 if leucine is bound (Chantranupong *et al.*, 2014; Saxton *et al.*, 2016; Wolfson *et al.*, 2016; Wolfson *et al.*, 2017) (Fig B1 C).

Most of the studies on the function of mTORC1 were performed in yeast or mammalian cell lines. Nevertheless, mTORC1 was also found to play a major role in T cell activation, differentiation and effector function (Powell *et al.*, 2012). Among the signals described above, signaling via the TCR in combination with co-stimulatory molecules can induce mTORC1 activity. This upstream signal is unique in T cells (Pollizzi & Powell, 2015; Powell *et al.*, 2012).

### 3.4 mTORC1 in T cells

Also in T cells S6K1 and 4E-BP1 were described as downstream targets of the serine/threonine kinase activity of mTORC1 (Hukelmann *et al.*, 2016; Yang *et al.*, 2013; Zeng *et al.*, 2013).

One of the main features of mTOR is the induction of the metabolic switch from OXPHOS to glycolysis, called Warburg effect (Fox *et al.*, 2005; Jones & Thompson, 2007; MacIver *et al.*, 2013; van der Windt & Pearce, 2012; Vander Heiden *et al.*, 2009). Resting T cells are found to be in a catabolic state. Upon stimulation, T cells become anabolic and switch to glycolysis and nutrient uptake.

PI3K signaling by the co-stimulatory receptor CD28 leads to Akt activation and thus the expression of glucose transporters via mTORC1 (Frauwirth *et al.*, 2002; Frauwirth & Thompson, 2002, 2004; Macintyre *et al.*, 2014; Powell *et al.*, 2012).

The question of how mTORC1 signaling affects T cell differentiation was mainly addressed by inhibiting mTORC1 signaling with the very potent inhibitor rapamycin or in T cells with deleted signaling components of mTORC1.

## B Introduction

It was found that T cells with abrogated mTORC1 activity proliferated less than wildtype cells in response to *in vitro* stimulation with anti-CD3/28 or cognate peptide as well as *in vivo* upon adoptive transfer into irradiated or RAG-deficient mice (Delgoffe *et al.*, 2009a; Delgoffe *et al.*, 2009b; Delgoffe *et al.*, 2011; He *et al.*, 2011; Tan *et al.*, 2017a; Tan *et al.*, 2017b; Yang *et al.*, 2013; Zeng *et al.*, 2013; Zhang *et al.*, 2011). Furthermore, a decrease in cell size was found early upon stimulation, indicating that mTORC1 plays a crucial role in T cell growth and proliferation (Pollizzi *et al.*, 2015; Yang *et al.*, 2013).

It was shown that mTORC1 and mTORC2 are both critical for T helper cell development and fate decision. T cells in mice with mTOR-deficiency were not able to develop into Th1, Th2 or Th17 cells. Instead, an increase in the FoxP3<sup>+</sup> T cell compartment was detected even under normal stimulation conditions (Delgoffe *et al.*, 2009b). Further studies using mice deficient in the mTORC1 activator Rheb showed more specifically that mTORC1 regulates the development of Th1 and Th17 cells in *in vitro* stimulation assays. Adoptively transferred OT-II T cells in mice infected with Vaccinia-OVA failed to express IFN $\gamma$ , IL-17 as well as the transcription factors GATA-3 and Ror $\gamma$ t. Furthermore, EAE scores and Th17 infiltrates were significantly reduced in mice carrying Rheb-deficient T cells. The same study showed that Th2 differentiation relies on mTORC2 signaling, since *in vitro* stimulated Rictor-deficient T cells failed to express IL-4 under Th2 skewing conditions (Delgoffe *et al.*, 2011; Lee *et al.*, 2010). Nevertheless, in T cells with compromised mTORC1 signaling by Raptor-deficiency, an impaired development of the Th2 phenotype was found (Yang *et al.*, 2013). Even though mTOR-deficient T cells tend to develop into a regulatory T cell phenotype, the same was not true in T cells with abrogated mTORC1 function. In T cells deficient for either Rheb or Raptor, Treg cells were found to rely on mTORC1 activity to program and maintain their metabolic and suppressive function (Delgoffe *et al.*, 2011; Zeng *et al.*, 2013).

The contribution of mTORC1 on memory formation was mainly studied in *in vitro* stimulated CD8<sup>+</sup> T cells. T memory cell numbers were increased upon transient mTORC1-inhibition with rapamycin; anergy in turn was decreased (Araki *et al.*, 2009; Jenkins, 1992; Pearce *et al.*, 2009; Powell *et al.*, 1999; Rao *et al.*, 2010). Nevertheless, long-term inhibition of mTORC1 abrogated memory formation (Li *et al.*, 2012).

Recent studies developed a correlation between mTORC1 activity and the active regulation of the translational activity in T cells. Proteomic analysis of rapamycin-

## B Introduction

treated P14 cells *in vitro* differentiated into CTLs with cognate peptide, showed lower global protein levels. A reduction was mainly found in proteins associated with cytotoxicity and glycolysis as well as ribosomal proteins and translation factors associated with protein synthesis mainly encoded by 5' TOP mRNA (Hukelmann *et al.*, 2016; Thoreen *et al.*, 2012). Similar results were detected in Raptor-deficient T cells stimulated *in vitro* with anti-CD3/28 for 16 hours (Tan *et al.*, 2017a). Moreover, signaling from the TCR is crucial for ribosome synthesis and translation as shown in OT-I T cells deficient for the TCR signaling molecule Lck, stimulated with cognate peptide *in vitro* (Tan *et al.*, 2017b). A further study on P14 CD8<sup>+</sup> T cells, adoptively transferred into mice infected with LCMV Armstrong, showed an active regulation of translational activity by the increase of mRNA bound to polysomes. When treated with rapamycin, less mRNA encoding for ribosomal proteins was bound to polysomes. Furthermore, a TCR-dependent increase in polysome-bound mRNA was detected in experiments comparing responses to the acute LCMV strain Armstrong versus the chronic strain clone 13 on day eight, indicating that antigen persistence affects translational regulation (Araki *et al.*, 2017).

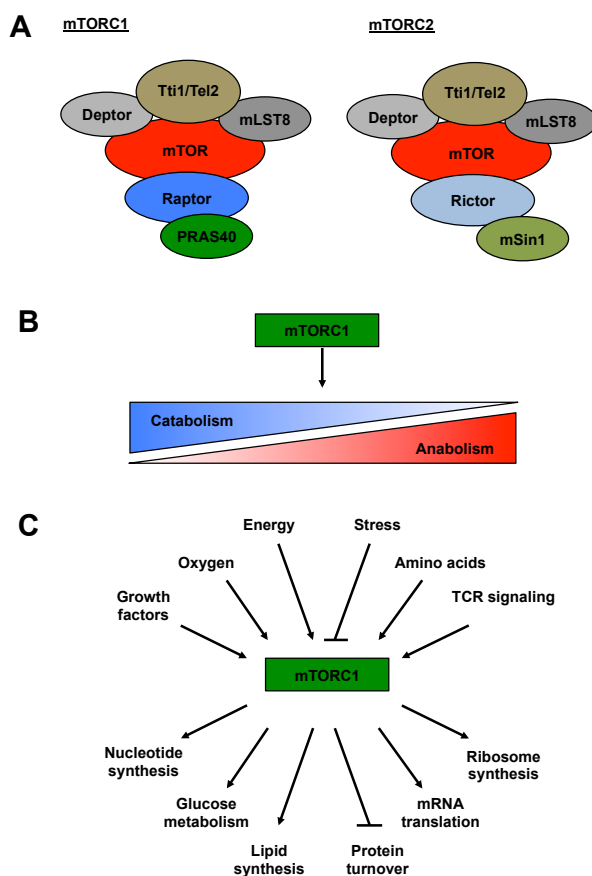


### Figure B1: The mammalian Target of Rapamycin - mTOR.

(A) The structure of mTORC1 and mTORC2.

(B) mTORC1 controls the balance between catabolism and anabolism.

(C) The major upstream and downstream targets of mTORC1. Modified from (Saxton & Sabatini, 2017)

### 4 Cell cycle in T cells

The cell cycle is a highly regulated, universal and conserved process in eukaryotic cells leading to the reproduction of a cell. This event can be divided into the S phase, in which the DNA of a cell is replicated and mitosis (M phase), in which the DNA is separated and partitioned in two daughter cells. S and M phase are separated by two gap phases:  $G_1$  before and  $G_2$  after S phase. In addition, most cells remain in a quiescent state in which they do not proliferate, the  $G_0$  phase. Upon activation, these cells can enter the cell cycle into  $G_1$  phase. The most critical event of a cell cycle is the replication and partitioning of the hereditary material, the DNA, during the S phase. A quantification of the DNA content of a cell helps to distinguish  $G_1$  from S and  $G_2/M$  phase (Nurse, 2000; Pardee, 1989).

In T cells, the cell cycle and proliferation plays a central role for activation and accompanies the differentiation of fully functional effector cells (Kaech & Cui, 2012; Masopust & Schenkel, 2013).

In 1980, Darzynkiewicz et al. demonstrated that not only the DNA, but also the RNA content of a cell changes during proliferation (Darzynkiewicz *et al.*, 1980). By visualizing DNA and RNA in several cell types including phytohaemagglutinin-stimulation of blood cells by acridine orange in flow cytometry, a better distinction of quiescent cells in  $G_0$  and cells in  $G_1$  was achieved compared to the forward scatter parameter (Darzynkiewicz *et al.*, 1980). One year later, Shapiro described the xanthene homolog of acridine orange, Pyronin Y as RNA-staining dye which could eliminate technical challenges accompanied with acridine orange staining, allowing RNA visualization in intact cells (Shapiro, 1981). Since then, Pyronin Y has occasionally been used to study the cell cycle in proliferating cells (Behbehani *et al.*, 2012; Challen *et al.*, 2009; Challen & Goodell, 2008; Crissman *et al.*, 1985; Cui *et al.*, 2003; Darzynkiewicz *et al.*, 2004; Janumyan *et al.*, 2003; Nakamura-Ishizu *et al.*, 2014; Passegue *et al.*, 2005; Qiu *et al.*, 2013; Schmid *et al.*, 2000). Quiescent, non-proliferating cells remain in  $G_0$ , characterized by diploid DNA and low RNA content. Upon stimulation, T cells enter  $G_1$  still having a diploid DNA content but increased RNA expression. From there, cells pass into the S-phase, in which they double their DNA content to  $4n$ , but also increase their amount of RNA. The S-Phase is followed by  $G_2$  and then the M phase when the genetic material and other macromolecules are distributed the two daughter cell. A critical regulation points in cell cycle that often dictates the speed of proliferation is the transition from  $G_1$  to S phase (Darzynkiewicz *et al.*, 1980; Pardee, 1989; Shapiro, 1981).

## B Introduction

Later on, specific molecules were defined characteristic for the transition into certain cell cycle phases. In this course, c-myc and the retinoblastoma protein were described as being critical for transitioning from G<sub>1</sub> to S phase (Sage *et al.*, 2000; Schorl & Sedivy, 2003; Weinberg, 1995). Furthermore, cyclins and cyclin-dependent kinases were defined as universal cell cycle regulators (Nurse, 2000).

In later studies, Dowling *et al.* used a transgenic mouse system, the FUCCI mouse, containing a red fluorescent reporter expressed during G<sub>1</sub> phase and a green fluorescent reporter expressed from the beginning of S phase to study the kinetics of cell cycle transitions in primary T cells *in vitro* (Dowling *et al.*, 2014).

In combination with *in vivo* performed studies using the cell division-sensitive fluorescent vital dye CFSE to assess the cell proliferation, gave closer insights on the duration of one cell cycle in a T cell. The time a T cell needs to complete one cell cycle is between ten and twelve hours *in vitro* and quite faster (four to eight hours depending on the intensity and duration of the TCR stimulus) *in vivo* (Dowling *et al.*, 2014; Lawrence & Braciale, 2004; Yoon *et al.*, 2010; Yoon *et al.*, 2007).

### 5 RNA expression in T cells

In highly proliferative cells, approximately 80% of transcription is invested into ribosome synthesis (Moss *et al.*, 2007; Moss & Stefanovsky, 2002; Warner, 2001). Ribosomes consist of 28S, 18S, 5.8S and 5S ribosomal RNA and 92 proteins. 2-300 proteins are involved in processing and assembly of ribosomes in the nucleolus. The first three named rRNAs have a common precursor, the 47S rRNA. The expression of this precursor is regulated via RNA Polymerase I. RNA Polymerase III regulates the expression of 5S rRNA (Moss *et al.*, 2007; Warner, 2001). The production of ribosomes starts at the end of mitosis, increases during G<sub>1</sub>- and has its maximum during G<sub>2</sub>-phase (Gebrane-Younes *et al.*, 1997). Molecules that drive cell cycle progression are the cyclin-dependent kinases (CDKs). Cdk1 negatively regulates the expression of RNA Polymerase I at the beginning of mitosis by phosphorylating RNA polymerase I specific transcription factors, thus preventing DNA binding (Sirri *et al.*, 1999).

Metabolism and specific environmental challenges are responsible for the regulation of the transcription of rRNA genes (Derenzini *et al.*, 1998; Hannan *et al.*, 1998). The MAPK-dependent activation of TIF-IA and UBF are the initial signals to induce RNA Polymerase I. In association with fibrillarin and nucleophosmin they serve essential functions in rRNA maturation (Grummt & Langst, 2013; Voit *et al.*, 1999). Newly synthesized RNA is processed and assembled in subnuclear structures called nucleoli.

### 6 The nucleolus

The nucleolus is a sub-compartment in the nucleus, which mediates the early steps of ribosome biogenesis and the assembly as well as function of non-ribosomal ribonucleoprotein complexes. It controls cell cycle progression and senses environmental stress. The nucleolar morphology changes depending on the transcriptional activity of a cell and in turn dictates nuclear pathways that affect transcription, replication and DNA repair. Thus it is a key player regulating cell growth, survival, senescence and stress responses (Hutten *et al.*, 2011; Pederson, 2010).

The nucleolus is composed of three compartments: the fibrillar centers (FC), dense fibrillar centers (DFC) and granular components (GC) (Scheer & Hock, 1999). The transcription of rRNA genes by RNA Polymerase I occurs at the interface between FCs and DFCs, while processing of pre-rRNA and assembly with ribosomal proteins takes place in the GC of the DFC (Nemeth & Grummt, 2018; Thiry *et al.*, 2011). The mammalian nucleolus is remarkably plastic and reorganizes during each cell cycle. The early event of nucleolar assembly starts at the telophase of the mitoses and occurs during a relatively long period of the cell cycle. It depends on the coordination between the transcription of rDNA and the expression of RNA processing complexes. During S-Phase, RNA Polymerase I is transiently released from rDNA to prevent collision with the replication machinery. With entry of the mitotic metaphase, the nucleolus disassembles which allows nucleolar proteins to associate with the surface of metaphase chromosomes (Hernandez-Verdun *et al.*, 2002; Smirnov *et al.*, 2016).

### 7 Aims of this thesis

It has been shown that mTORC1 serves as a mediator of extracellular signals and cell functionality. In T cells, T cell receptor stimulation induces mTORC1 activity, which is indispensable for rapid T cell proliferation. Furthermore, mTORC1 regulates the expression of transcription factors associated with RNA Polymerase I activity and thus the expression of ribosomal RNA. If this also affects proliferation in T cells is not fully understood, yet. This study addresses the question whether there is a direct correlation between mTORC1-dependent RNA Polymerase I activity and thus ribosomal RNA biosynthesis and proliferation in T cells. This hypothesis was tested, by (I) analyzing the requirement of mTORC1 activity for T cell proliferation *in vivo*, (II) the global and ribosomal RNA synthesis in mTORC1-deficient T cells *in vitro* and (III) showing a direct correlation between RNA Polymerase I activity and proliferation.

## **B Introduction**

In a second project, the Krüppel-associated box KRAB, fused to the DNA-binding domain of the tet-repressor was used to improve the leaky peptide expression in iOVA mice, a new model for transient antigen expression *in vivo*. Thus, functional analysis of OT-I T cells in response to cognate antigen expression was tested in the presence of the KRAB repressor. Furthermore, a doxycycline-inducible OVA<sub>257-264</sub> expressing virus was created and tested under the absence or presence of the Krüppel-associated box-domain. With these approaches, the influence of persistent antigen-presentation in comparison to transient antigen-stimuli on CD8<sup>+</sup> T cell development was tested under non-inflammatory conditions.

### C Material and Methods

#### 1 Material

##### 1.1 Chemicals and Solutions

---

2-Deoxy-D-Glucose	Sigma-Aldrich, St. Louis, MO, USA now: Merck, Kenilworth, NJ, USA
2-Mercaptoethanol	Carl Roth, Arlesheim, Switzerland
Actinomycin D	Hölzel Diagnostika GmbH, Köln, Germany
Agarose	Peqlab, Erlangen, Germany
Antibiotic/antimycotic	GE Healthcare, Chalfont St Giles, UK
Brefeldin A	Sigma-Aldrich, St. Louis, MO, USA now: Merck, Kenilworth, NJ, USA
Casy ton	Roche, Basel, Switzerland
4',6-diamidino-2-phenylindole (DAPI)	Invitrogen, Carlsbad, CA, USA
DMEM (Powderly <i>et al.</i> )	AppliChem, Darmstadt, Germany
DMSO	Sigma-Aldrich, St. Louis, MO, USA now: Merck, Kenilworth, NJ, USA
dNTPs	Peqlab, Erlangen, Germany
Doxycycline	AppliChem, Darmstadt, Germany
EDTA (Gibco)	Life Technologies, Carlsbad, CA, USA
Ethanol	Diagonal, Münster, Germany
Ethidium bromide (1% solution)	AppliChem, Darmstadt, Germany
FCS (Gibco)	Life Technologies, Carlsbad, CA, USA
Ficoll (PAA)	GE Healthcare, Chalfont St Giles, UK
FVD (eFluor450, eFluor660, eFluor780)	eBioscience, San Diego, CA, USA
Gelatin	Sigma-Aldrich, St. Louis, MO, USA now: Merck, Kenilworth, NJ, USA
Gene ruler (Fermentas)	Thermo Fisher Scientific, Waltham, MA, USA
Glycerin	AppliChem, Darmstadt, Germany
HEPES (PAA)	GE Healthcare, Chalfont St Giles, UK
Ionomycin	Diagonal, Münster, Germany
Isopropanol	Diagonal, Münster, Germany
L-Glutamine (PAA)	GE Healthcare, Chalfont St Giles, UK
H <sub>2</sub> O	AppliChem, Darmstadt, Germany
Orange G	Sigma-Aldrich, St. Louis, MO, USA now: Merck, Kenilworth, NJ, USA

## C Material and Methods

OVA <sub>257-264</sub>	Peptides & Elephants, Potsdam, Germany
Paraformaldehyde	Diagonal, Münster, Germany
PCR Buffer	Peqlab, Erlangen, Germany
PCR Enhancer	Peqlab, Erlangen, Germany
Perm Buffer III BD Phosphoflow	BD, Franklin Lakes, NJ, USA
PMA	Diagonal, Münster, Germany
Proteinase K	Diagonal, Münster, Germany
Pyronin Y	Sigma-Aldrich, St. Louis, MO, USA now Merck, Kenilworth, NJ, USA
Quarfloxin	Hölzel Diagnostika GmbH, Köln, Germany
RBC Lysis Buffer	Biolegend, San Diego, CA, USA
RPMI 1640 + GlutaMAX Supplement	Life Technologies, Carlsbad, CA, USA
RPMI 1640 Methionin-free	Life Technologies, Carlsbad, CA, USA
Streptavidin (APC-Cy7, PE)	Biolegend, San Diego, CA, USA
Taq polymerase	Peqlab, Erlangen, Germany
Tigecyclin	Sigma-Aldrich, St. Louis, MO, USA now: Merck, Kenilworth, NJ, USA
Torin 1	Hölzel Diagnostika GmbH, Köln, Germany
TRIS	AppliChem, Darmstadt, Germany
Triton X-100 (Fluka)	Sigma-Aldrich, St. Louis, MO, USA now: Merck, Kenilworth, NJ, USA
Trizol LS reagent	Life Technologies, Carlsbad, CA, USA
Trypan Blue	Carl Roth, Arlesheim, Switzerland
Volvic, Water	Danone Waters, Frankfurt, Germany

---

### 1.2 Buffers and Media

#### **Agarosegel (1%)**

---

Agarose	1.5 g
TAE (1x)	150 mL

---

#### **Ethidiumbromid**

---

H <sub>2</sub> O	7,44 mL
Ethidiumbromid (1%)	650 µL

---

#### **Cell Transfer Buffer**

---

DMEM	
HEPES	10mM

---

#### **CFSE/CTV staining medium**

---

## C Material and Methods

---

PBS (1x)	
BSA	0.1%

---

### **DMEM (pH 7.0)**

---

H <sub>2</sub> O	add up to 1 L
DMEM (w/v)	
Natriumhydrogencarbonat	3.7 g
HEPES	10 mL
BSA	50 mL out of 20%

---

### **Doxycyclin (20 mg/mL)**

---

H <sub>2</sub> O (Volvic)	add up to 50 mL
Doxycyclin	1 g

---

### **FACS-Medium**

---

DMEM	
HEPES	10 mM
BSA (w/v)	1%

---

### **GeneRuler**

---

Marker	100 µL
1x TAE	700 µL
Loading buffer (6x)	200 µL

---

### **DNA isolation buffer (10x)**

---

H <sub>2</sub> O	
TRIS, pH 8,8	670 mM
(NH <sub>4</sub> ) <sub>2</sub> SO <sub>4</sub>	166 mM
MgCl <sub>2</sub>	65 mM
Gelatin	0.1%

---

### **Loading Buffer (6x)**

---

Orange G	250 mg
Glycerin (30%)	30 mL
H <sub>2</sub> O	70 mL

---

### **MACS Buffer**

---

PBS (1x)	
BSA (w/v)	0.5%
EDTA	1mM

---

### **Paraformaldehyde pH 7.4 (4%)**

---

H <sub>2</sub> O	add up to 100 mL
Paraformaldehyde	4g
PBS (10x)	10 mL

---

### **PCR Mastermix**

---

H <sub>2</sub> O	
PCR Buffer	1x
PCR Enhancer	0.5x

---

## C Material and Methods

Oligonucleotide 1	0.5 $\mu$ M
Oligonucleotide 2	0.5 $\mu$ M
dNTPs	0.2 mM
Taq polymerase	0.026 U/ $\mu$ L

### **PBS (1x)**

H <sub>2</sub> O	add up to 1 L
PBS (10x)	100 mL

### **PBS (10x)**

H <sub>2</sub> O	add up to 1 L
NaCl	90 g
Na <sub>2</sub> HPO <sub>4</sub> ·2H <sub>2</sub> O	14.33 g
KH <sub>2</sub> PO <sub>4</sub>	2.17 g

### **TAE (1x)**

H <sub>2</sub> O	add up to 1 L
TAE (50x)	20 mL

### **TAE (50x)**

H <sub>2</sub> O	add up to 1 L
TRIS Base	242 g
Acetic acid (99%)	57.1 mL
EDTA, pH8 (0.5 M)	100 mL

### **Tissue digestion buffer**

H <sub>2</sub> O	
DNA isolation buffer	1x
Triton-X-100	0.5%
Proteinase K	0.3 mg/mL

### **TE**

H <sub>2</sub> O	
TRIS, pH 7,6	10mM
EDTA	1mM

### **T cell medium / RPMI Full**

RPMI 1680 GlutaMAX	
FCS (w/v) heat inactivated	0.1%
Antibiotic/Antimycotic (100x)	1x
2-Mercaptoethanol	5 $\mu$ M

### **Trypan Blue Solution (10x)**

PBS	
Trypan Blue (w/v)	0.05%

## C Material and Methods

### 1.3 Oligonucleotides

Oligonucleotides for mice genotyping were purchased from Eurofins MWG Operon, Ebersberg, Germany.

Target	Primer name	Sequences (5' - 3')
OT-I	RO459	CAGCAGCAGGTGAGACAAAGT
	RO460	GGCTTTATAATTAGCTTGGTCC
CD45.1	RO489	CATGGGGTTTAGATGCAGGA
	RO490	GCAAGGCAGGATGCTAGAAA
CD45.2	RO484	GAGCCTGTATCTAAACCTGAGT
	RO487	GGCAACATGCCCTTAACT
Ii-rTA	RO281	GTCTCAGAAGTGGGGGCATA
	RO282	GGACAGGCATCATACCCACT
TIM	RO235	CTCATCTCAAACAAGAGCCA
	RO236	CACTGCTTACTTCCTGTACC
TSO	RO267	TGTAAGCTCTTGGGGAATGG
	RO268	TGGAGGGTGTCCGAATAGAC
KRAB	RO405	GAGTGGAAGCTGCTGGACAC
	RO406	CAGGATGGGTCTCTTGGTGA
Raptor	RO291	ATGGTAGCAGGCACACTCTTCATG
	RO292	GCTAAACATTCAGTCCCTAATC
Rictor	RO293	TTATTAAGTGTGTGTGGGTTG
	RO294	CGTCTTAGTGTTGCTGTCTAG
CD4-cre	RO289	TGTGGCTGATGATCCGAATA
	RO290	GCTTGCATGATCTCCGGTAT
NR4	RO445	CGGGTCAGAAAGAATGGTGT
	RO446	CAGTTTCAGTCCCCATCCTC
R26	RO599	AAGACCGCAAGAGTTTGTC
	RO600	AAAGTCGCTCTGAGTTGTTAT
	RO601	GGAGCGGGAGAAATGGATATG

## C Material and Methods

### 1.4 Antibodies

specificity	conjugate	species	Isotype	Clone	Company
CD3	purified	arm. hamster	IgG1	145-2C11	BioXcell, West Lebanon, NH, USA
CD4	bio	rat	IgG2a, κ	RM4-5	Biologend, San Diego, CA, USA
CD4	PE	rat	IgG2a, κ	RM4-5	eBioscience, San Diego, CA, USA now: Thermo Fischer Scientific, Waltham, MA, USA
CD4	Al647	rat	IgG2b, κ	Gk1.5	eBioscience, San Diego, CA, USA now: Thermo Fischer Scientific, Waltham, MA, USA
CD4	Al647	rat	IgG2a, κ	RM4-5	Biologend, San Diego, CA, USA
CD8a	Al647	rat	IgG2a, κ	53-6.7	Biologend, San Diego, CA, USA
CD8a	PerCP	rat	IgG2a, κ	53-6.7	Biologend, San Diego, CA, USA
CD8a	bio	rat	IgG2a, κ	53-6.7	Biologend, San Diego, CA, USA
CD11b	bio	rat	IgG2b, κ	M1/70	Biologend, San Diego, CA, USA
CD11c	bio	arm. hamster	IgG	N418	Biologend, San Diego, CA, USA
CD16/32 (Fc-block)	purified	rat	IgG2a, λ	93	eBioscience, San Diego, CA, USA now: Thermo Fischer Scientific, Waltham, MA, USA
CD28	purified	syrian hamster	IgG2	37.51	BioXcell, West Lebanon, NH, USA
CD40	purified	rat	IgG2a	FGK4.5	BioXcell, West Lebanon, NH, USA
CD44	PE-Cy7	rat	IgG2b, κ	IM7	eBioscience, San Diego, CA, USA now: Thermo Fischer Scientific, Waltham, MA, USA
CD45.1	PE-Cy7	mouse	IgG2a, κ	A20	Biologend, San Diego, CA, USA
CD45.1	PerCP/Cy5.5	mouse	IgG2a, κ	A20	Biologend, San Diego, CA, USA
CD45.2	APC	mouse	IgG2a, κ	104	Biologend, San Diego, CA, USA
CD45R	bio	rat	IgG2a, κ	RA3-6B2	Biologend, San Diego, CA, USA
CD49b	bio	rat	IgM, κ	DX5	Biologend, San Diego, CA, USA
CD62L	PE	rat	IgG2a, κ	MEL-14	Biologend, San Diego, CA, USA
CD69	PE	arm. Hamster	IgG	H1.2F3	Biologend, San Diego, CA, USA
CD73	PE	rat	IgG1, κ	TY/11.8	Biologend, San Diego, CA, USA

## C Material and Methods

CD71	PE	rat	IgG2a, κ	RI7217	Biolegend, San Diego, CA, USA
CD90.1	Al647	mouse	IgG1, κ	OX-7	Biolegend, San Diego, CA, USA
CD127	PE	rat	IgG2a, κ	A7R34	eBioscience, San Diego, CA, USA now: Thermo Fischer Scientific, Waltham, MA, USA
CD183 (CXCR3) CD279 (PD-1)	PE	arm. Hamster	IgG	CXCR3-173	Biolegend, San Diego, CA, USA
Histone H3-P (Ser28)	Al488	rat	IgG2a, κ	HTA28	Biolegend, San Diego, CA, USA
IFN $\gamma$	APC	rat	IgG1, κ	XMG1.2	eBioscience, San Diego, CA, USA now: Thermo Fischer Scientific, Waltham, MA, USA
Isotype control	Al488	rat	IgG2a, κ	RTK2758	Biolegend, San Diego, CA, USA
Isotype control	Al488	rabbit	IgG	DA1E	eBioscience, San Diego, CA, USA now: Thermo Fischer Scientific, Waltham, MA, USA
Ly6C	FITC	rat	IgM, κ	AL-21	eBioscience, San Diego, CA, USA now: Thermo Fischer Scientific, Waltham, MA, USA
LY6G/LY6C (GR-1)	bio	rat	IgG2b, κ	RB6-85C	Biolegend, San Diego, CA, USA
p-S6	Al488	rabbit	IgG	2F9	eBioscience, San Diego, CA, USA now: Thermo Fischer Scientific, Waltham, MA, USA
phospho-Rb (pS807/pS811)	Al488	mouse	IgG2a, κ	J112-9060	eBioscience, San Diego, CA, USA now: Thermo Fischer Scientific, Waltham, MA, USA
Streptavidin	Pe				eBioscience, San Diego, CA, USA now: Thermo Fischer Scientific, Waltham, MA, USA
Ter119	bio	rat	IgG2b, κ	TER-119	Biolegend, San Diego, CA, USA
TNF $\alpha$	FITC	rat	IgG1, κ	MP6-XT22	Biolegend, San Diego, CA, USA
V $\alpha$ 2	FITC	rat	IgG2a, $\lambda$	B20.1	Biolegend, San Diego, CA, USA
V $\beta$ 3	FITC	arm. hamster	IgG2, κ	Kj25	Benoist, Mathis

### 1.5 Cytokines

rhIL-2 PeproTech, Rocky Hill, NJ, USA

rmIL-7 Immunotools, Friesoythe, Germany

## C Material and Methods

### 1.6 Enzymes

---

Proteinase K	Diagonal, Münster, Germany
Peg Gold Taq DNA Polymerase	Peqlab, Erlangen, Germany
RNase A	Thermo Fischer Scientific, Waltham, MA, USA

---

### 1.7 Peptides

---

Q4H7 SIIQFEHL peptides & elephants GmbH, Hennigsdorf, Germany
---

---

### 1.7 Consumables

---

Casy cups	Roche, Basel, Switzerland
Cell culture plate, 96-well round bottom	Sarstedt, Nümbrecht, Germany
Cell strainer (100 µm, sterile)	BD, Franklin Lakes, NJ, USA
Cover slides (glass)	Diagonal, Münster, Germany
Dissecting scissors	WPI-Europe, Hertfordshire, UK
Ear punch, 10 cm, 2 mm diameter	WPI-Europe, Hertfordshire, UK
Cannulas 23G blue	Carl Roth, Arlesheim, Switzerland
FACS tubes	Sarstedt, Nümbrecht, Germany
Filter tips OneTip, 1-10ul	Starlab, Hamburg, Germany
Filter tips OneTip, 2-20ul	Starlab, Hamburg, Germany
Filter tips, 1000 µL	Diagonal, Münster, Germany
Glaspipette 5 mL	Diagonal, Münster, Germany
Gloves Small	Diagonal, Münster, Germany
Insulin syringes 0.5 mL 0.30 x 8 mm	Diagonal, Münster, Germany
Insulin syringes 1 mL 0.33(29G) x 12.7 mm	Diagonal, Münster, Germany
MACS LS columns	Miltenyi, Bergisch-Gladbach, Germany
Microfine Syringes	BD, Franklin Lakes, NJ, USA
Omnifix 20 mL syringes	Diagonal, Münster, Germany
Operating scissors	WPI-Europe, Hertfordshire, UK
PCR reaction tubes stripes	Diagonal, Münster, Germany
PCR-plates, 96-well	Diagonal, Münster, Germany
Petri dish 60 mm x 15 mm	Diagonal, Münster, Germany
Pipette tips 20-200 µL, yellow	Brand, Wertheim, Germany
Pipette tips 50-1000 µL, blue	Brand, Wertheim, Germany

## C Material and Methods

Polyamide-mesh, pore size 150 µm and 89 µm	RCT, Heidelberg, Germany
Reaction tube rack	Carl Roth, Arlesheim, Switzerland
Reaction tubes round-bottom 4 mL and 14 mL	BD, Franklin Lakes, NJ, USA
Reaction tubes Safeseal 1.5 mL	Sarstedt, Nümbrecht, Germany
Reaction tube 50 mL	Greiner, Kremsmünster, Austria
Rotilabo-Abdeckfolien für PCR-Platten	Carl Roth, Arlesheim, Switzerland
Serological pipettes (5mL, 10 mL, 25 mL)	Sarstedt, Nümbrecht, Germany
Steril filter Millex-GP 0.22 µm	Diagonal, Münster, Germany
Synrignes 1 mL Omnifix	Diagonal, Münster, Germany
TPP Bottle-Top-Filter 500 mL, 0.22 µm	Sigma-Aldrich, St. Louis, MO, USA now: Merck, Kenilworth, NJ, USA

---

### 1.8 Kits

---

CFDA-SE Cell Tracer Kit	USA Invitrogen, Carlsbad, CA, USA
CTV Cell Tracer Kit	USA Invitrogen, Carlsbad, CA, USA
Click-iT HPG	Thermo Fischer Scientific, Waltham, MA, USA

---

### 1.9 Laboratory Equipment

---

BD FACSAriaIII	BD, Franklin Lakes, NJ
BD FACSCalibur	BD, Franklin Lakes, NJ
BD FACSCantoll	BD, Franklin Lakes, NJ
Casy Counter	Innovatis/OLS OMNI Life Science GmbH & Co. KG, Bremen, Germany
Centrifuge 5417R	Eppendorf, Hamburg, Germany
Centrifuge 5424	Eppendorf, Hamburg, Germany
Centrifuge Rotanata 460R	Hettich, Tuttlingen, Germany
Electrophoresis Power supply (EPS200)	Pharmacia Biotech, Upsalla, Sweden
Fridge, Freezer	Liebherr, Bulle, Switzerland
GelDoc XR+	BioRad, Hercules, CA, USA
Heatblock Thermomixer 5436	Eppendorf, Hamburg, Germany
Ice machine	Scotsman, Radevormwald, Germany
Incubator	Heracus, Hanau, Germany

## C Material and Methods

Incubator FlowSafe B-[MaxPro]2-190	Berner International GmbH, Elmshorn, Germany
Laminar airflow cabinet HeraSafe	Heraeus, Hanau, Germany
Microscope Labovert FS	Leitz, Wetzlar, Germany
Microscope Leica	Leica Microsystems GmbH, Wetzlar, Germany
Microwave	DAEWOO, Seoul, South Korea
Multifuge X3R	Heraeus, Hanau, Germany
Pipette	Brand, Wertheim, Germany
Pipette 0.2 - 2 $\mu$ L	Eppendorf, Hamburg, Germany
Pipette 8-channel, 0,1-10 $\mu$ L	Eppendorf, Hamburg, Germany
Pipette, 12-channel, 20-200 $\mu$ L	Brand, Wertheim, Germany
Pipettes	Brand, Wertheim, Germany
Thermocycler T1	Biometra, Göttingen, Germany
Thermocycler TADVANCED	Biometra, Göttingen, Germany
Vortex Genie 2	Bender & Hobein AG, Zurich, Switzerland
Water bath	Lauda, Lauda-Köningshofen, Germany

---

### 1.10 Software

---

BD cell quest	BD, Franklin Lakes, NJ, USA
Graph Pad Prism 5.0c and 7.0d for Mac	GraphPad, La Jolla, CA, USA
MS Office for Mac	Microsoft, Redmont, WA, USA
FACSDiva	BD, Franklin Lakes, NJ, USA
FlowJo 8.8.7 for Mac	Treestar Ashland, OR, USA

---

## C Material and Methods

### 2 Methods

#### 2.1. Mice

Mice were bred and maintained at the animal facility of the Institute for Immunology, Ludwig-Maximilians-University Munich in Munich, Germany. All experiments were performed in compliance with German federal guidelines.

Line Name	Official Line Name	Background	MHC	Source	Reference
AND x 45.1	Tg(TcrAND)53Hed; Ptpca	B10.BR/lfl	H-2 <sup>k</sup>	CB, DM	(Kaye et al., 1989)
AND x 90.1	Tg(TcrAND)53Hed; Thy1a	B10.BR/lfl	H-2 <sup>k</sup>	CB, DM	(Kaye et al., 1989)
AND x NR4	Tg(TcrAND)53Hed; Tg(Nr4a1-EGFP/cre)820Khog	B10.BR/lfl	H-2 <sup>k</sup>	The Jackson Laboratory	(Moran et al., 2011)
AND T-Rptor <sup>-/-</sup>	Tg(TcrAND)53Hed Tg(Cd4-cre)1Cwi; Rptortm1.1Dmsa	B10.BR/Jax	H-2 <sup>k</sup>	The Jackson Laboratory	(Lee et al., 2001; Sengupta et al., 2010)
B10.BR/Jax	B10.BR-H2k; H2- T18a/SgSnJ 5045	B10.BR/Jax	H-2 <sup>k</sup>	The Jackson Laboratory	(Stimpfling & Richardson, 1965)
B6	C57BL/6	C57BL/6	H-2 <sup>b</sup>	The Jackson Laboratory	
Bm1	H-2K <sup>bm1</sup>	C57BL/6	H-2 <sup>bm1</sup>	Veit Buchholz	(McKenzie et al., 1977)
Bm12	H2-Ab1 <sup>bm12</sup>	B6KhEgJ	H-2 <sup>bm12</sup>	The Jackson Laboratory	(McKenzie et al., 1979)
iMCC	li-rTAxTIM. Tg(Cd74- rtTA)#Doi; Tg(tetO- Cd74/MCC)#Doi	B10.BR/lfl	H-2 <sup>k</sup>	CBDM	(Obst et al., 2005; van Santen et al., 2004)
iOVA	Tg(tetO- Cd74/MCC)#Doi; Tg(TetO-OVA)7Obst	C57BL/6	H-2 <sup>b</sup>	Reinhard Obst	(Rabenstein et al., 2014)
iOVA-KRAB	Tg(Cd74rtTA)#Doi;Tg (TetO- OVA)7Obst;CD11c- DTR; HPGKtTR- KRAB	C57BL/6	H-2 <sup>b</sup>	Reinhard Obst	(Barde et al., 2009; Rabenstein et al., 2014)
OT-I x 45.1	Tg(TcraTcrb)1100Mjb ; Ptpca	C57BL/6	H-2 <sup>b</sup>	Thomas Brocker	(Hogquist et al., 1994)
OT-I x 90.1	Tg(TcraTcrb)1100Mjb ; Thy1a	C57BL/6	H-2 <sup>b</sup>	Thomas Brocker	(Hogquist et al., 1994)
OT-I x NR4	Tg(TcraTcrb)1100Mjb ;Tg(Nr4a1-	C57BL/6	H-2 <sup>b</sup>	The Jackson	(Moran et al., 2011)

## C Material and Methods

	EGFP/cre)820Khog			Laboratory	
OT-I T-Rptor <sup>-/-</sup>	Tg(TcraTcrb)1100Mjb; Tg(Cd4-cre)1Cwi; Rptortm1.1Dmsa	C57BL/6	H-2 <sup>b</sup>	The Jackson Laboratory	(Lee et al., 2001; Sengupta et al., 2010)
R26-rtTA-M2 x KRAB	Gt(ROSA)26Sor <sup>tm1(rt1)</sup> A <sup>M2</sup> Jae; HPGKtTR-KRAB	C57BL/6	H-2 <sup>b</sup>	Vigo Heissmeyer	(Barde et al., 2009; Hochedlinger et al., 2005)
RAG <sup>-/-</sup>	Rag1 <sup>tm1Mom</sup>	C57BL/6	H-2 <sup>b</sup>	Thomas Brocker	(Mombaerts et al., 1992)
T-Rictor <sup>-/-</sup>	Tg(Cd4-cre)1Cwi; Rictortm1.1Klg	C57BL/6	H-2 <sup>b</sup>	The Jackson Laboratory	(Lee et al., 2001; Tang et al., 2012)
T-Rptor <sup>-/-</sup>	Tg(Cd4-cre)1Cwi; Rptortm1.1Dmsa	C57BL/6	H-2 <sup>b</sup>	The Jackson Laboratory	(Lee et al., 2001; Sengupta et al., 2010)

### 2.1.1 Wildtype mice

Wildtype C57/Bl6 (H-2<sup>b</sup>) and B10.Br/Jax (H-2<sup>k</sup>) mice were both originally obtained from The Jackson Laboratory and bred in the mouse facility of the Institute for Immunology, LMU Munich.

### 2.1.2 Congenic marker

In order to identify adoptively transferred T cells, the congenic markers CD45.1 and CD90.1 were used. They originally derived from Ptprca and Thy1a mice, respectively. Ptprca and Thy1a mice were purchased from The Jackson Laboratory.

### 2.1.3 TCR transgenic mice

AND TCR transgenic mice (Tg(TcrAND)53Hed Tg(Cd4-cre)1Cwi2.1.4) were received from Diane Mathis and Christophe Benoist (Harvard Medical School, Boston, MA, USA). The TCR of AND T cells predominantly consists of the V $\alpha$ 11 (clone: AN6.2) and V $\beta$ 3 chain (clone: 5C.C7) and recognizes a peptide, derived from moth cytochrome c (MCC<sub>93-103</sub>) in the context of H-2E<sup>k</sup>.

OT-I TCR transgenic mice (Tg(TcraTcrb)1100Mjb) were received from Thomas Brocker (Ludwig-Maximilians-University Munich, Munich, Germany). The TCR of OT-I T cells predominantly consists of the V $\alpha$ 2 and V $\beta$ 5 chain (clone: 149.42) and recognize a peptide derived from chicken ovalbumin (OVA<sub>257-264</sub> /SIINFEKL) in the context of H-2K<sup>b</sup>. TCR transgenic animals were crossed with mice expressing the congenic marker CD45.1 or CD90.1.

## C Material and Methods

### 2.1.4 TCR signaling reporter mice

To visualize early TCR activity, a mouse strain was used, carrying a BAC-transgene consisting of a Nur77-GFP reporter cassette (Tg(Nr4a1-EGFP/cre)<sup>820Khog</sup>). Mice were purchased from The Jackson Laboratory. The expression of Nur77-GFP was measured by flow cytometry and is described to be upregulated within hours upon TCR stimulation, correlating with the strength of the TCR stimulus. It remains high up to two days post-antigen-pulse *in vitro* (Moran *et al.*, 2011).

Transgenic mice were crossed with AND and OT-I mice carrying the congenic markers CD90.1 and CD45.1 on H-2<sup>k</sup> or H-2<sup>b</sup> background, respectively.

### 2.1.5 T cell specific mTORC1/2- deficient mice

T cell specific mTORC1 (Tg(Cd4-cre)<sup>1Cwi</sup>; Rptortm1.1Dmsa)- and mTORC2 (Tg(Cd4-cre)<sup>1Cwi</sup>; Rictortm1.1Klg)-deficient mice were purchased from the Jackson Laboratory and bred on B6 background. The Mouse Genome Informatics database gives this detail: “Cre recombinase is expressed under the control of mouse Cd4 regulatory elements. The Cd4 enhancer, promoter and silencer collectively drive expression at sequential stages specifically of CD4<sup>+</sup> T cell development.”<sup>1</sup> For mTORC1-deficient T cells, the Mouse Genome Informatics database reports: “Exon 6 was flanked by 5' and 3' LoxP sites located 111 bp upstream and 547 bp downstream, respectively, and an FRT flanked neo cassette was inserted via homologous recombination. The neo cassette was removed by flp mediated recombination.”<sup>2</sup> For mTORC2-deficient mice, the Mouse Genome Informatics database describes: “A targeting vector was designed to insert a loxP site followed by a frt-flanked neomycin resistance (neo) cassette upstream of exon 11, and a second loxP site downstream of exon 11. Flp-mediated recombination removed the neo cassette and left exon 11 floxed.”<sup>3</sup>

Both mice were crossed with OT-I and AND mice carrying the congenic marker CD45.1 on H-2<sup>b</sup> and H-2<sup>k</sup> background, respectively.

### 2.1.6 Bm1 and Bm12 mice

Bm1 mice were received from Dr. Veit Buchholz (Technical University Munich, Munich, Germany). The Mouse Genome Informatics database gives this detail: “The bm1 mutation contains 7 nucleotide differences resulting in amino acid substitutions at codon 152 (glutamate to alanine), codon 155 (arginine to tyrosine) and codon 156

---

<sup>1</sup> <http://www.informatics.jax.org/allele/key/8393>; retrieved on 23.11.2018

<sup>2</sup> <http://www.informatics.jax.org/allele/key/636375>; retrieved on 23.11.2018

<sup>3</sup> <http://www.informatics.jax.org/allele/key/822979>; retrieved on 23.11.2018

## C Material and Methods

(leucine to tyrosine)<sup>4</sup>, thus binding and presenting a different repertoire of self-peptides in the context of MHC-I.

Bm12 mice were purchased from The Jackson Laboratory. The Mouse Genome Informatics database gives this detail: “Three non-consecutive nucleotide changes occurred, resulting in three amino acid substitutions in the beta1 exon. The amino acid changes consist of codon 67 (isoleucine to phenylalanine), codon 70 (arginine to glutamine) and codon 71 (threonine to lysine). These changes were likely the product of gene conversion of H2-Ab1<sup>b</sup> with sequence from H2-Eb<sup>b</sup>.”<sup>5</sup> Hence, Bm12 mice bind and present a different repertoire of self-peptides in the context of MHC-II.

### 2.1.7 RAG-deficient mice

RAG-deficient mice were kindly provided by Thomas Brocker (Ludwig-Maximilians-University Munich, Munich, Germany). The recombination activation gene 1 (RAG1) is essential for the V(D)J recombination in B and T cells. RAG1-deficient mice have small lymphoid organs and no mature B and T cells. In these mice a neomycin cassette replaced a 1356 bp genomic fragment of the Rag1 gene, encoding the nuclear localization signal and the zinc-finger motif.

Upon adoptive transfer, T cells start to vigorously proliferate in these lymphopenic mice.

### 2.1.8 Double-transgenic mice

iMCC double-transgenic (dtg) mice (li-rTAxTIM. Tg(Cd74-rtTA)#Doi; Tg(tetO-Cd74/MCC)#Doi) were provided from Diane Mathis and Christophe Benoist (Harvard Medical School, Boston, MA, USA). li-rTA mice were crossed with mice carrying the tetracycline inducible invariant chain in cooperation with MCC<sub>92-103</sub> (TIM) in MHC-II positive cells. Mice were bred on the B10.BR background.

iOVA dtg mice (Tg(TetO-OVA)7Obst) were generated by crossing li-rTA mice with mice carrying a tetracycline regulated signal sequence in cooperation with OVA<sub>257-264</sub> (TSO) in MHC-II positive cells in the laboratory of Reinhard Obst (Ludwig-Maximilians-University Munich, Munich, Germany). Mice were bred on the C57/Bl6 Background.

Both recipient mice carry a transgene for the improved S2 mutant of the reverse tet-activator under the control of the invariant chain (li) promoter and the H-2Ea enhancer element from the pDOI-6 transgene expression vector. The S2 mutant consists of a tetracycline binding domain and a transactivator (Urlinger *et al.*, 2000).

---

<sup>4</sup> <http://www.informatics.jax.org/allele/key/42193>; retrieved on 23.11.2018

<sup>5</sup> <http://www.informatics.jax.org/allele/key/39181>; retrieved on 23.11.2018

## C Material and Methods

The expression is regulated via the invariant chain (Ii) promoter and the H-2E $\alpha$  enhancer element derived from pDOI-6 transgene expression vector.

In iMCC mice, the CLIP region of the Ii was replaced by MCC<sub>92-103</sub> and named TIM. The expression of TIM is under the control of the CMV<sub>core</sub> promoter and seven tet-operator (tetO) sequences. In addition the efficiency of the transgene expression was improved by an intron from rabbit  $\beta$ -globulin, which was inserted downstream of the transcription start site.

In iOVA mice, the TSO transgene encodes a minigene combination of the OVA<sub>257-264</sub> and the H2-K<sup>b</sup> signal sequence, which mediates a translation into the endoplasmatic reticulum. This fusion is followed by two stop codons and the human growth hormone splice substrate required for efficient expression. The expression of the cognate antigen of OT-I is independent of proteasomal processing and TAP-transport and under the control of an improved tetracycline response element in which an interferon response element was removed from the spacers separating the seven tetO sequences. In addition the spacer region was shortened so that the tetO sequences were separated by 3.5 instead of 4 helical turns, which enabled the transactivator molecule to alternatively bind on opposite sites of the DNA. Furthermore, an enhancer element was removed from the CMV<sub>core</sub> promoter.

In iMCC mice MCC<sub>93-103</sub> is expressed on MHC-II upon doxycycline treatment, iOVA mice express OVA<sub>257-264</sub> on MHC-I, thus presenting cognate antigen to AND and OT-I T cell, respectively.

iOVA mice were crossed to transgenic mice expressing the tetracycline-dependent transrepressor KRAB, generating iOVA-KRAB mice. KRAB is a fusion protein that consists of the DNA binding domain of the tetracycline repressor from *E. coli* and the Krüppel-associated box (KRAB) domain of the human Kox1 zinc finger protein (Deuschle *et al.*, 1995). It is expressed under the human phosphoglycerate kinase promoter and constitutively active in the absence of doxycycline (Barde *et al.*, 2009). KRAB domains recruit histone deacetylases and histone methyltransferases and thus mediate a reversible transcriptional repression of target genes (Groner *et al.*, 2010; Margolin *et al.*, 1994). If bound to doxycycline, the tetracycline-dependent transrepressor will be inactivated and in turn the transactivator can bind and induce the expression of OVA<sub>257-264</sub> on MHC-I.

### 2.1.9 R26-rtTA-M2 mice

The Rosa26 locus is ubiquitously expressed. The Mouse Genome Informatics database gives this detail: " An optimized form of reverse tetracycline controlled

## C Material and Methods

transactivator (rtTA-M2) was inserted downstream of the Gt(ROSA)26Sor promoter and was followed by a PGK-puro selection cassette. This mutant form of rtTA termed M2 has five amino acid substitutions in the tetR moiety of tTA: S12G, E19G, A56P, D148E and H179R. This mutated form of transactivator protein has increased doxycycline sensitivity. Mice have widespread expression of the rtTA-M2 protein.<sup>6</sup> R26-rtTA-M2 mice were crossed to KRAB expressing mice.

### 2.2 Mice Typing

#### 2.2.1 Tissue digestion

DNA was harvested from the tail tip. The tissue was digested in 100 µl tissue digestion buffer for 7 hours at 56°C, followed by 10 minutes at 90°C for protein denaturation. The lysate was diluted 1:10 in dH<sub>2</sub>O for PCR.

#### 2.2.2 Polymerase Chain Reaction

DNA from digested tissue samples (1 µL) was mixed with 24 µL of the master mix described below. DNA was initially denaturated for 5 minutes at 95 °C followed by 35 cycles of denaturation (30 seconds at 95 °C), primer annealing (45 seconds at 55 °C) and DNA elongation (45 seconds at 72 °C). A final elongation period for 5 minutes at 72 °C and a cooling period for 10 seconds at 20 °C was added.

#### PCR master mix

---

PCR H <sub>2</sub> O	
PCR Buffer	1x
PCR Enhancer	0.5x
Oligonucleotide 1	0.5 µM
Oligonucleotide 2	0.5 µM
dNTPs	0.2 mM
Taq polymerase	0.026 U/µL

---

#### 2.2.3 Gel electrophoresis

For size separation of PCR products, a 1% agarose gel (in 1xTAE buffer with 0.005% ethidiumbromide) with a 100 bp ladder marker was used. The PCR products were loaded on the gel with loading buffer in a 1:5 ratio. The electrophoresis was performed at 120 Volt in a horizontal gel chamber for 25 minutes. The results were visualized in a gel documentation system using a UV light source.

---

<sup>6</sup> <http://www.informatics.jax.org/allele/key/52600>; retrieved on 22.11.2018

## C Material and Methods

### 2.3 Cell extraction from mouse organs

Mice were sacrificed by CO<sub>2</sub> exposure in accordance with the German Protection of Animals Act. Spleen and lymph nodes (axillary, inguinal, brachial and cervical or axillary, inguinal and brachial only from recipients of adoptively transferred T cells) were removed under non-sterile conditions and homogenized in FACS Medium either using a sterile cell strainer (150 µm) if intended for cell culture or adoptive T cell transfer or glass cover slides for flow cytometry analysis. In order to remove erythrocytes, splenocytes were centrifuged through a Ficoll cushion for 10 minutes at 2000 rpm/ 450 x g and brake set on 5 of 9. The interphase was collected. Single cell suspension was pelleted with 350 x g for 5 minutes and resuspended in FACS medium, 1xPBS or DMEM. Cell numbers were measured with the Casy Counter.

### 2.4 Intra peritoneal injection of anti-CD40

Mice were treated with 20 or 40 µg anti-CD40 in order to stabilize antigen presentation on APCs to T cells. Sterile solutions of anti-CD40 in 1xPBS were prepared and injected intraperitoneally with a maximum of 100 µL per mouse.

### 2.5 CFSE/CTV labeling of naïve T cells

A stock of 5 mM CTV or CFSE was used to assess cell proliferation. Both dyes bind to proteins and thus get diluted in half with every cell division. The number of divisions can be calculated by following:  $N = \log_2(\text{CFSE MFI}_{\text{ctr}}/\text{CFSE MFI}_{\text{sample}})$ .

Cell labeling was performed with 20 million cells per mL in prewarmed CFSE/CTV labeling medium with 10 µM CFSE or CTV for naïve, not enriched cells and 5µM for Magnetic-Activated Cell Sorting purified cells, while gently vortexing. Cells were incubated for 10 minutes in a 37 °C warm water bath in the dark with an additional step of swirling after 5 minutes. Adding equal amounts of CFSE/CTV labeling medium blocked the reaction. 1-3 mL heat-inactivated FCS was underlayered to provide nutrients. Cells were centrifuged at 1500 rpm at 4°C for 5 minutes and washed twice with transfer medium if cells were used for adoptive transfer or FACS Medium if cells were cultured *in vitro*.

### 2.6 Adoptive T cell transfer

For *in vivo* stimulation assays, lymphocytes were harvested from lymph nodes (axillary, inguinal, brachial) in DMEM without BSA. Cells that were pre-stimulated *in vitro* before transfer were harvested from cell culture and washed with DMEM without BSA to remove remaining BSA from T cell medium. If indicated, cells were labeled with CFSE or CTV and transferred in a maximum of 100 µL DMEM without BSA intravenously.

## C Material and Methods

Cell numbers varied between  $0.1 \times 10^6$  and  $2 \times 10^6$  cells per mouse depending on the experimental setup.

### 2.7 Doxycycline treatment

Mice were treated with 100  $\mu\text{g}/\text{mL}$  doxycycline in water with low divalent cations (Volvic, Danone Waters, Frankfurt, Germany), if indicated.

### 2.8 Immunization

#### 2.8.1 Immunization with MVA-Ova

MVA-encoding OVA (MVA-OVA) SC126 5A 13-13 stock:  $9.09 \times 10^9$  TC ID<sub>50</sub>/mL (Bavarian Nordic GmbH, Planegg-Martinsried, Germany) was used to induce ovalbumin expression on myeloid dendritic cells to generate adoptively transferred effector (d8) and memory (d36) OT-I T cells.  $5 \times 10^7$  TC ID<sub>50</sub>/mL was injected intravenously in 100  $\mu\text{L}$  1xPBS per mouse on day one before adoptive transfer of TCR transgenic OT-I T cells.

#### 2.8.2 Immunization with MHV-68\_OVA

The murine gamma herpes virus 68\_OVA (MHV-68\_OVA) bacterial artificial chromosome (BAC) was generated in collaboration with Prof. Heiko Adler (Helmholtz Center for Environmental Health, Munich). The expression cassette of TSO (described in 2.1.8) was inserted into the MHV-68 genome between ORF27 and ORF29b at position 46347 (Supplementary figure 12). In the presence of the reverse tetracycline-transactivator (rtTA<sup>M2</sup>), OVA<sub>257-264</sub> expression can be induced on H2-K<sup>b</sup> in virus-infected cells.

For immunization, host mice were injected intravenously with  $2 \times 10^5$  PFU MHV-68\_OVA in 100  $\mu\text{L}$  1xPBS per mouse one day after adoptive transfer of TCR transgenic OT-I T cells.

### 2.9 Magnetic purification of CD4<sup>+</sup> and CD8<sup>+</sup> T cells

In order to purify CD4<sup>+</sup> or CD8<sup>+</sup> T cells, Magnetic-Activated Cell Sorting, a technique based on the usage of paramagnetic anti-biotin microbeads to separate cells labeled with biotinylated antibodies on a column placed in a strong magnetic field, was used. Single cell suspensions of lymph nodes and spleen were prepared as described in 2.3 and pooled before incubation with biotinylated mAb. Biotinylated mAb were added according to the following table in 200  $\mu\text{L}$  FACS medium per donor mouse.

## C Material and Methods

CD8 <sup>+</sup>	CD4 <sup>+</sup>		/mouse
CD4	CD8	T cells	8 $\mu$ l
CD45R	CD45R	B cells	8 $\mu$ l
CD49	CD49	NK cells	5 $\mu$ l
Gr-1	Gr-1	Granulocytes	5 $\mu$ l
CD11b	CD11b	Macrophages	5 $\mu$ l
CD11c	CD11c	DCs	5 $\mu$ l
TER119	TER119	Erythrocytes	5 $\mu$ l

Cells were incubated for 15 minutes on ice and washed three times in FACS medium at 1500 rpm for 5 minutes. The pellet was resuspended in 100  $\mu$ L FACS Medium per mouse, 10  $\mu$ L anti-biotin-beads were added. Cells were incubated for 20 minutes at 4°C (swirled after 10 minutes) and washed twice (first step with FACS Medium, second step with MACS buffer). For negative selection an LS column was placed in a magnetic field and equilibrated with 3 mL MACS buffer. Pellet was resuspended in 2 mL MACS buffer per mouse and loaded on the LS columns (maximum of cells from two mice per column). Columns were subsequently washed twice with 3 mL MACS buffer. The flow-through was collected. The obtained cells were centrifuged as indicated. The pellet was resuspended in FACS medium and cell number was measured with the Casy Counter.

For quality control an aliquot before and after purification was taken for flow cytometry analysis.

### 2.10 Stimulation with anti-CD3 and anti-CD28

In order to coat anti-CD3 and anti-CD28 to cell culture plates, 96-well U-bottom plates were incubated with 10  $\mu$ g/mL anti-CD3 and 10  $\mu$ g/mL anti-CD28 in 70  $\mu$ L 1xPBS per well for 2 hours at 37°C and 5% CO<sub>2</sub>. Subsequently, plates were washed twice with cold 1xPBS. MACS-purified cells (see 2.9) were adjusted to a concentration of 0.5 x 10<sup>6</sup> cells/mL in T cell medium, 5 ng/mL IL-7 was added and 10 ng/mL IL-2 if indicated. Cells were cultured in 200  $\mu$ L per well up to 3 days at 37°C and 5% CO<sub>2</sub>.

### 2.11 Stimulation with PMA and ionomycin

A single cell suspension from lymph node and spleen was generated as described in 2.3 and pooled for further treatment. 0.2 x 10<sup>6</sup> cells were transferred into a 96-well plate and stimulated in 200  $\mu$ L RPMI Full with 10 ng/mL PMA (for stimulation of protein

## C Material and Methods

kinase C) and 25 ng/mL Ionomycin (a  $\text{Ca}^{2+}$  - ionophore) for 20 minutes to 2 hours at 37°C and 5%  $\text{CO}_2$ .

### 2.12 Inhibitor treatment

Inhibitors were added with a start concentration as listed below. In twelve steps, inhibitors were serially diluted two-fold or four-fold ranging from 1:2 or 1:4 to 1:2048 or 1:42000000 for actinomycin D, respectively in 100  $\mu\text{l}$  RPMI Full Medium with drug-free medium as control. Cells were purified and stimulated as described in 2.9 and 2.10 with the exception that cells were adjusted to a concentration of  $1 \times 10^6$  cells/mL with IL-7 (10ng/mL). 100  $\mu\text{L}$  of the cell suspension were added to 100  $\mu\text{L}$  inhibitor solution, which lead to a final concentration of  $0.5 \times 10^6$  cells/mL and 5 ng/mL IL-7. Cells were incubated for 48 hours *in vitro* at 37°C and 5%  $\text{CO}_2$ .

Inhibitor	Target	Stock conc.	Start conc.	Dilution
Torin 1	mTORC1 and mTORC2	4 mM	1 $\mu\text{M}$	1:2
2-DG	Glycolysis	305 mM	2 mM	1:2
Actinomycin D	RNA Polymerase I and II	40 mM	4 $\mu\text{M}$	1:4
Quarflorin	RNA Polymerase I	16.5 mM	0.2 $\mu\text{M}$	1:2
Tigecyclin	Mitochondrial ribosomes	5.11 mM	40 $\mu\text{M}$	1:2

### 2.13 Cell preparation for flow cytometry

The flow cytometers BD FACSCalibur and FACSCanto II were used for data acquisitions and analysis was performed with FlowJo 8. In order to remove aggregates, antibody dilutions were centrifuged at 14000 rpm in 1.5 mL reaction tubes for 10 minutes at 4°C. Staining was performed in 96-well plates in the dark at 4°C for 20 minutes. Cells were washed once with FACS Medium and filtered through a mesh with a pore size of 80  $\mu\text{m}$  before analysis.

#### 2.13.1 Antibody staining

Staining and washing was performed in FACS Medium when DAPI or 1xPBS when fixable viability dye (FVD eFluor450, eFluor660, eFluor780) was used for dead cell discrimination. All antibodies were diluted 1:400, SA-conjugated fluorochromes and FVD 1:2000 and DAPI 1:1000.  $0.01-1 \times 10^6$  cells were washed and pelleted at 1500 rpm at 4°C for 3 minutes. The pellet was resuspended in 50  $\mu\text{L}$  antibody mix and incubated as indicated above.

## C Material and Methods

### **2.13.2 Fixation with 4% PFA**

In order to fix cells, T cells stained for extracellular markers as described in 2.13.1 were washed once with 1xPBS at 250xg and 4°C for 3 minutes and subsequently resuspended in 100 µL freshly thawed 4% paraformaldehyde. Cells were incubated for 10 minutes at room temperature protected from light. Subsequently, cells were washed twice with 1xPBS at 350 x g for 5 minutes and stored in 100 µL 1xPBS at 4°C in the dark or further treated as described in 2.13.3.

### **2.13.3 Permeabilization with Perm III Buffer**

Permeabilization of fixed cells was performed using Perm III Buffer (BD, Franklin Lakes, NJ, BD Phosphoflow). Cells were resuspended in 100 µL Perm III Buffer and incubated for 5 minutes at room temperature, followed by two washing steps with 1xPBS at 250xg for 5 minutes.

### **2.13.4 Intracellular antibody staining for phospho-proteins**

For intracellular staining of phosphorylated proteins, cells were stained for extracellular markers, fixed and permeabilized as described under 2.13.1 2.13.2 and 2.13.3. Before, intracellular antibody staining was performed, non-specific binding was prevented by anti-CD16/CD32 treatment in a dilution of 1:400 in 1xPBS for 15 minutes. Subsequently, cells were washed once in 1xPBS for 5 minutes at 350xg and resuspended in antibody mix containing anti-phospho antibodies diluted in 1x PBS. In addition antibodies, which have been used at the first staining step to discriminate extracellular markers were added to the solution.

<b>mAb</b>	<b>dilution</b>
pS6-AI488	1:100
H3P-AI488	1:10
pRb-AI488	1:50

### **2.13.5 RNA and DNA staining with Pyronin Y and DAPI**

To visualize nucleic acids, DAPI and Pyronin Y were used. While DAPI exclusively intercalates into DNA, Pyronin Y can stain both DNA and RNA. To guarantee a specific binding only to RNA, Pyronin Y was added after incubation with DAPI to block DNA binding sites. Both parameters were acquired on a linear scale.

Equivalent numbers of enriched CD4<sup>+</sup> and/or CD8<sup>+</sup> T cells (0.5 to 2 x 10<sup>6</sup> each) were treated together in the same well of a 96-well plate. The cells were washed twice and stained for intracellular markers and FVD as indicated in 2.13.1. After one washing

## C Material and Methods

step with 1x PBS at 1500 rpm and 4°C for 3 minutes, cells were fixed as described in 2.13.2. Cells were washed twice with 1xPBS at 250xg for 5 minutes at room temperature and could then be stored over night at 4°C. To continue, cells were permeabilized with Perm III Buffer (BD, Franklin Lakes, NJ, BD Phosphoflow™) for 5 minutes at room temperature, followed by two washing steps with 1xPBS as described in 2.13.3. DAPI (stock: 250 mg/mL) was added at a 1:1000 dilution in 100 µL 1xPBS per well for 10 minutes at room temperature in the dark. Subsequently Pyronin Y (stock: 1 mg/mL) was added in a 1:200 dilution (final dilution 1:400) in 100 µL 1xPBS for 10 minutes at room temperature. Cells were pelleted at 350xg for 5 minutes at room temperature and resuspended in FACS medium for analysis at BD FACSCanto II. DAPI has an excitation maximum at 350 nm and can be detected at 470nm. The excitation maximum of Pyronin Y lies at 546 nm and can be detected at 565 nm.

### **2.13.6 Intracellular cytokine staining**

The FoxP3 staining kit (eBioscience, San Diego, CA, USA) was used as indicated in the manufacturer's instructions for intracellular staining of transcription factors and cytokines. Before fixation and permeabilization, cells were stained with surface molecules and FVD in 1xPBS for at least 20 minutes on ice. After fixation in 100 µl Fix/Perm, cells were washed twice in 150 µl Perm/Wash per well (cells could now be stored at 4°C in Perm/Wash over night). Unspecific antibody binding was blocked by anti-CD16/CD32 Fc-receptor blockage in a 1:400 dilution for 15 minutes. Cells were washed and stained intracellular for at least 20 minutes in antibody dilutions as indicated below.

Specificity	Fluorochrome	Dilution
IFN $\gamma$	APC	1:400
TNF $\alpha$	Al488	1:100

### **2.13.7 Visualization of translational activity**

The Click-iT HPG Alexa Fluor Protein Synthesis Assay Kit was used, in order to monitor the translation of proteins at a defined time window of 30' post-stimulation for 48 hours. With this approach, the incorporation of the L-methionine analogue L-homopropargylglycine (L-HPG) containing an alkyne moiety was measured. The detection of the incorporated amino acid utilized a chemoselective ligation or click reaction between an azide and alkyne, where the alkyne-modified protein was detected with Alexa Fluor 488 azide.

## C Material and Methods

Cells were treated following the manufacturer's protocol.

Thus, all reagents were thawed and warmed to room temperature and Click-iT HPG reagent (Component A) was briefly centrifuged to maximize reagent recovery. Next a 10x stock solution of the Click-iT HPG reaction buffer additive was prepared by adding 2 mL of deionized water to Component E. Click-iT HPG reaction buffer was diluted 1:10 in deionized water to prepare a 1x solution.

Polyclonal T cells were purified and stimulated as described in 2.9 and 2.10. T cell Medium was removed and exchanged with 100  $\mu$ L/well L-Methionine free medium containing 50  $\mu$ M (1:1000 dilution) Component A. Cells were incubated for 30 minutes at 37°C and 5% CO<sub>2</sub> in the dark. After incubation, the medium containing Click-iT<sup>®</sup> HPG was removed and cells were washed twice with 1xPBS. CD4<sup>+</sup> and CD8<sup>+</sup> T cells were mixed and stained for CD8 (1:400) and viability with FVD780 (1:2000) in 1xPBS for 15 minutes on ice in the dark. Cells were washed once with 1xPBS. 1xPBS was removed and cells were fixed with 4% PFA for 10 minutes at room temperature in the dark. Cells were washed twice with 1xPBS and subsequently permeabilized with Perm Buffer III (methanol based permeabilization) at room temperature for 5 minutes in the dark. The Click-iT reaction cocktail was prepared according to the protocol provided by the company.

<b>Reaction Component</b>	<b>Amount needed (100 <math>\mu</math>L/well)</b>
1x Click-iT HPG reaction buffer	86 $\mu$ L
Copper [III] Sulfate [CuSO <sub>4</sub> ] (Component D)	4 $\mu$ L
Alexa Fluor 488 azide (Component B)	0.25 $\mu$ L
1x Click-iT HPG buffer additive (1:10 dilution of 10x Click-iT HPG buffer additive in deionized water)	10 $\mu$ L
Total volume	100 $\mu$ L

Cells were washed twice with 1xPBS. 1xPBS was removed and 100  $\mu$ L of the reaction cocktail were added. Cells were incubated for 30 minutes at room temperature protected from light. The reaction cocktail was removed and cells were washed once with Click-iT reaction rinse buffer (Component F). Rinse buffer was removed and cells were resuspended in 1xPBS and subsequently analyzed by flow cytometry with BD FACS Canto II.

## C Material and Methods

### 2.14 RNase digestion of fixed and permeabilized cells.

Cells were fixed and permeabilized as described in 2.13.2 and 2.13.3. RNase was added in 50  $\mu$ L 1xPBS with a concentration of 2 mg/mL (stock: 10 mg/mL). Cells were incubated for 30 minutes at 37°C in the heatblock. RNase was washed away twice with 1xPBS for 5 minutes at 350xg and subsequently stained as described in 2.13.5.

### 2.15 Total RNA Sequencing

#### 2.15.1 Cell sorting

Cells were treated as indicated in 2.9 and 2.10. In order to exclude apoptotic and dead cells from total RNA sequencing, between 1.5 and 4 x 10<sup>6</sup> cells were incubated in 300  $\mu$ L antibody solution containing MFG8-GFP in a 1:250 dilution and FVD780 in a 1:1000 dilution in 1x PBS. MFG8-GFP was kindly provided by Dr. Jan Kranich. Cells were incubated for 30 minutes and washed once with 1xPBS and resuspended in 1 mL 1xPBS. Cell sorting was performed on FACSAriaIII with a 70 micro nozzle, and a sheath pressure of 70 by Lisa Richter at the Core Facility for Flow Cytometry of the Biomedical Center LMU Munich. Gating strategy is monitored in Supplementary figure 5.

#### 2.15.2 Trizol treatment

Sorted cells were pelleted at 250xg for 3 minutes and resuspended in 250  $\mu$ L 1xPBS in a 1.5 mL reaction tube. 750  $\mu$ L Trizol-LS was added and the reaction tube was inverted 5 to 10 times. Cells were incubated for 1 minute at room temperature and subsequently stored at -80°C.

#### 2.15.3 RNA Preparation

Prepared samples were delivered to *vertis Biotechnologie AG* for total RNA sequencing.

Total RNA was isolated and purified using RNeasy columns (Qiagen), including DNase treatment. The total RNA preparations were examined by capillary electrophoresis using Shimadzu MultiNA microchip electrophoresis system and Qubit in order to discriminate 18/28S RNA and total RNA amounts, respectively.

#### 2.15.4 cDNA synthesis

RNA samples were first fragmented using ultrasound (4 pulses of 30 s each at 4°C). Then, an oligonucleotide adapter was ligated to the 3' end of the RNA molecules. First-strand cDNA synthesis was performed using M-MLV reverse transcriptase and the 3' adapter as primer. The first-strand cDNA was purified and the 5' Illumina TruSeq

## C Material and Methods

sequencing adapter was ligated to the 3' end of the antisense cDNA. The resulting cDNA was PCR-amplified to about 10-20 ng/ $\mu$ L using a high fidelity DNA polymerase. Cycle numbers are indicated in following table. The TruSeq barcode sequences, which are part of the 5' and 3' TruSeq sequencing adapters, are included. The cDNA was purified using the Agencourt AMPure XP kit (Beckman Coulter Genomics) and was analyzed by capillary electrophoresis.

<b>Sample no.</b>	<b>Barcode i5</b>	<b>Barcode i7</b>	<b>PCR cycles</b>
1	AGGCTATA	ATTACTCG	12
2	GCCTCTAT	ATTACTCG	12
3	AGGATAGG	ATTACTCG	13
4	TCAGAGCC	ATTACTCG	13
5	CTTCGCCT	ATTACTCG	12
6	TAAGATTA	ATTACTCG	12
7	ACGTCCTG	ATTACTCG	13
8	GTCAGTAC	ATTACTCG	12
9	ATAGAGAG	ATTACTCG	12
10	AGAGGATA	ATTACTCG	13
11	CTCCTTAC	ATTACTCG	12
12	TATGCAGT	ATTACTCG	13
13	TACTCCTT	ATTACTCG	12
14	AGGCTTAG	ATTACTCG	12
15	ATTAGACG	TCCGGAGA	12
16	CGGAGAGA	TCCGGAGA	13
25	CTAGTCGA	TCCGGAGA	14
26	CTTAATAG	TCCGGAGA	13
27	ATAGCCTT	TCCGGAGA	13
28	TAAGGCTC	TCCGGAGA	12
29	TCGCATAA	TCCGGAGA	15
30	AGTCTTCT	TCCGGAGA	13
31	CATTGCT	TCCGGAGA	14
32	TCTACTCT	TCCGGAGA	12
33	ATCCTGTG	TCCGGAGA	13
34	TACAGGTC	TCCGGAGA	13
35	AGTCCAAC	TCCGGAGA	13

## C Material and Methods

### 2.15.5 Pool generation and size fractionation

For Illumina NextSeq sequencing, the samples were pooled in approximately equimolar amounts. The cDNA pool was size fractionated in the size range of 150 - 500 bp using a preparative agarose gel. An aliquot of the size-fractionated pool was analyzed by capillary electrophoresis.

### 2.15.6 Description of the cDNA

The cDNAs have a size of about 150 – 500 bp. The 3' and 5' adapters and the primers used for PCR amplification were designed for small RNA sequencing according to the instructions of Illumina. The following adapter sequences flank the DNA insert:

TruSeq\_Sense\_primer i5 Barcode 5'-AATGATACGGCGACCACCGAGATCTACAC-  
NNNNNNNN-ACACTCTTCCCTACACGACGCTCTTCCGATCT-3'

TruSeq\_Antisense\_primer i7 Barcode 5'-CAAGCAGAAGACGGCATACGAGAT-NNNNNNNN-  
GTGACTGGAGTTCAGACGTGTGCTCTTCCGATCT-3'

The combined length of the flanking sequences is 136 bases.

### 2.15.7 Illumina sequencing

The cDNA pool was sequenced on an Illumina NextSeq 500 system using 75 bp read length.

Step 2.15.3 – 2.15.7 were performed by *vertis Biotechnologie AG*.

### 2.15.8 RNA sequencing analysis

Data generated in 2.15.7 were analyzed in collaboration with Dr. Tobias Straub of the Bioinformatics Core Unit, Ludwig-Maximilians-Universität Munich, Biomedical Center.

Adapter sequences were removed using cutadapt (v.1.16) keeping only reads with a minimum length of 25bp. Sequences mapping to rRNA sequences with bowtie2 (v2.2.9) were counted and removed. The remaining sequences were mapped to mouse genes (genome version GRCm38, annotation version GRCm38.92) using STAR (v2.6.0a, parameters "--outFilterMultimapNmax 200 --winAnchorMultimapNmax 200") and expression was estimated using RSEM (v.1.3.0).

rRNA database contained the sequences of a) rRNA genes extracted from ENSEMBL Mus\_musculus.GRCm38.92.gtf, b) manually selected sequences from the NCBI database (Rn45s (NR\_046233.2 and BK000964.1), Rn4.5s (NR\_002841.2), n-R5s136

## C Material and Methods

(NR\_046144.1), Rn5s (NR\_030686.1)) c) manually selected blast hits of unaligned reads (AH002076.2, AH002077.2, BK000964.3, JQ247698.1, GU372691.1, J00623.1, X55996.1, X82564.1, V00849.1, V00850.1, V00851.1, X00525.1, X56974.1, D17318.1, D17317.1, D14835.1, D14834.1, D14833.1, D14832.1, X00686.1, X04886.1, X71804.1, J01871.1, M27441.1, M27443.1, M57716.1, M57714.1, K01366.1, M18066.1, M18065.1, M18064.1, M18063.1, M18062.1, M20154.1, M35283.1, M57720.1, M57723.1, K01367.1, M57708.1, K02235.1, M19226.1, M55272.1, M27358.1, K01380.1, M31319.1) d) the silva rRNA database for mouse and human (arb-silva.de, date stamp 2018-06-16).

tRNA database contained the sequences obtained from gtrnadb.ucsc.edu (mm10-tRNAs.fa). Alignment rates were  $\leq 0.5\%$ .

### 2.16 *In vivo* killing assay

To test the capability of TCR transgenic OT-I T cells to kill target cells presenting the cognate peptide OVA<sub>257-364</sub>, congenically marked, peptide pulsed splenocytes from C57/Bl6 mice were transferred into recipients of OT-I T cell one day before being analyzed. The spleen was dissected from CD45.1.2<sup>+</sup> C57/Bl6 mice and homogenized. The cell suspension was centrifuged at 1500 rpm for 5 minutes. The pellet was resuspended in FACS Medium at a concentration of  $2 \times 10^6$  cells/mL. 1  $\mu$ g/mL, 0.01  $\mu$ g/mL or no Q4H7 peptide was added to the cell suspension, respectively. Cells were incubated for 4 hours at 37 °C and 5% CO<sub>2</sub>. Splenocytes pulsed with 1  $\mu$ g/mL peptide were labeled with 5 nM CTV and cells pulsed with 0.1  $\mu$ g/mL with 0.5 nM CTV as described under 2.5. Unpulsed cells kept unlabeled. This allows a discrimination of all three populations *ex vivo*. Pulsed and unpulsed cells were mixed in a 1:1:1 ratio with the equivalent of  $1 \times 10^6$  cells per population and transferred in 100  $\mu$ L DMEM w/o BSA into recipient mice of OT-I T cells, 4 or 29 days post-transfer, respectively. Mice were sacrificed 16 hours later

### 2.17 Statistic analysis

Statistic analysis was performed on Prism 5.0c and 7.0d. Mean and p-values have been generated from unpaired two-tailed student's t-test, if not indicated otherwise.

## D Results

### I mTORC1-dependent RNA synthesis in proliferating T cells

#### 1 mTORC1-dependent physiological changes upon TCR stimulation

Antigen-recognition rapidly induces a series of signals, downstream of the TCR, which lead to T cell activation, blast formation and eventual clonal expansion of the cell. Besides the transduction of NFAT, Jun, Fos and NF $\kappa$ B to the nucleus, the TCR ligation to cognate antigen triggers a PI3K-dependent activation of mTOR in collaboration with CD28 (Finlay *et al.*, 2012; Gaud *et al.*, 2018).

##### 1.1 The phosphorylation of S6 in stimulated T cells is mTORC1-dependent

The source of the signals that lead to the phosphorylation of mTORC1 downstream targets during T cell activation was further investigated. Thus, we tested whether TCR signaling alone is sufficient to activate mTORC1 or if co-stimulation via CD28 is needed to induce the phosphorylation of downstream targets of mTORC1. Polyclonal CD4<sup>+</sup> and CD8<sup>+</sup> T cells from mouse spleen and lymph nodes were stimulated with immobilized anti-CD3, anti-CD28, both antibodies combined (anti-CD3/28) or PMA/IM for 2 hours *in vitro*. The activity of mTORC1 was measured by flow cytometry for the presence of phosphorylated S6 ribosomal protein at Ser240/244 (pS6) by S6K1, a direct target of mTORC1. Figure D1.1 A and B show an ~80-fold increase of pS6 in CD4<sup>+</sup> and ~45-fold increase in CD8<sup>+</sup> T cells upon stimulation with anti-CD3/28 in comparison to unstimulated cells. The omission of CD28 reduced the gMFI of S6 phosphorylation by ~55% in CD4<sup>+</sup> and ~70% in CD8<sup>+</sup> T cells, indicating the amplifying effects of co-stimulation. A treatment by PMA/IM does not directly induce mTORC1 signaling via PI3K/Akt but rather indirect by a crosstalk via Erk/Tsc1/Rheb (Powell *et al.*, 2012). PMA/IM induced an increase in the phosphorylation of S6 up to 45-fold in CD4<sup>+</sup> and 23-fold in CD8<sup>+</sup> T cells. This result is in line with previous data showing anti-CD3 can induce the phosphorylation of S6 but signaling via CD28 is required to stabilize the phosphorylation of S6 at later time points (16 hours) (Yang & Chi, 2013). To test the expression of pS6 in Raptor-deficient T cells, T-Rptor<sup>-/-</sup> and T-WT cells were stimulated with PMA/IM for two hours *in vitro*. Even though mTORC1 was disrupted in T-Rptor<sup>-/-</sup> cells, an induction of S6 phosphorylation was detected, albeit with a 1.5- to two-fold lower magnitude than in T-WT cells probably due to mTORC1-independent

## D Results

activation of S6K (Fig. D1.1C, D). Hence, TCR signaling induces a phosphorylation of S6, which partially depends on the presence of mTORC1.

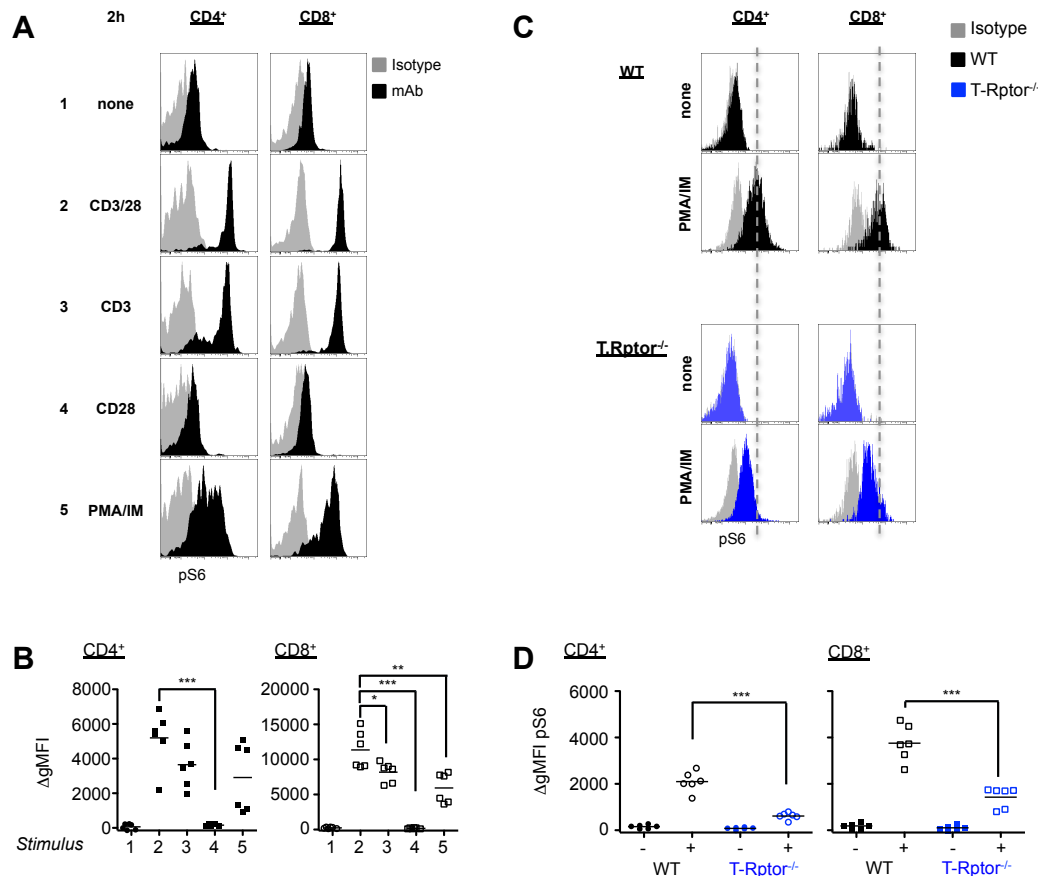


**Figure D1.1: TCR stimulation induces mTORC1 dependent S6 phosphorylation.** (A)  $0.2 \times 10^6$  cells pooled from six sub-cutaneous (s.c.) lymph nodes and spleen from B6 mice were incubated in 96-well plates for two hours *in vitro* with immobilized antibodies ( $10 \mu\text{g/mL}$ ) or PMA/IM. The phosphorylation of S6 in T cells was monitored by flow cytometry with the rabbit IgG mAb 2F9-AI488 (black) and rabbit IgG-AI488 isotype control. Results are representative of 6 independent experiments. (B) Geometrical mean fluorescence intensities (gMFIs) were quantified and normalized to isotype controls. (C)  $0.2 \times 10^6$  WT and T-Raptor<sup>-/-</sup> cells pooled from lymph nodes and spleen were stimulated as indicated and analyzed two hours later. Stimulated T-WT cells are shown in black, T-Raptor<sup>-/-</sup> cells in blue and the specific isotype control in grey (n=6). (D) Geometrical fluorescence intensities were quantified and normalized to isotype controls. Statistical analysis was performed using Student's t-test with \*:  $p < 0.05$ , \*\*  $p < 0.01$ , \*\*\*  $p < 0.001$ .

### 1.2 T cell blast formation is delayed in mTORC1-deficient T cells

In numerous studies, a correlation between mTORC1 activity and cell growth has been detected. They demonstrated a reduced blast formation early upon T cell stimulation (Pollizzi & Powell, 2015; So *et al.*, 2016; Yang *et al.*, 2013). To test whether mTOR

## D Results

activity affects T cell blast formation not only 24 hours post-stimulation, but also at later time points, MACS-purified T-WT, T-Rptor<sup>-/-</sup> and T-Rictor<sup>-/-</sup> cells were stimulated with anti-CD3/28 for 48 hours *in vitro* and analyzed by flow cytometry. T cell blast formation was measured by the increase of the forward scatter area (FSC-A). The detection signal of the FSC-A visualizes the light diffraction of cells and is proportional to the cell diameter. Hence, the FSC-A correlates with the size of a cell (Tzur *et al.*, 2011).

Within 48 hours of stimulation, both CD4<sup>+</sup> and CD8<sup>+</sup> T cells increased two-fold in size in comparison to naïve T cells. T cells deficient in either mTORC1 or mTORC2 were able to increase in size to the same degree as T-WT cells could by this time point. T-Rictor<sup>-/-</sup> cells were even slightly bigger than T-WT cells (Fig. D1.2 A and B).

To investigate changes in cell size over time *in vivo*, naïve T-WT and T-Rptor<sup>-/-</sup> AND or OT-I TCR transgenic cells specific for MCC<sub>93-103</sub> or OVA<sub>257-264</sub>, were co-transferred into iMCC or iOVA mice, respectively and monitored in the spleen. iMCC mice can express MCC<sub>93-103</sub> on H-2E<sup>k</sup>, iOVA mice express OVA<sub>257-264</sub> on H-2K<sup>b</sup>. Only if orally treated with 100 µg/mL doxycycline in the drinking water, the tet-responsive transactivator can bind to the tet-operator and induce the expression of their respective peptides on either MHC-II in iMCC and MHC-I in iOVA mice (Rabenstein *et al.*, 2014). In this experiment, antigen-expression was induced one day before transfer by doxycycline and continued until the end of the experiment. Both T-WT and T-Rptor<sup>-/-</sup> cells increased in size upon stimulation *in vivo*. Albeit, T-Rptor<sup>-/-</sup> cells were slower in comparison to T-WT cells (Fig. D1.2 C, D). Thus, T cell blast formation is rather delayed in mTORC1-deficient T cells than completely reduced.

## D Results

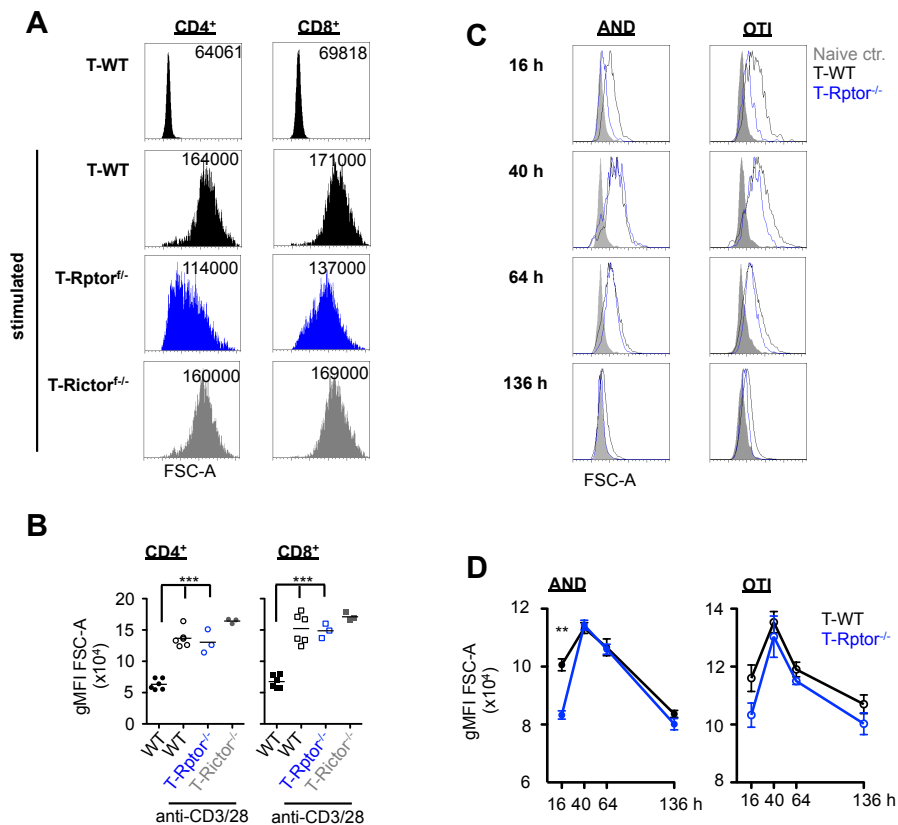


**Figure D1.2: Blast formation of T-Rpator<sup>-/-</sup> cells is delayed upon TCR stimulation.** (A)  $0.1 \times 10^6$  magnetically purified T-WT, T-Rpator<sup>-/-</sup> and T-Rictor<sup>+/-</sup> CD4<sup>+</sup> and CD8<sup>+</sup> T cells were incubated with 5 ng/mL IL-7 in the presence or absence of 10  $\mu$ g/mL immobilized anti-CD3/28 antibodies for 48 hours *in vitro*. The FSC-A was determined by flow cytometry. Results are representative of six independent experiments. (B) Quantification of the geometrical MFI of the FSC-A. (C) FSC-A of *in vivo* stimulated AND and OT-I T-WT (black) and T-Rpator<sup>-/-</sup> (blue) cells over time.  $1 \times 10^6$  naive AND or OT-I T-WT and T-Rpator<sup>-/-</sup> cells were transferred into iMCC and iOVA mice, respectively, pre-treated with 40  $\mu$ g anti-CD40 antibody, respectively and persistently fed with doxycycline starting one day before transfer. Same experiment as shown in chapter D 2.2. (D) Quantification of the data shown in (C). Statistical analysis was performed using Student's t-test with \*:  $p < 0.05$ , \*\*  $p < 0.01$ , \*\*\*  $p < 0.001$ .

## 2 Clonal expansion and survival of T-Rpator<sup>-/-</sup> cells *in vivo*

The successful priming of a T cell results in a population of expanded clones. In 2009, Jonathan Powell and others have shown a reduced proliferation rate in mTORC1-deficient T cells *in vitro* (Delgoffe *et al.*, 2009b; Yang *et al.*, 2013). To test whether this is also the case *in vivo*, mTORC1-sufficient and deficient T cells were isolated from congenically marked mice, labeled with CFSE, and adoptively transferred under different conditions.

## D Results

### 2.1 Impaired GvH response of T-Rptor<sup>-/-</sup>

The parent-into-F1 model has been used to study autoimmune diseases such as lupus. In this model the transfer of homozygous T cells from the parental generation into non-irradiated semi-allogeneic F1 mice induces a graft-versus-host (GvH) response. It is mediated by naïve T cells that develop into mature effector T cells and start to proliferate upon the recognition of allo-antigens (Via, 2010).

To examine the alloresponse of T-WT and T-Rptor<sup>-/-</sup> cells, an experimental system for graft-versus-host response was used by the adoptive transfer of  $10 \times 10^6$  CFSE-labeled bulk naïve cells from lymph node and spleen of an H-2A<sup>b/b</sup> CD45.1/1<sup>+</sup> mouse into CD45.2<sup>+</sup> recipients, expressing allogeneic MHC class I (H-2K<sup>b/bm1</sup>) or class II (H-2A<sup>b/bm12</sup>). Five days post-transfer, CD4<sup>+</sup> and CD8<sup>+</sup> T-WT cells started to divide up to eight times or more in H-2A<sup>b/bm12</sup> and H-2-K<sup>b/bm1</sup> recipient mice, respectively. In contrast, T-Rptor<sup>-/-</sup> cells showed a much lower response (Fig. D2.1 A and B). Furthermore, T-Rptor<sup>-/-</sup> cells accumulated 15- to 26-times less *in vivo* up to day five post-stimulation. Thus, either fewer T-Rptor<sup>-/-</sup> cells can responded to alloantigen or more cells died upon proliferation than T-WT cell, resulting in an impaired graft-versus-host response in T-Rptor<sup>-/-</sup> cells.

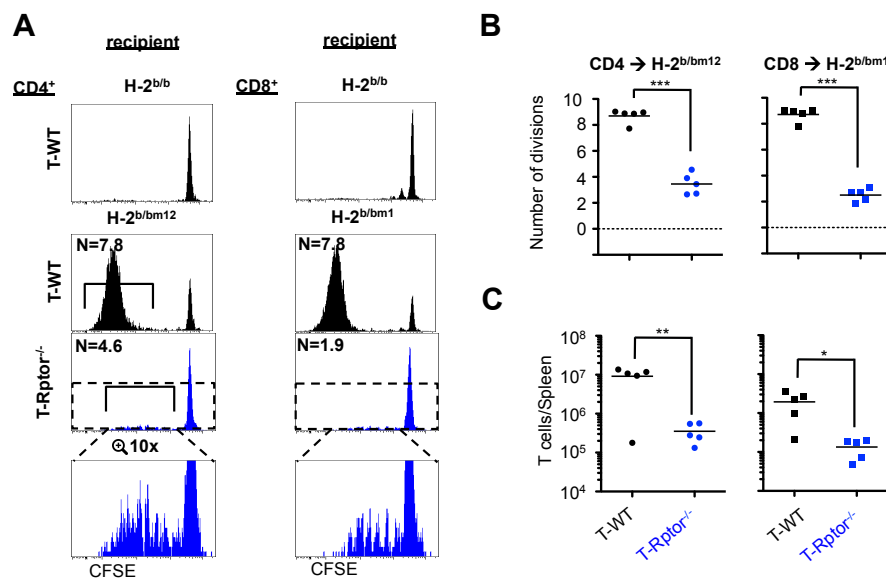


**Figure D2.1: Reduced proliferation and survival of T-Rptor<sup>-/-</sup> cells in an allogenic-mediated GvH response.**

(A)  $10 \times 10^6$  CFSE-labeled T lymphocytes from pooled lymph nodes and spleen from CD45.1<sup>+</sup> T-WT and T-Rptor<sup>-/-</sup> animals were transferred into either B6 (H-2<sup>b/b</sup>), bm1 (H2K<sup>b/bm1</sup>) or bm12 (H-2A<sup>b/bm12</sup>) mice that have been injected with 20  $\mu$ g anti-CD40 antibody 24 hours before cell transfer. CFSE dilution of alloresponsive splenic T-WT and T-Rptor<sup>-/-</sup> cells was monitored five days post-adoptive transfer by flow cytometry. Results are shown for CD45.1<sup>+</sup> donor cells only. Results are representative of five

## D Results

independent experiments. (B) Average division number of proliferative-active transferred T cells was calculated as  $N = \log_2(\text{gMFI}_{\text{ctrl}}/\text{gMFI}_{\text{sample}})$ . (C) The total number of transferred T cells was quantified in the spleens of the recipient mice. Statistical analysis was performed using Student's t-test with \*:  $p < 0.05$ , \*\*  $p < 0.01$ , \*\*\*  $p < 0.001$ .

### 2.2 T-Rptor<sup>-/-</sup> cells proliferate slower and accumulate less in response to antigen

We next tested an antigen-specific response to cognate antigen by monitoring the proliferation of AND CD4<sup>+</sup> and OT-I CD8<sup>+</sup> TCR transgenic T cells. Purpose of the experiment was to analyze proliferation and accumulation of T-WT and T-Rptor<sup>-/-</sup> cells in response to persistent antigen-presentation side by side under similar conditions at different time points during clonal expansion.

Equal numbers of CFSE-labeled AND or OT-I T-WT and T-Rptor<sup>-/-</sup> cells isolated from six lymph nodes were co-transferred into either iMCC or iOVA mice, treated with 20 or 40  $\mu\text{g}$  anti-CD40 per mouse, respectively one day before transfer and 100  $\mu\text{g}/\text{mL}$  doxycycline in the drinking water starting 24 hours before transfer until the end of the experiment (Fig. D2.2 A and E). Absolute T cell numbers and proliferation by the dilution of CFSE was monitored by flow cytometry over time (Fig. D2.2 B and F) and translated into average division numbers (Fig. D2.2 C and G). Upon 40 hours post-transfer T-WT and T-Rptor<sup>-/-</sup> cells from AND or OT-I have started to proliferate, even though not all T-Rptor<sup>-/-</sup> cells have started their first division, yet. Whereas AND and OT-I T-WT cells display an average division number higher than three, T-Rptor<sup>-/-</sup> cells have not divided more than twice. Between 40 and 64 hours post-transfer, a further division has been detected every seven hours in AND and eleven hours in OT-I T-WT cells. In contrast, the division rate was two-times lower in T-Rptor<sup>-/-</sup> cells. Six days post-transfer, T-WT cells have divided eight-times or higher, whereas T-Rptor<sup>-/-</sup> cells divided five-times in average. Moreover, the total number of transferred T-Rptor<sup>-/-</sup> cells per spleen was 50 to 90-fold reduced (Fig. 2.2 D and H).

In summary, not only the first cell cycle entry in T-Rptor<sup>-/-</sup> cells appears to be delayed but also later divisions. In total, all T-Rptor<sup>-/-</sup> cells were able to divide, albeit slower, but show a hampered accumulation due to cell death.

## D Results

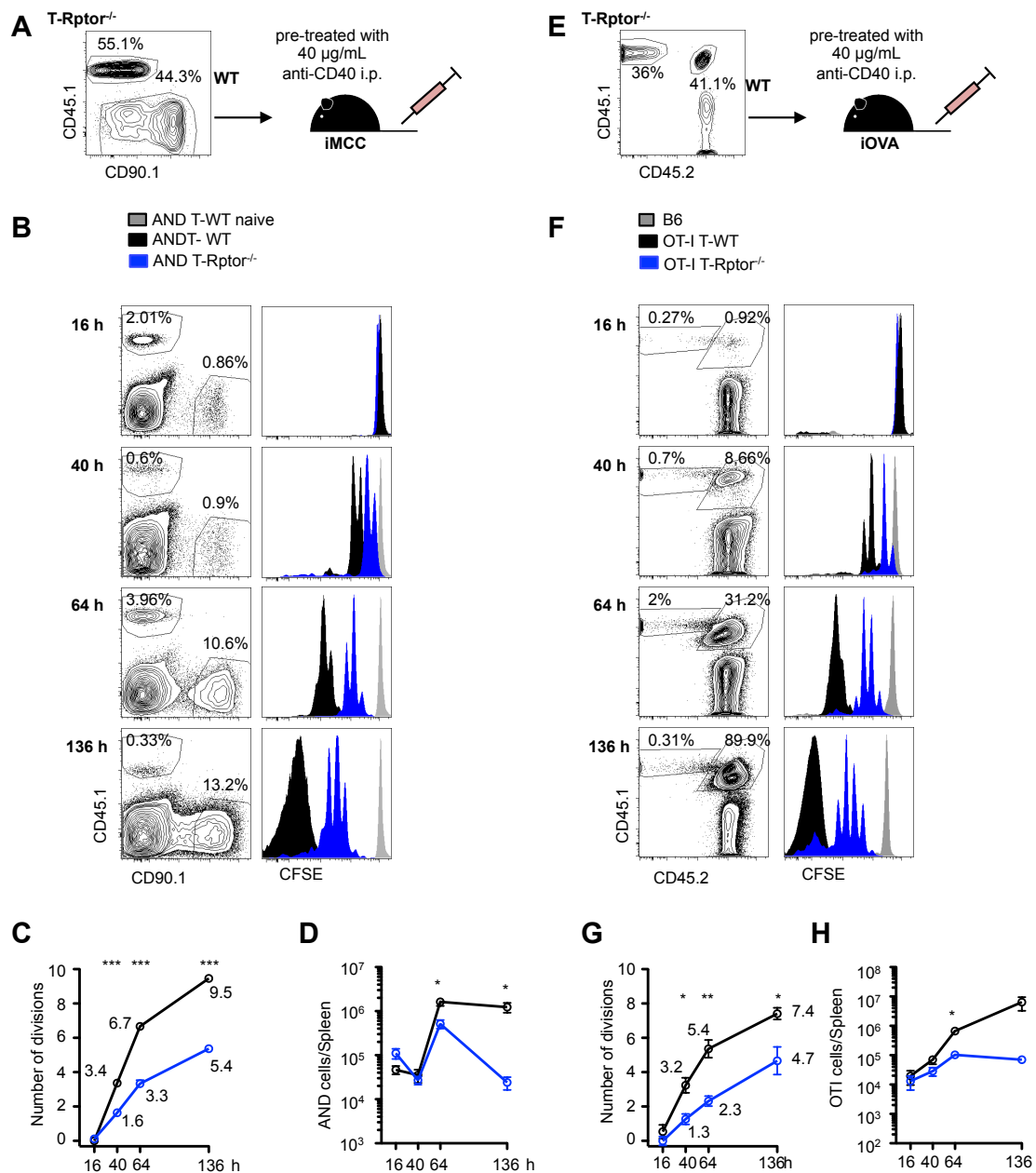


**Figure D2.2: Reduced proliferation rate and survival of TCR transgenic T-Rptor<sup>-/-</sup> cells in an antigen-specific response.**

(A, E)  $1 \times 10^6$  CFSE-labeled AND (A-D) or OT-I T-WT and T-Rptor<sup>-/-</sup> cells from bulk lymph node cells were co-transferred into iMCC (A-D) or iOVA mice that have been treated with 40 µg anti-CD40 antibody one day before transfer, respectively. The respective antigen-expression was induced by 100 µg/mL doxycycline in the drinking water from one day before transfer on until the end of the experiment. (B, F) CFSE dilution of transferred control (A) naïve (gray) AND T cells or (E) OTI<sup>-/-</sup> as well as OTI<sup>+/+</sup> T-WT (black) and T-Rptor<sup>-/-</sup> (blue) cells was monitored over time in the spleen by flow cytometry. Results are representative of three independent experiments. (C, G) Average division number of transferred T cells was calculated as  $N = \log_2(\text{gMFI}_{\text{ctrl}}/\text{gMFI}_{\text{sample}})$ . (D, H) Total number of transferred T cells was quantified in the recipient spleen. Statistical analysis was performed using Student's test with \*:  $p < 0.05$ , \*\*  $p < 0.01$ , \*\*\*  $p < 0.001$ .

## D Results

### 2.3 T-Rptor<sup>-/-</sup> OT-I T cells expand less in response to transient TCR stimulation

It has been published that a short antigen pulse is sufficient to induce clonal expansion of CD8<sup>+</sup> T cells (Rabenstein *et al.*, 2014). We asked if mTOR-deficient TCR transgenic OT-I T cells proliferate upon a transient TCR stimulus to the same extent as T-WT cells. Thus, naïve CD8<sup>+</sup> T-WT, T-Rptor<sup>-/-</sup> and T-Rictor<sup>-/-</sup> cells were magnetically purified and primed *in vitro* for 48 hours and subsequently labeled with CFSE and separately transferred into B6 hosts. As positive control, *in vitro* primed OT-I T-WT cells were transferred into iOVA mice. Proliferation in the context of CFSE dilution was monitored three days later by flow cytometry (Figure D2.3 A). Upon stimulation, T-WT and T-Rictor<sup>-/-</sup> cells divided up to five-times independent of antigen persistence. However, T-Rptor<sup>-/-</sup> cells divided up to two-times upon transient TCR stimulation, indicating a reduced antigen-independent expansion in T-Rptor<sup>-/-</sup> cells (Figure D2.3 B, C).

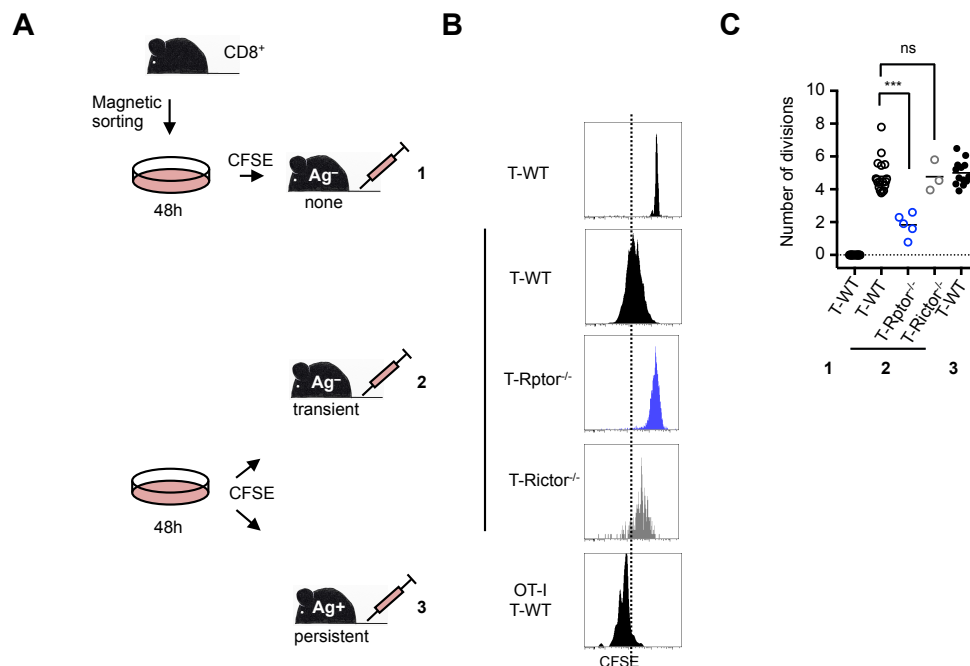


**Figure D2.3: Impaired response to a transient antigen stimulus in OT-I T-Rptor<sup>-/-</sup> cells.**

(A) Experimental outline. Magnetically sorted CD45.1.1<sup>+</sup> T-WT, T-Rictor<sup>-/-</sup> and T-Rptor<sup>-/-</sup> cells were cultured in the absence (condition 1) or presence of anti-CD3/CD28 for 48 hours and subsequently labeled with CFSE.  $2 \times 10^6$  cells were transferred into CD45.2.2<sup>+</sup>, cognate Ag-free (condition 1 and 2) or -expressing (condition 3) recipients and analyzed three days later. (B) Representative histograms of the CFSE dilution of congenically identified splenic AND and OT-I T cells. (C) The average division number  $N$  is calculated as  $N = \log_2(\text{CFSE MFI}_{\text{ctr}}/\text{CFSE MFI}_{\text{sample}})$ . Results are representative of 3-18 independent experiments. Statistical analysis was performed using Student's *t*-test with \*:  $p < 0.05$ , \*\*  $p < 0.01$ , \*\*\*  $p < 0.001$ .

## D Results

### 2.4 T-Rptor<sup>-/-</sup> cells expand and persist less in response to an infection with MVA-OVA

To investigate whether additional signals, such as virus-induced cytokine expression might benefit a proliferation in mTORC1-deficient T cells, the same numbers of OT-I T-WT and T-Rptor<sup>-/-</sup> cells were co-transferred in recipient mice that had subsequently been infected with OVA-expressing Modified Vaccinia Ankara Virus (MVA-OVA) (Fig. D2.4 A). The expansion of T-WT and T-Rptor<sup>-/-</sup> cells was monitored side by side under equal conditions. MVA is known to preferentially target dendritic cells, with viral life cycle arrest before late gene expression, limiting the presentation of antigen to the turnover of the infected DCs and thus induced a short antigen pulse only. Furthermore, an infection with MVA-OVA is reported to induce CD8<sup>+</sup> T cell activation and a differentiation into cytotoxicity T lymphocytes (Liu *et al.*, 2008).

By eight days post-infection, OT-I T-WT cells had expanded up to 38-fold in comparison to naïve OT-I cells transferred into uninfected mice. Also OT-I T-Rptor<sup>-/-</sup> cells had expanded, however three times less than T-WT cells. Five weeks post-infection, OT-I T-Rptor<sup>-/-</sup> cells were only detected in half of all recipient mice. The accumulation was nine-fold reduced in mice that still had T-Rptor<sup>-/-</sup> cells. T-Rptor<sup>-/-</sup> cells showed a reduced response to MVA-OVA early and late after infection. Thus, the expansion and survival of T-Rptor<sup>-/-</sup> cells is impaired in response to an MVA-OVA infection.

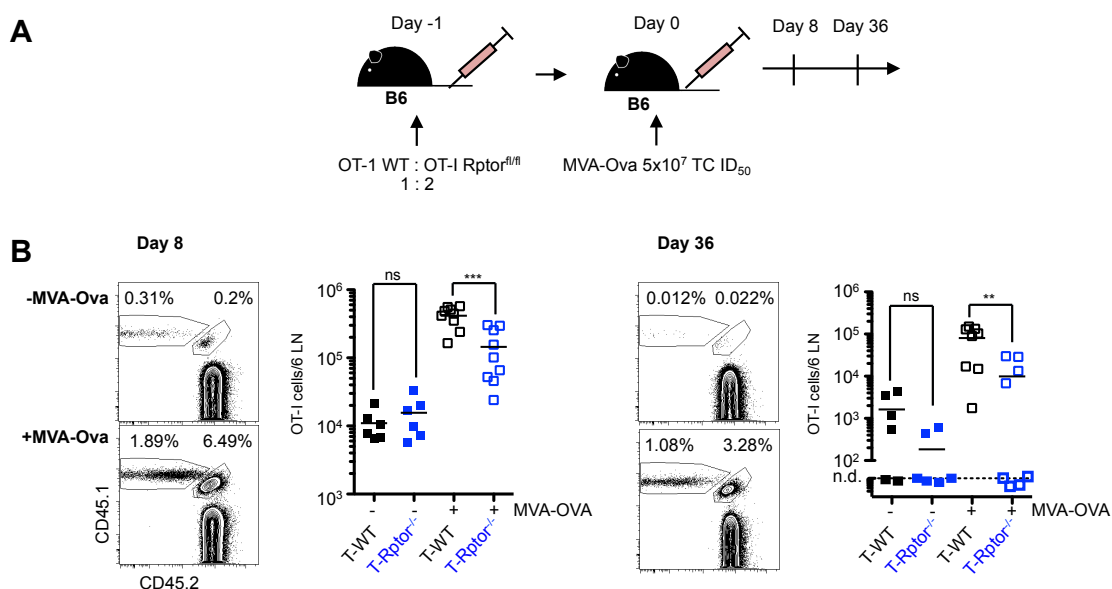


**Figure D2.4: Reduced antigen-driven and homeostatic expansion and accumulation in response to MVA-OVA in OT-I T-Rptor<sup>-/-</sup> cells.**

(A)  $0.1 \times 10^6$  OT-I T-WT and T-Rptor<sup>-/-</sup> cells were co-transferred (d-1) into B6 mice that

## D Results

were infected with  $5 \times 10^7$  TC ID<sub>50</sub> i.v. 24 hours later (d0). (B) The total number of transferred T cells was quantified in the recipient lymph nodes on day 8 and day 36 post-infection. Results are representative of three independent experiments, of which one was done without uninfected recipient mice. Statistical analysis was performed using Student's t-test with \*:  $p < 0.05$ , \*\*  $p < 0.01$ , \*\*\*  $p < 0.001$ .

### 2.5 Lymphopenic-driven expansion is diminished in T-Rptor<sup>-/-</sup> cells

It has been reported that T cells rapidly divide and persist in lymphopenic mice (Bell *et al.*, 1987; Bruno *et al.*, 1996; Kieper *et al.*, 2001; McDonagh & Bell, 1995; Pereira & Rocha, 1991; Rocha *et al.*, 1989; Sprent *et al.*, 1991). We next tested the proliferative capacity of T-Rptor<sup>-/-</sup> cells under homeostatic conditions. CFSE-labeled T-WT and T-Rptor<sup>-/-</sup> cells were co-transferred into lymphopenic, RAG1-deficient hosts. RAG1-deficient mice are not able to perform V(D)J recombination and thus B and T cell differentiation arrests at an early stage (Mombaerts *et al.*, 1992).

Five days post-transfer around 50% of all CD8<sup>+</sup> T-WT but only 8% T-Rptor<sup>-/-</sup> cells have started to proliferate in the lymph nodes of the recipient mouse (Fig. D2.4). Hence demonstrating reduced proliferation capacity of T-Rptor<sup>-/-</sup> cells under homeostatic conditions *in vivo*. In agreement with Yang *et al.*, 2013, T-Rptor<sup>-/-</sup> cells responded less to non-infectious, homeostasis-induced signals. Nevertheless, also T-WT cells only divided up to four-times in RAG1<sup>-/-</sup> mice, which is less than previously described. This could be due to environmental conditions in the animal facility of the Biomedical Center at the LMU, Munich. In agreement with others, we found diminished lymphopenic proliferation in T-Rptor<sup>-/-</sup> cells (Li *et al.*, 2011; Rathmell *et al.*, 2001; Yang *et al.*, 2013).

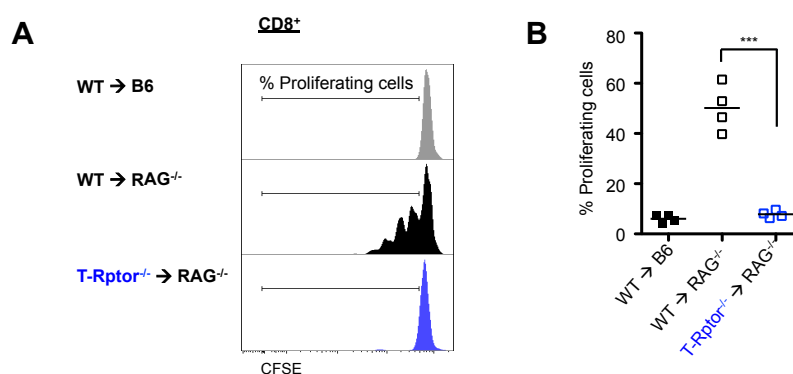


**Figure D2.5: T-Rptor<sup>-/-</sup> cells proliferate less in RAG1<sup>-/-</sup> mice.**

(A) Co-transfer of  $2 \times 10^6$  CFSE-labeled CD8<sup>+</sup> T-WT (black) and T-Rptor<sup>-/-</sup> (blue) cells into RAG1-sufficient or deficient (black, blue) mice. CFSE dilution was monitored by flow cytometry five days post-transfer in the lymph nodes of the recipient mice. Results are representative of four independent experiments (B) The percentage of proliferating cells was quantified. Statistical analysis was performed using Student's t-test with \*:  $p < 0.05$ , \*\*  $p < 0.01$ , \*\*\*  $p < 0.001$ .

### 3 rRNA expression limits T cell proliferation

In a proliferating cell, the biosynthetic demands are expected to be very high. It has been estimated that around 80% of the energy consumption is used for the synthesis of Ribosomes (Moss *et al.*, 2007; Warner, 2001). Also in yeast, around 80% of nucleolar transcription is dedicated to the assembly of the translational machinery, in mammalian cell lines around 50% (Moss & Stefanovsky, 2002). Two studies in tumor cell lines have shown that the transcription of ribosomal DNA is regulated via an mTORC1-dependent phosphorylation of RNA Polymerase I specific transcription factors TIF-1A (Rrn3) and Ubf by S6K1 (Hannan *et al.*, 2003; Mayer & Grummt, 2006). The aim of the following experiments was to establish a link between mTORC1-dependent expression of RNA with clonal expansion in T cells.

#### 3.1 The expression of RNA Polymerase I subunits is mTORC1-dependent

In 2017, Chi and colleagues performed total and phospho-proteomic experiments of *in vitro* stimulated T-WT and T-Rptor<sup>-/-</sup> cells (Tan *et al.*, 2017a). To determine the expression of RNA Polymerase I subunits on protein level, the data generated in Chi's lab were re-analyzed in this study in collaboration with Prof. Axel Imhof at the BMC. Upon stimulation with anti-CD3/28, an increase of the expression of RNA Polymerase I subunits was detected, while the expression of RNA Polymerase II subunits was high and independent of TCR stimulation. Furthermore, the expression of RNA Polymerase II subunits did not rely on mTORC1-signaling. In contrast, T-Rptor<sup>-/-</sup> cells showed lower expression levels of RNA Polymerase I subunits (Fig. D3.1). Thus, the increased expression of RNA Polymerase I subunits upon TCR stimulation was partially dependent on the activity of mTORC1.

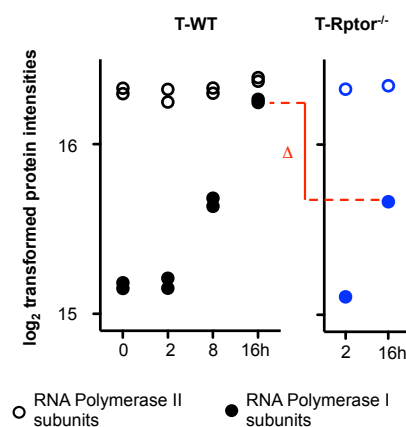


**Figure D3.1: mTORC1-dependent increase of expression of RNA Polymerase I subunits.**

## D Results

Proteomic analysis of *in vitro* stimulated (anti-CD3/CD28) T cells at indicated time points. Data were retrieved from Tan *et al.*, 2017 and analyzed by Prof. Axel Imhof, Core Facility Proteomics, Biomedical Center, Munich. Statistical analysis was performed using Student's t-test with \*:  $p < 0.05$ , \*\*  $p < 0.01$ , \*\*\*  $p < 0.001$ .

### 3.2 TCR induced expression of total and ribosomal RNA is mTORC1 dependent - quantity versus specificity

To explore whether mTORC1 activity affects RNA Polymerase I mediated expression of rDNA only or also other RNA species, total RNA sequencing was performed as previously described (Westermann *et al.*, 2016). MACS-purified CD4<sup>+</sup> and CD8<sup>+</sup> T-WT and T-Rpator<sup>-/-</sup> cells were stimulated with anti-CD3/28 *in vitro* for 48 hours and subsequently sorted to remove dead cells from the suspension (Gating strategy Supplementary Figure 4). Viable cells were discriminated as FVD780<sup>-</sup> and MFG8-GFP<sup>-</sup> and lysed in Trizol to purify RNA using RNeasy columns (Qiagen), including DNase treatment. A quantification of total RNA and 28S rRNA was performed by Dr. Fritz Thümmeler at Vertis Biotechnology AG by two different methods and compared with sorter-determined cell numbers.

The amount of RNA per cell increased 44-times in CD4<sup>+</sup> and 26-times in CD8<sup>+</sup> T-WT cells upon stimulation. T-Rpator<sup>-/-</sup> cells showed a 23-fold increase in RNA expression in CD4<sup>+</sup> T cells and a 10-fold increase in CD8<sup>+</sup> T cells, which was 2.6 to 2.8-times lower than in T-WT cells (Fig. 3.2 A). The amount of 28S rRNA was detected on quite similar levels as global RNA expression at around 0.5  $\mu\text{g}$  per  $10^5$  cells, which indicates ribosomal RNA being the most common of all RNA species in the cell. Also among rRNA species, activated T-Rpator<sup>-/-</sup> cells show an approximately 2.5-fold reduced upregulation in comparison to T-WT cells (Fig. D2.3 B).

cDNA libraries were generated from fragmented RNA and total RNA sequencing performed. Figure D3.2 C, D and Table 1 show the percentage distribution of all mappable RNA species. With around 83% of the mappable RNA reads belong to 45S and 5S ribosomal RNA in naïve CD4<sup>+</sup> and CD8<sup>+</sup> T-WT cells. Even though the amount of global and ribosomal RNA species increased upon stimulation, the relative amounts of the RNA species remained mostly unchanged. However, the proportion of mRNA increased slightly two-fold upon stimulation in CD8<sup>+</sup> T-WT cells. In turn snoRNA dropped accordingly.

In general, the reduced RNA expression following the activation of T-Rpator<sup>-/-</sup> cells observed before affected all RNA species to a similar extend.

Ribosomes consist of 28S, 18S, 5.8S and 5S rRNA and approximately 92 proteins. First three rRNAs are processed from a common 47S precursor, which is expressed

## D Results

from hundreds of genes by RNA Polymerase I, whereas 5S rRNA is synthesized by RNA Polymerase III (Moss *et al.*, 2007; Warner, 2001). To compare 47S rRNA processing in activated T-WT and T-Rptor<sup>-/-</sup> cells, the expression levels of 28S, 18S and 5.8S rRNA were analyzed. No strong difference has been detected in T-WT and T-Rptor<sup>-/-</sup> as well as T-Rictor<sup>-/-</sup> cells, hence showing no detectable influence of mTORC1 and 2 activities on 47S rRNA processing (Fig. D3.2 E). However, the number of reads across the 47S rRNA is highly variable across the sequence, likely due to secondary structures interfering with primer ligation during cDNA synthesis. In addition, the spread within ETS and ITS is higher than within the 28S, 18S and 5.8S rRNA itself, indicating a higher variation in total 47S rRNA synthesis but not in processing of the ribosomal subunits (Fig. D3.2 E).

Worth to mention, tRNA could not be mapped within this assay probably also due to secondary structures. Thus, other than RNA Polymerase I and II activity, RNA Polymerase III activity can hardly be accessed with this method.

### ***Number of mappable reads:***

stimulation	T-WT				T-Rptor <sup>-/-</sup>			
	CD4 <sup>+</sup>		CD8 <sup>+</sup>		CD4 <sup>+</sup>		CD8 <sup>+</sup>	
	-	+	-	+	-	+	-	+
rRNA	83.300 ± 1.21	85.800 ± 2.68	84.300 ± 0.04	85.400 ± 1.56	82.700 ± 1.05	86.600 ± 0.87	83.900 ± 0.56	86.400 ± 1.10
protein_coding	6.040 ± 1.23	7.900 ± 3.21	4.560 ± 0.61	8.360 ± 1.73	5.490 ± 1.24	5.570 ± 1.33	4.240 ± 1.02	6.040 ± 1.73
snoRNA	3.770 ± 1.72	2.280 ± 0.51	5.390 ± 0.79	2.150 ± 0.72	4.410 ± 0.39	2.920 ± 0.51	5.600 ± 0.66	2.920 ± 0.65
Mt_rRNA	3.530 ± 0.36	1.510 ± 0.18	2.380 ± 0.10	1.370 ± 0.22	3.120 ± 0.70	1.900 ± 0.28	2.070 ± 0.52	1.920 ± 0.50
snRNA	1.880 ± 0.80	1.380 ± 0.25	2.100 ± 0.27	1.390 ± 0.23	2.890 ± 1.00	1.890 ± 0.28	2.840 ± 1.16	1.420 ± 0.33
lincRNA	0.432 ± 0.03	0.534 ± 0.11	0.444 ± 0.00	0.777 ± 0.07	0.416 ± 0.07	0.497 ± 0.04	0.416 ± 0.03	0.659 ± 0.11
misc_RNA	0.475 ± 0.03	0.230 ± 0.04	0.385 ± 0.04	0.242 ± 0.01	0.408 ± 0.09	0.276 ± 0.02	0.415 ± 0.07	0.291 ± 0.05
miRNA	0.127 ± 0.03	0.124 ± 0.04	0.103 ± 0.01	0.116 ± 0.02	0.131 ± 0.05	0.131 ± 0.04	0.130 ± 0.07	0.142 ± 0.03
scaRNA	0.237 ± 0.00	0.041 ± 0.01	0.226 ± 0.01	0.037 ± 0.00	0.232 ± 0.02	0.077 ± 0.01	0.250 ± 0.04	0.067 ± 0.00
processed_transcript	0.035 ± 0.00	0.059 ± 0.01	0.028 ± 0.00	0.060 ± 0.00	0.035 ± 0.01	0.046 ± 0.00	0.029 ± 0.00	0.050 ± 0.00
TEC	0.062 ± 0.02	0.026 ± 0.01	0.043 ± 0.01	0.026 ± 0.00	0.054 ± 0.01	0.037 ± 0.01	0.042 ± 0.00	0.035 ± 0.01
antisense	0.046 ± 0.01	0.030 ± 0.01	0.033 ± 0.00	0.028 ± 0.00	0.041 ± 0.01	0.026 ± 0.00	0.032 ± 0.01	0.030 ± 0.01
Mt_tRNA	0.009 ± 0.00	0.023 ± 0.01	0.011 ± 0.00	0.021 ± 0.00	0.012 ± 0.00	0.017 ± 0.00	0.011 ± 0.01	0.019 ± 0.01
processed_pseudogene	0.019 ± 0.01	0.019 ± 0.01	0.014 ± 0.00	0.020 ± 0.01	0.018 ± 0.00	0.020 ± 0.01	0.017 ± 0.00	0.022 ± 0.01
sense_intronic	0.007 ± 0.00	0.002 ± 0.00	0.005 ± 0.00	0.002 ± 0.00	0.006 ± 0.00	0.004 ± 0.00	0.004 ± 0.00	0.004 ± 0.00
TR (V, D, J, C)	0.013 ± 0.00	0.007 ± 0.00	0.008 ± 0.00	0.007 ± 0.00	0.015 ± 0.00	0.006 ± 0.00	0.009 ± 0.00	0.005 ± 0.00

**Table D1: RNA type distribution in activated T-WT versus T-Rptor<sup>-/-</sup> cells.**

MACS-purified CD4<sup>+</sup> and CD8<sup>+</sup> T-WT or T-Rptor<sup>-/-</sup> cells were incubated in 96-well plates *in vitro* with 5 ng/mL IL-7 in the presence or absence of 10 µg/mL anti-CD3/28 mAbs for 48 hours. Viable (FVD780<sup>-</sup>, MFG8-GFP<sup>-</sup>) cells were sorted and resuspended in Trizol. Total RNA was purified and fragmented using ultrasound. cDNA was synthesized and amplified with 12-15 PCR cycles. Illumina NextSeq sequencing was done of three independent experiments. Relative percentage of all detected RNA species with standard deviation are shown.

## D Results

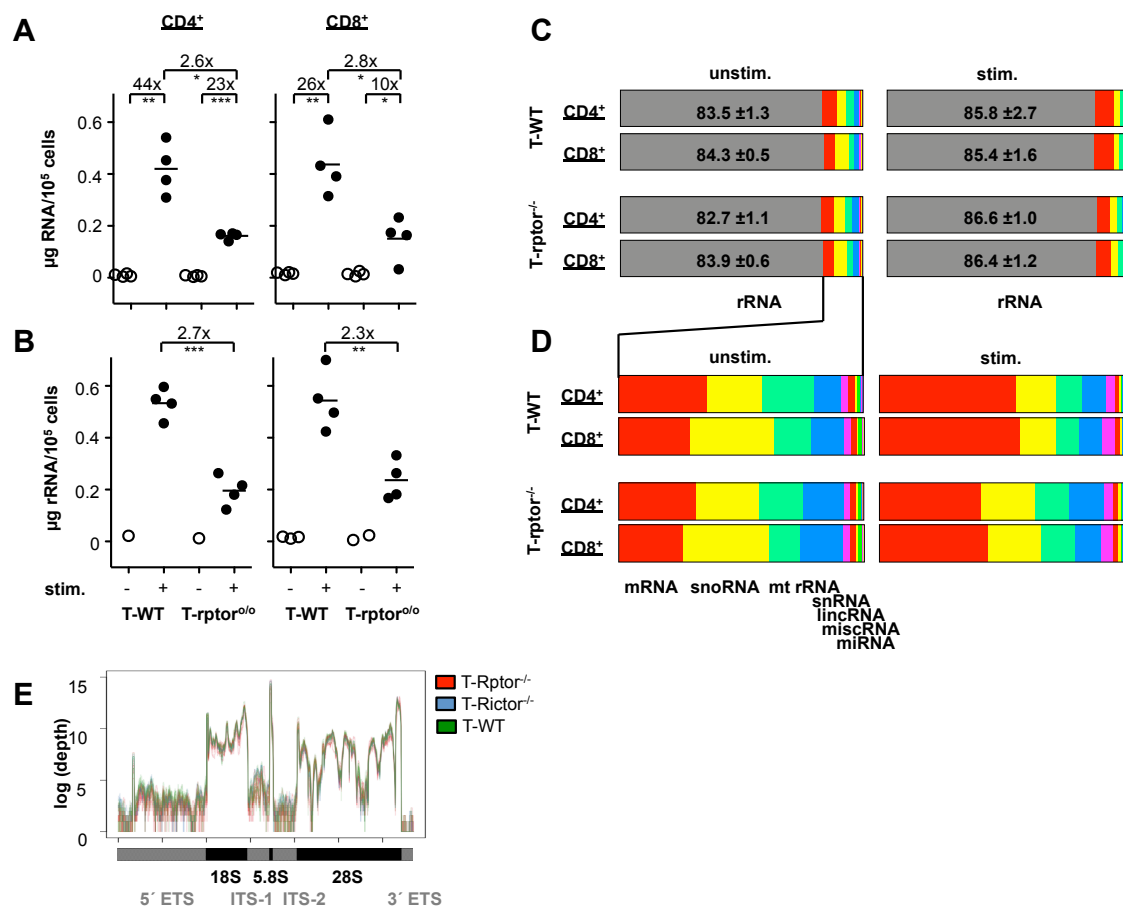


**Figure D3.2: Total RNA sequencing in activated T-WT versus T-Rpctor<sup>-/-</sup> cells shows reduced global RNA expression in T-Rpctor<sup>-/-</sup> cells.**

(A-D) MACS-purified CD4<sup>+</sup> and CD8<sup>+</sup> T-WT or T-Rpctor<sup>-/-</sup> cells were incubated in 96-well plates *in vitro* with 5 ng/mL IL-7 in the presence or absence of 10 µg/mL anti-CD3/28 antibodies for 48 hours. Viable (FVD780<sup>+</sup>, MFG8-GFP<sup>+</sup>) cells were sorted and resuspended in Trizol. Total RNA was purified and measured by (A) Qubit and (B) Shimadzu MultiNA microchip electrophoresis; n=1-4. (C, D) The RNA was fragmented using ultrasound, synthesized to cDNA and amplified with 12-15 PCR cycles. Illumina NextSeq sequencing was performed for three independent experiments. Relative percentage of all detected RNA species was plotted. (E) Expression level of processed 45S rRNA (18S, 5.8S, 28S) was measured in stimulated T-WT (green), T-Rpctor<sup>-/-</sup> (red) and T-Rictor<sup>-/-</sup> cells relative to unstimulated T cells. Statistical analysis was performed using Student's t-test with \*: p<0.05, \*\* p < 0.01, \*\*\* p< 0.001.

### 3.3 Visualization of RNA synthesis by flow cytometry

To further analyze the expression of RNA in T-WT, T-Rpctor<sup>-/-</sup> and T-Rictor<sup>-/-</sup> cells on a single cell level, a staining strategy for flow cytometry was established. RNA content was visualized in fixed and permeabilized cells applying the fluorescent xanthene dye Pyronin Y. It intercalates into double stranded nucleic acids, thus binding not only RNA but also enhances DNA staining. The interaction with DNA can be blocked by prior

## D Results

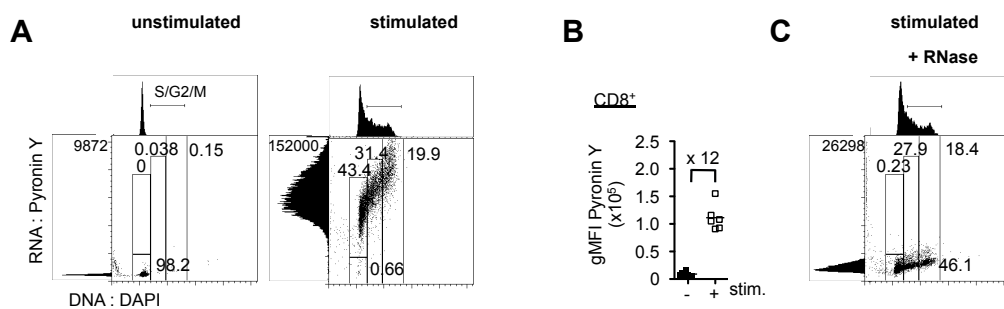
staining with Hoechst, a dye only intercalating into DNA (Shapiro, 1981). In this thesis, the application of 4',6-diamidino-2-phenylindole (DAPI) was used instead of Hoechst. DAPI allows assessing the cell cycle phases  $G_0/G_1$ , S and  $G_2/M$ .

Figure D3.3 A shows  $CD8^+$  T-WT cells cultured for 48h *in vitro*, subsequently PFA-fixed and methanol permeabilized and stained with Pyronin Y and DAPI. The Pyronin Y staining of naïve cells was very low. Upon stimulation with anti-CD3/28, the level of Pyronin Y increased 12-fold in comparison to unstimulated cells.

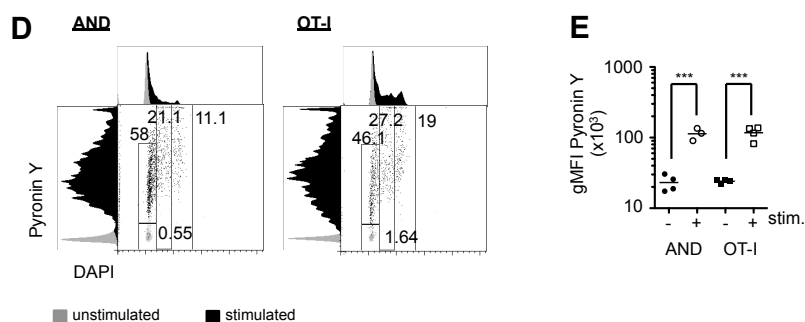
To test whether Pyronin Y exclusively stained RNA and not DNA in this experimental setup, fixed and permeabilized cells were treated with RNase before RNA and DNA staining. A treatment with RNase had no effect on DNA staining levels, but remarkably reduced the level of Pyronin Y to a basal level (Fig D 3.3 A-C).

To investigate the expression of RNA *in vivo*, TCR transgenic AND and OT-I T cells were either transferred into iMCC or iOVA mice treated with doxycycline. Cells from lymph node and spleen of the recipient mice were pooled 48 hours post-transfer and magnetically purified for either  $CD4^+$  or  $CD8^+$  T-WT cells in order to enrich the cells of interest for Pyronin Y staining. A staining with Pyronin Y increased five-fold in activated AND and OT-I T cells in comparison to cells transferred into antigen-free hosts. Thus, Pyronin Y can be used to assess RNA expression on a single cell level by flow cytometry in naïve and stimulated T cells (Fig D3.3 D, E).

### *in vitro*



### *in vivo*



## D Results

### Figure D3.3: RNA expression in single cells with Pyronin Y *in vitro* and *in vivo*.

(A-C) MACS-purified CD8<sup>+</sup> T cells were incubated in 96-well plates *in vitro* with IL-7 in the presence or absence of 10 µg/mL anti-CD3/28 antibodies for 48 hours. Fixed and permeabilized cells were treated with (C) or without (A, B) RNase for 30 minutes at 37°C. Cells were stained with DAPI (250 µg/mL) and Pyronin Y (625 µg/mL). Results are representative of 2-6 independent experiments (D, E) 1 x 10<sup>6</sup> congenically marked TCR transgenic AND and OT-I T cells were transferred into either iMCC or iOVA mice that have been pre-treated with 20 or 40 µg anti-CD40 mAb, respectively. Two days post-transfer, cells from lymph node and spleen were pooled and magnetically separated for either CD4<sup>+</sup> or CD8<sup>+</sup> T cells. The fixed and permeabilized CD4<sup>+</sup> and CD8<sup>+</sup> T cells were stained with DAPI and Pyronin Y in the same reaction tube and analyzed by flow cytometry. (B, E) The expression of Pyronin Y was quantified by the gMFI for 4-6 independent experiments. Statistical analysis was performed using Student's t-test with \*: p<0.05, \*\* p < 0.01, \*\*\* p< 0.001.

### 3.4 RNA expression in T cells correlates with cell cycle entry – kinetics

To further investigate the kinetics of RNA expression in T-WT cells, AND and OT-I T cells were stimulated *in vitro* for different periods of time and analyzed by flow cytometry. Even though TCR signaling was already seen four hours post-stimulation as visualized by the expression of Nur77-GFP (Moran *et al.*, 2011) (Fig. D3.4 B), RNA expression was first detected after 24 hours, whereby OT-I T cells increased RNA levels up to 104-fold and AND T cells 74-fold (1.4 times lower than in OT-I T cells) in comparison to unstimulated cells. The RNA expression levels further increased up to 48 hours and 72 hours post-stimulation in AND T cells and plateaued on a very high level in OT-I T cells. Cell cycle entry was determined as percentage of cells that had entered S/G<sub>2</sub>/M-phases. 24 hours post-stimulation less than 0.1% AND and ~20% OT-I T cells had entered the cell cycle. The number further increased upon ongoing stimulation up to half of the cells being found in S/G<sub>2</sub>/M-phases 72 hours post-stimulation (Fig. D3.4 A and B). Cell cycle entry directly correlated with RNA expression patterns (Fig. D3.4 A). In addition, AND and OT-I T cells started to form blasts and upregulated the transferrin receptor CD71 regulated by the activity of mTORC1 (Zheng *et al.*, 2007), with comparable kinetics (Fig. D3.4 B). Thus, RNA expression upon TCR stimulation correlates with cell blasting, cell cycle entry and mTORC1 activity *in vitro*. Since CD4<sup>+</sup> and CD8<sup>+</sup> T cells were different at their activation status 24 hours post-stimulation, further experiments were performed at 48 hours.

## D Results

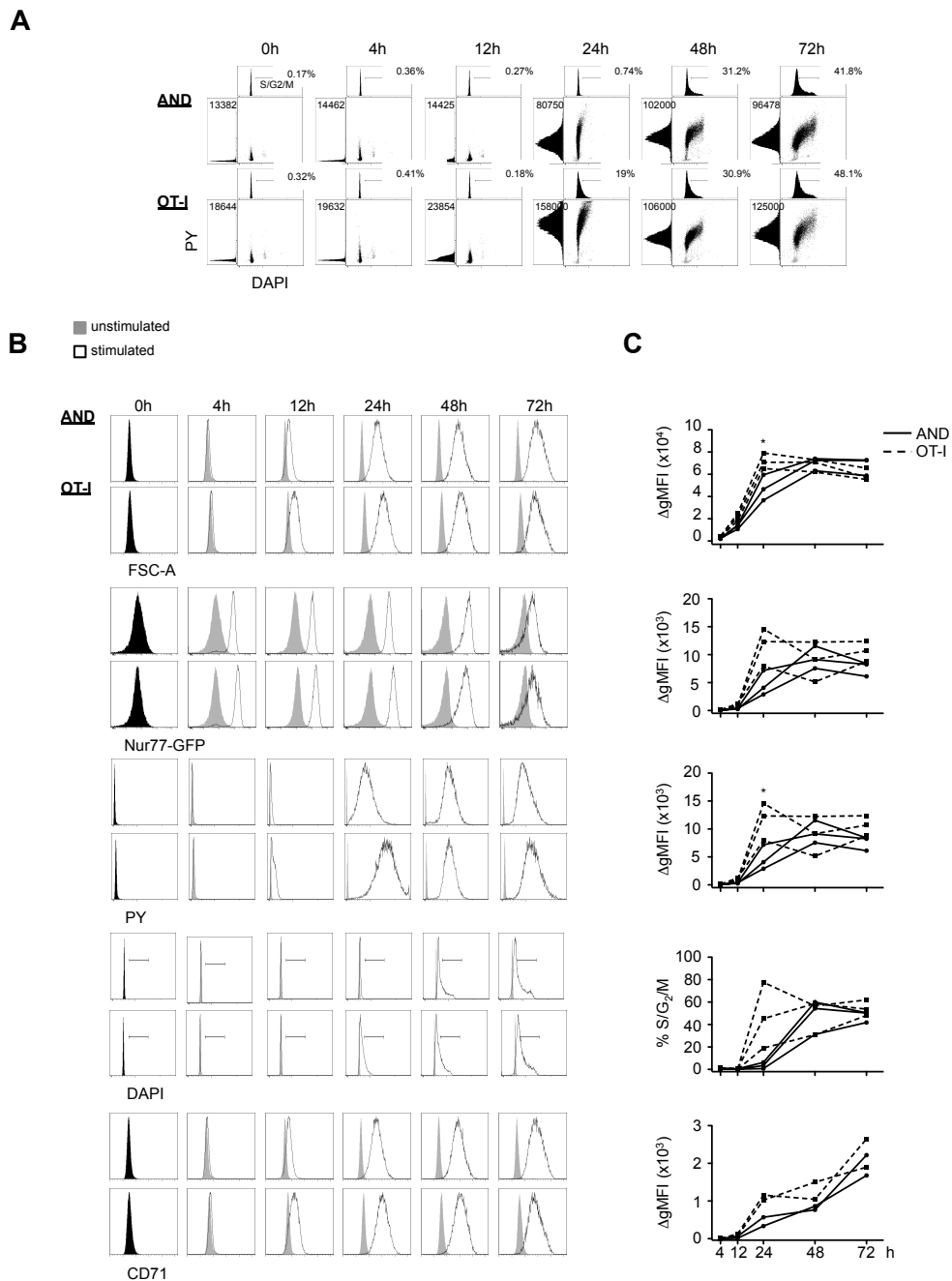


**Figure D3.4: RNA expression in activated T cells over time.**

(A) MACS-purified CD4<sup>+</sup> and CD8<sup>+</sup> T cells were incubated in 96-well plates *in vitro* with 5 ng/mL IL-7 in the presence or absence of 10  $\mu$ g/mL anti-CD3/28 antibodies over time. After 48 hours of stimulation anti-CD3/28 was replaced by 10 ng/mL IL-2 in fresh T cell medium. Cells were incubated for further 24 hours. Fixed and permeabilized. CD4<sup>+</sup> and CD8<sup>+</sup> T cells were stained with DAPI (250  $\mu$ g/mL) and Pyronin Y (625  $\mu$ g/mL) in the same reaction tube and analyzed by flow cytometry. Results are representative of three independent experiments. (B) The increase of FSC-A, Nur77-GFP, Pyronin Y, DAPI and CD71 in unstimulated (gray) and stimulated (black) T cells plotted in histograms and (C) quantified as percentage of cells in the indicated gate or relative to naïve control for 3 independent experiments. Statistical analysis was performed using Student's t-test with \*:  $p < 0.05$ , \*\*  $p < 0.01$ , \*\*\*  $p < 0.001$ .

## D Results

### 3.5 RNA expression in activated T-WT versus T-Rptor<sup>-/-</sup> and T-Rictor<sup>-/-</sup> cells

The in this study established staining method with Pyronin Y was next used to visualize RNA expression in T-Rptor<sup>-/-</sup> and T-Rictor<sup>-/-</sup> cells. Magnetically purified CD4<sup>+</sup> and CD8<sup>+</sup> T-WT, T-Rptor<sup>-/-</sup> and T-Rictor<sup>-/-</sup> cells were stimulated with anti-CD3/28 *in vitro* for 48 hours. CD4<sup>+</sup> and CD8<sup>+</sup> T cells were subsequently stained with Pyronin Y and DAPI together in the same tube. Upon stimulation CD4<sup>+</sup> T-WT cells upregulated RNA expression up to 9-fold, CD8<sup>+</sup> T-WT cells up to 12-fold in comparison to unstimulated cells. Accordingly, 45% of T-WT cells were detected in S/G<sub>2</sub>/M-phases. T-Rptor<sup>-/-</sup> cells showed a 2-fold lower upregulation of RNA. Nevertheless, 17% of CD4<sup>+</sup> and 31% of CD8<sup>+</sup> T-Rptor<sup>-/-</sup> cells were found in the S/G<sub>2</sub>/M stages. T-Rictor<sup>-/-</sup> cells even showed a ~1.5 times higher expression of RNA than T-WT cells, with comparable if not slightly more cells in S/G<sub>2</sub>/M-phases (Fig. D3.5). In agreement with observations described in 2.2, showing that TCR transgenic T-Rptor<sup>-/-</sup> cells could proliferate albeit slower upon transfer into antigen-presenting mice, T-Rptor<sup>-/-</sup> cells were able to enter cell cycle upon *in vitro* stimulation for 48 hours, but with a lower extend than T-WT cells. Furthermore, T-Rptor<sup>-/-</sup> cells were not able to upregulate RNA expression to the same extend as T-WT cells. This indicates a defect in RNA upregulation in T-Rptor<sup>-/-</sup> but not T-Rictor<sup>-/-</sup> cells, which results in less cells in S/G<sub>2</sub>/M-phases.

## D Results

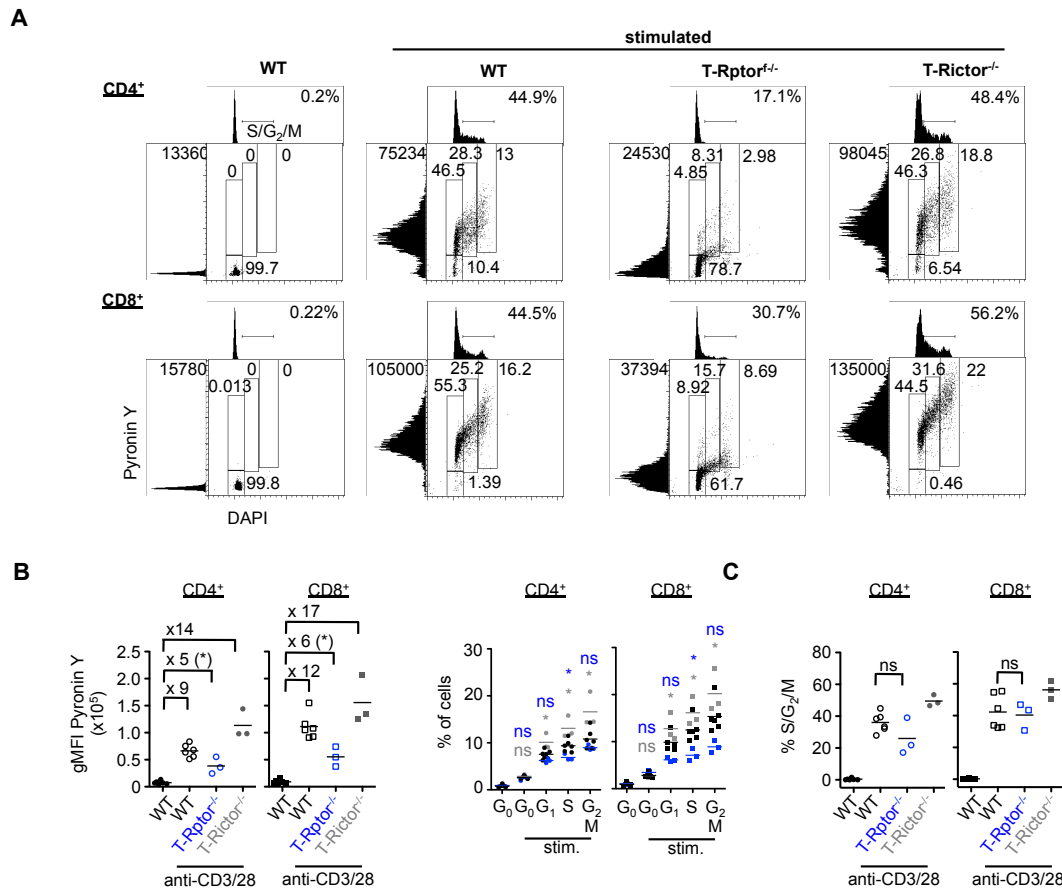


**Figure D3.5: RNA expression in activated T-WT versus T-Rptor<sup>-/-</sup> and T-Rictor<sup>-/-</sup> cells.**

(A) MACS-purified CD4<sup>+</sup> and CD8<sup>+</sup> T cells were incubated in 96-well plates *in vitro* with 5ng/mL IL-7 in the presence or absence of 10  $\mu$ g/mL anti-CD3/28 antibodies for 48 hours. Fixed and permeabilized CD4<sup>+</sup> and CD8<sup>+</sup> T cells were stained with DAPI (250  $\mu$ g/mL) and Pyronin Y (625  $\mu$ g/mL) in the same reaction tube and analyzed by flow cytometry. Results are representative of 3-6 independent experiments. (B) Quantification of gMFI or (C) percentage was calculated for 3-6 independent experiments. Statistical analysis was performed using Student's t-test with \*: p<0.05, \*\* p < 0.01, \*\*\* p< 0.001.

### 3.6 Differential translational activity in mTORC1-deficient T cells

It is published that mTORC1 is crucial for the translation of a specific group of mRNAs, the 5' TOP mRNA. 5' TOP mRNAs mainly encode for proteins involved into RNA and protein synthesis as well as ribosomal assembly (Araki *et al.*, 2017; Hukelmann *et al.*, 2016; Iadevaia *et al.*, 2012; Tan *et al.*, 2017a; Thoreen *et al.*, 2012). In this study we found a significantly reduced expression of global and ribosomal RNA in T-Rptor<sup>-/-</sup> cells. We further tested whether this has an impact on the translational activity of activated T-Rptor<sup>-/-</sup> cells.

## D Results

CD4<sup>+</sup> T-WT and T-Rpator<sup>-/-</sup> were stimulated with anti-CD3/28 for 48 hours *in vitro* and metabolically labeled with the fluorescence-tagged methionine analogue L-homopropargylglycine (L-HPG) for 30 minutes (Fig. D3.6 A). At this particular time point, a lack of mTORC1 did show a significant reduction of the translational activity in CD4<sup>+</sup> T-Rpator<sup>-/-</sup> cells. Nevertheless, both T-WT and T-Rpator<sup>-/-</sup> cells increased their translational activity up to 80-fold and 70-fold upon stimulation, respectively. Thus, translational activity was not completely diminished but significantly reduced in mTORC1-deficient CD4<sup>+</sup> T cells. This reduction can be due to the impaired translation of 5' TOP mRNAs. The translational activity over time needs to be further investigated in CD4<sup>+</sup> and CD8<sup>+</sup> T cells. Moreover, the effect on the abundance of total protein is not tested so far.

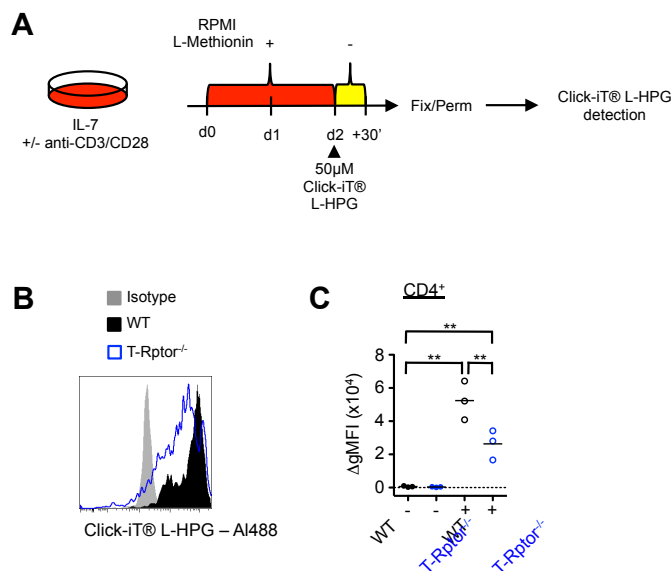


**Figure D3.6: Differential translational activity in CD4<sup>+</sup> T-Rpator<sup>-/-</sup> cells.**

(A) Magnetically purified CD4<sup>+</sup> T-WT (black) or T-Rpator<sup>-/-</sup> (blue) cells were incubated with 5 ng/mL IL-7 in the presence (black, blue) or absence (gray) of 10 µg/mL anti-CD3/28 antibodies for 48 hours *in vitro*. The medium was replaced by L-Methionine free medium and incubated with Click-iT L-HPG for 30 minutes. Incorporated L-HPG was detected in fixed and permeabilized cells by chemoselective ligation (also known as click reaction) between azide and alkyne, where the alkyne-modified protein is detected with Alexa Fluor 488. (B) Incorporated Click-iT L-HPG –AI488 in unstimulated (gray) or stimulated WT (black) or T-Rpator<sup>-/-</sup> (blue) cells measured by flow cytometry. Results are representative of three independent experiments. (C) Geometrical intensities were quantified and normalized to the intensities of AI-488 in cells treated without Click iT L-HPG. Statistical analysis was performed using Student's t-test with \*: p<0.05, \*\* p < 0.01, \*\*\* p< 0.001.

## D Results

### 3.7 Drug-induced inhibition of RNA Polymerase I reduces the expression of RNA and limits cell cycle entry in vitro

To further dissect which downstream targets of mTORC1 contribute to proliferation in T cells, an inhibition of RNA expression was induced with drugs interfering with the mTORC1-signaling pathway. Torin 1 is a very potent inhibitor of mTOR selectively inhibiting kinase activities of mTORC1 and 2 (Liu *et al.*, 2012). Together with 2-deoxy-D-glucose (2-DG), a glucose analogue which terminates glycolysis, it functioned as a positive control inducing a similar phenotype observed in T-Rptor<sup>-/-</sup> cells (Cham *et al.*, 2008). Tigecycline binds to 30S ribosomal subunits and therefore inhibits the activity of mitochondrial ribosomes (Skrtic *et al.*, 2011). To inhibit the activity of RNA Polymerases I and II, actinomycin D and quarfloxin (CX-5343) were used (Bywater *et al.*, 2012; Drygin *et al.*, 2011; Perry & Kelley, 1970). Quarfloxin exclusively inhibits RNA Polymerase I and thus the synthesis of 47S RNA and actinomycin D the activity of both Polymerases in a dose dependent manner. Magnetically enriched CD4<sup>+</sup> and CD8<sup>+</sup> T-WT cells were stimulated with anti-CD3/28 for 48h in the absence or presence of the named inhibitors with increasing doses. With very high doses of torin 1 and 2-DG, not only cell cycle entry and proliferation were blocked but also a ten- to twenty-fold reduction of RNA contents were detected in comparison to untreated activated T cells (Fig. D3.7 A and B). Furthermore, cell cycle entry, RNA expression, T cell blasting and proliferation were affected in a dose-dependent manner (Fig. D3.7 C-F). An inhibition with actinomycin D has shown similar patterns as torin 1 and 2-DG: a dose-dependent reduction of cell cycle entry, RNA expression, blasting and proliferation resulting in completely blocking of clonal expansion with very high doses. An inhibition of RNA Polymerase I activity alone with very high doses of quarfloxin, was also able to block proliferation and cell cycle entry but to a lesser extent than torin 1, 2-DG and actinomycin D. Furthermore, the highest inhibitor dose possible, merely showed a four-fold reduction of RNA expression in comparison to untreated cells in CD4<sup>+</sup> and a two-fold reduction in CD8<sup>+</sup> T cells, being in line with RNA expression levels in T-Rptor<sup>-/-</sup> cells (Fig. D3.7 A-F). Thus, an exclusive inhibition of RNA Polymerase I dependent rRNA synthesis by quarfloxin, was enough to phenocopy the RNA expression and cell cycle progression patterns of T-Rptor<sup>-/-</sup> cells. In contrast, even very high doses of tigecycline had no effect on global RNA expression and proliferation in stimulated T cells, as expected, since it only targets mitochondrial ribosomal RNA expression. Of note, CD4<sup>+</sup> T cells were more susceptible to torin 1, 2-DG, actinomycin D and quarfloxin.

## D Results

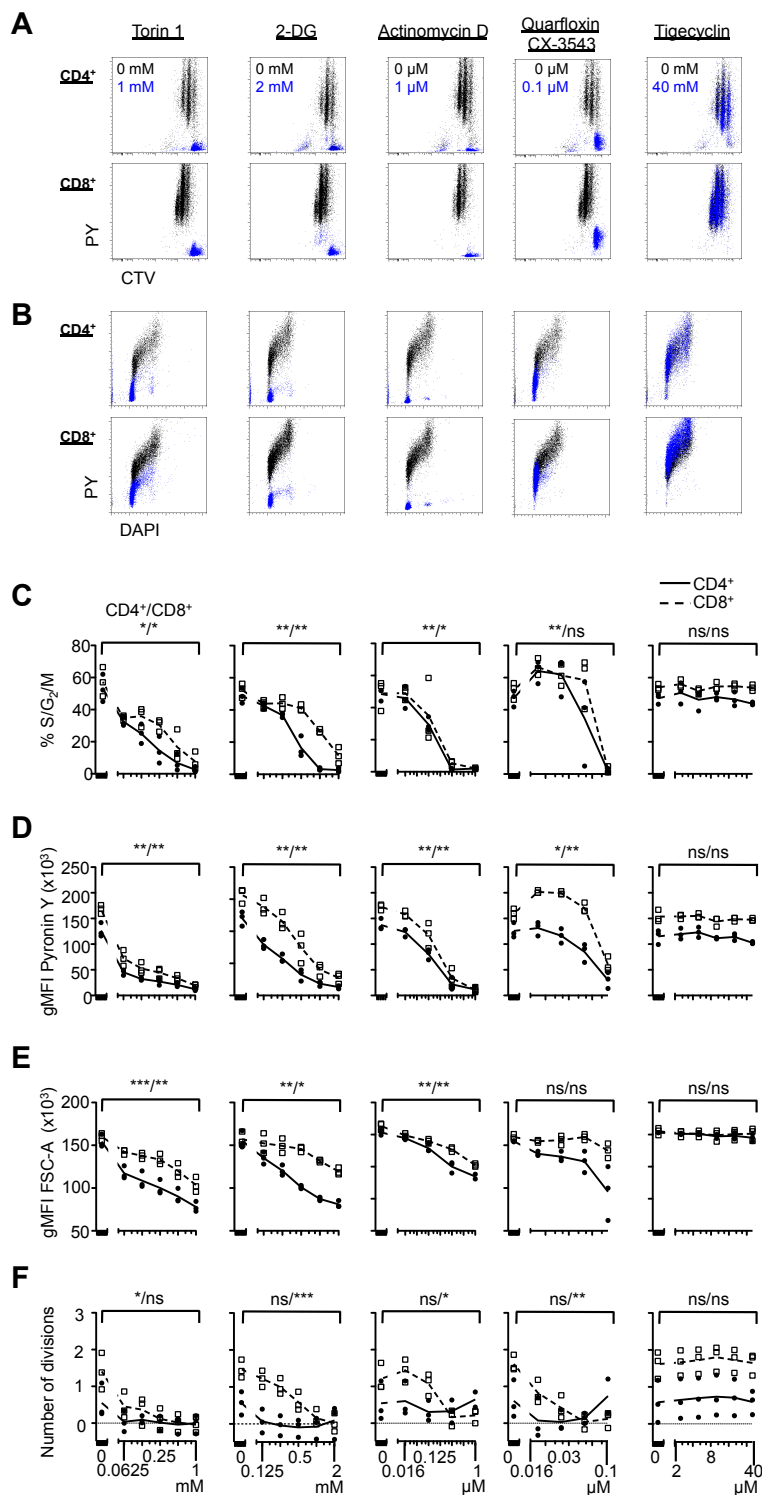


**Figure D3.7: RNA Polymerase I inhibition in T-WT cells is sufficient to phenocopy RNA expression and proliferation patterns from T-Rptor<sup>-/-</sup> cells.**

(A-F) MACS-purified CD4<sup>+</sup> and CD8<sup>+</sup> T-WT cells were CTV-labeled and incubated in 96-well plates *in vitro* with 5ng/mL IL-7 in the presence or absence of 10μg/mL anti-CD3/28 antibodies for 48 hours with increasing levels of torin 1, 2-DG, actinomycin D, quarfloxin and tigecyclin. Fixed and permeabilized CD4<sup>+</sup> and CD8<sup>+</sup> T cells were stained with DAPI (250 μg/mL), Pyronin Y (625 μg/mL) and for CD71 in the same

## D Results

reaction tube and analyzed by flow cytometry. Pyronin Y was plotted against CTV (A) and DAPI (B) with (blue) or without (black) inhibitors in indicated concentrations. Results are representative of 3 independent experiments (C-F) Percentage of cells in S/G<sub>2</sub>/M-phases (C) gMFI of Pyronin Y (D) and FSC-A (E) as well as the average cell division number defined as  $N = \log_2(\text{gMFI}_{\text{ctrl}}/\text{gMFI}_{\text{sample}})$  (F) were monitored in CD4<sup>+</sup> (line) and CD8<sup>+</sup> (dashed) T cells; x-axes shown in log<sub>2</sub> scale. Statistical analysis was performed using paired Student's t-test with \*: p<0.05, \*\* p < 0.01, \*\*\* p< 0.001.

### 4 Persistent RNA synthesis is required for T cell proliferation

A previously published study by Yang and colleagues demonstrated that mTORC1 activity is critical for the transition from quiescent G<sub>0</sub> to S phase and becomes less important after cell cycle entry (Yang *et al.*, 2013). The next experiment addressed the question if this is also true for RNA Polymerase I activity or if ongoing rRNA synthesis is required for cell cycle progression.

To address this question, CD4<sup>+</sup> and CD8<sup>+</sup> T-WT cell were stimulated *in vitro* for 24 hours (Fig. D4 A). Within this period, both cell types increased two-fold in size and showed a 6-fold upregulation of global RNA expression, indicating an exit from quiescence into G<sub>1</sub> phase. Nevertheless, no proliferation was detected in CD4<sup>+</sup> and CD8<sup>+</sup> T cells 24 hours post-stimulation (Fig. D4 B, C). Next, 0.2 μM quarfloxin was added to stimulated cells for two more days (Fig D4 A). As shown in figure D3.7, an inhibition of RNA Polymerase I by quarfloxin was sufficient to fully diminish RNA expression and cell cycle progression, when added to the T cells at the time of activation. If administered 24 hours after an initial stimulation, global RNA expression and cell size was hardly affected in CD4<sup>+</sup> and CD8<sup>+</sup> T-WT cells. Nevertheless, proliferation was fully blocked in quarfloxin treated T-WT cells, whereas untreated cells were able to divide up to three-times within 72 hours. This indicates that other than mTORC1 activity, RNA Polymerase I induced rRNA expression is not only required early upon activation but also for continuous T cell proliferation.

## D Results

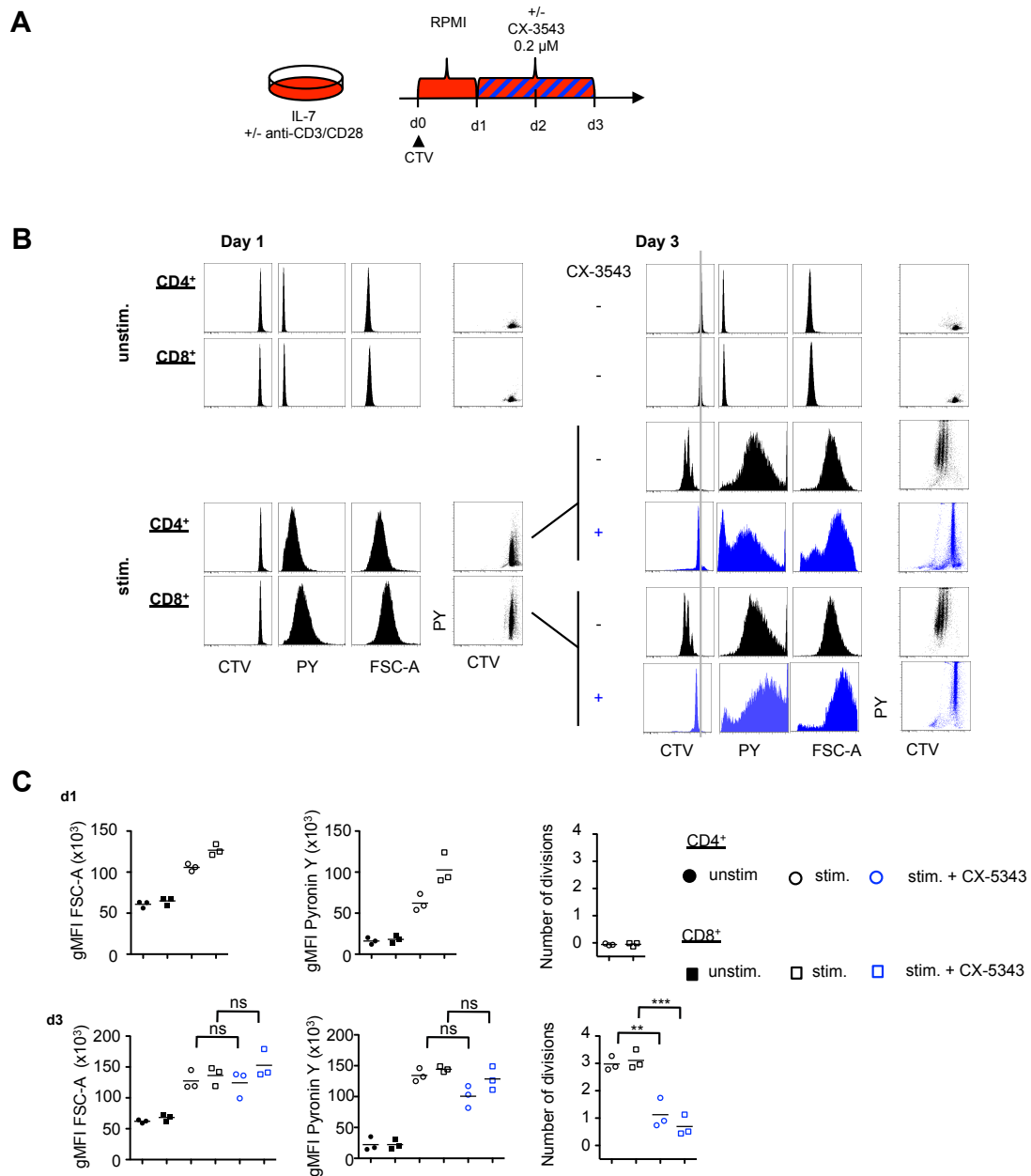


**Figure D4: Persistent RNA synthesis is required for T cell proliferation.**

(A) MACS-purified CD4<sup>+</sup> and CD8<sup>+</sup> T-WT cells were labeled with CTV and incubated in 96-well plates *in vitro* with 5 ng/mL IL-7 in the presence or absence of 10  $\mu$ g/mL anti-CD3/28 antibodies for 72 hours. If indicated 0.2  $\mu$ M CX-5343 was added 24 hours post-stimulation. (B) Fixed and permeabilized CD4<sup>+</sup> and CD8<sup>+</sup> T cells were stained with Pyronin Y (625  $\mu$ g/mL) in the same reaction tube and analyzed by flow cytometry. Results are representative of three independent experiments. (C) The gMFI of FSC-A and Pyronin Y as well as the average cell division number defined as  $N = \log_2(\text{gMFI}_{\text{ctrl}}/\text{gMFI}_{\text{sample}})$  was calculated. Statistical analysis was performed using Student's t-test with \*:  $p < 0.05$ , \*\*  $p < 0.01$ , \*\*\*  $p < 0.001$ .

### 5 T-Rptor<sup>-/-</sup> cells show a lower cell cycle progression with changed cell abundance in G<sub>0</sub>- and S-phase

Cell cycle analysis was performed to dissect which cell phase was slowed down in T-Rptor<sup>-/-</sup> cells. As described in 3.3, a DNA staining with DAPI can distinguish between G<sub>0</sub>/G<sub>1</sub>, S and G<sub>2</sub>/M-phase (Fig. D5 A). To clearly separate cells in G<sub>0</sub> from cells that already have entered G<sub>1</sub>-phase an antibody specific for phosphorylated retinoblastoma protein at Serine 780 (pRb) was used. When phosphorylated, Rb induces G<sub>0</sub> to G<sub>1</sub> transition. The detection of phosphorylated Histone H3 with fluorescently labeled anti-H3P allows distinction of cells specifically in M but not G<sub>2</sub> phase (Fig. D5 B).

As already described in Figure D3.3, less T-Rptor<sup>-/-</sup> than T-WT cells have entered cell cycle upon *in vitro* stimulation with anti-CD3/28 for 48h (Fig. D3.3; Fig D5 A). With 40% CD4<sup>+</sup> and 12% CD8<sup>+</sup> T-Rptor<sup>-/-</sup> cells being detected in G<sub>0</sub>, half as many cells have left G<sub>0</sub> in comparison to T-WT cells upon stimulation (Fig. D5 C). In contrast, similar levels of T-WT and T-Rptor<sup>-/-</sup> cells were detected in G<sub>1</sub>-phase. Between 40% and 50% of all stimulated cells can be found in this cell cycle phase. Furthermore, only minor but detectable differences have been observed in G<sub>2</sub> and M phases. A significant disadvantage of T-Rptor<sup>-/-</sup> cells was observed in the S-phase of the cell cycle with three times less CD4<sup>+</sup> (6.2%) and twice less CD8<sup>+</sup> (11.6%) T cells in S-phase in comparison to T-WT cells. Hence, T-Rptor<sup>-/-</sup> cells showed a disadvantage in transitioning from G<sub>0</sub> to G<sub>1</sub> and G<sub>1</sub> into S phase.

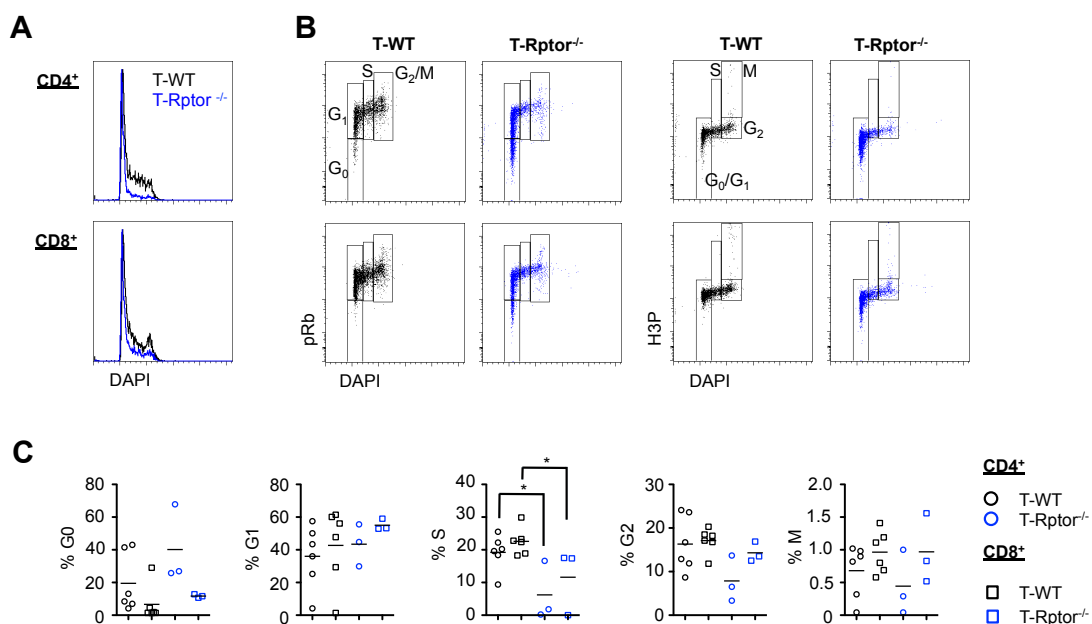


Figure D5: Lower cell cycle progression in G<sub>0</sub>- and S-phase in T-Rptor<sup>-/-</sup> cells.

## D Results

(A-C) MACS-purified CD4<sup>+</sup> and CD8<sup>+</sup> T-WT cells were incubated in 96-well plates *in vitro* with 5 ng/mL IL-7 in the presence or absence of 10 µg/mL anti-CD3/28 antibodies for 48 hours. Fixed and permeabilized cells were stained with DAPI (250 µg/mL) (A) and either pRb or H3P (B) and analyzed by flow cytometry. Results are representative of 3-6 independent experiments. (C) Percentage of cells in G<sub>0</sub>, G<sub>1</sub>, S, G<sub>2</sub> and M were calculated as indicated in (B). Statistical analysis was performed using Student's t-test with \*: p<0.05, \*\* p < 0.01, \*\*\* p< 0.001.

### **II Development of a mouse system to investigate CD8<sup>+</sup> T cell development upon acute and chronic antigen presentation under sterile conditions**

#### **1 Improved performance of iOVA by the Tet-repressor KRAB**

In order to improve the tools for the analysis of T cell responses to acute and chronic antigen-presentation under sterile conditions, a mouse system was developed that allowed inducing or withdrawing antigen-expression on MHC-I at defined time points. In the past, the termination of antigen-presentation could only be investigated in systems of bacterial infections by antibiotic treatment (Corbin & Harty, 2004; Williams & Bevan, 2004). Furthermore, studies with chronic and acute strains of the lymphocytic choriomeningitis virus (LCMV) were performed to analyze the duration of antigen presentation on T cell development (Wherry *et al.*, 2007). In these systems, a separation of the antigen stimulus from general inflammation is not necessarily possible. Thus in this work a doxycycline-inducible antigen expression system was developed that allowed a tuning of antigen-presentation on APCs and a separation of antigen-stimulus from inflammation.

Previously, a doxycycline-inducible antigen expression system of an MHC-I restricted T cell antigen was developed in this laboratory (Rabenstein *et al.*, 2014). Upon doxycycline treatment (100 µg/mL in drinking water), the tetracycline-transactivator converts into an active state and induces the expression of OVA<sub>257-264</sub> in the context of H-2K<sup>b</sup>. Adoptively transferred OT-I T cells recognize the peptide-MHC complex on APCs and start to expand (Fig. D6.1 A).

As shown in figure D1 C and published in Rabenstein *et al.*, 2014, CFSE-labeled OT-I T cells were able to proliferate extensively three days post-transfer into iOVA mice independent of doxycycline and the expression of the rtTA<sup>S2</sup> (Rabenstein *et al.*, 2014).

To abolish this leakiness, iOVA mice were crossed to transgenic mice expressing the tetracycline-dependent repressor KRAB, generating iOVA-KRAB mice. KRAB is a fusion protein of the DNA binding domain of the tetracycline repressor from *E. coli* and the Krüppel-associated box (KRAB) domain of the human Kox1 zinc finger protein (Deuschle *et al.*, 1995). It is expressed under the human phosphoglycerate kinase promoter and constitutively active in the absence of doxycycline (Barde *et al.*, 2009). KRAB domains recruit histone deacetylases and histone methyltransferases and thus mediate a reversible transcriptional repression of target genes (Groner *et al.*, 2010; Margolin *et al.*, 1994). In the presence of doxycycline, the tetracycline-dependent

## D Results

transrepressor will be inactivated and in turn the transactivator can bind and induce the expression of OVA<sub>257-264</sub> on MHC-I (Fig. D6.1 B). The tight expression of the target antigen is demonstrated in figure D1 C by a five-fold reduction of OT-I T cells responding to peptide-MHC expression in the presence of KRAB.

To further analyze the kinetics and time courses in which antigen-presentation can be turned on and off,  $1 \times 10^6$  CFSE-labeled OT-I T cells were transferred into iOVA-KRAB mice. The administration of doxycycline (100  $\mu\text{g}/\text{mL}$ ) in the drinking water was started and stopped at different time points. T cell responses were monitored three days post-transfer by the dilution of CFSE. Figure D1 D shows that a pre-treatment with doxycycline for one week was not enough to induce OT-I T cell proliferation. Rather a treatment of at least 14 days before transfer was necessary to induce proliferation in OT-I T cells. On the other hand, ten days were sufficient to withdraw antigen-presentation in APCs and thus proliferation of OT-I T cells. This resulted in an experimental setup further described in figure D6.3.

## D Results

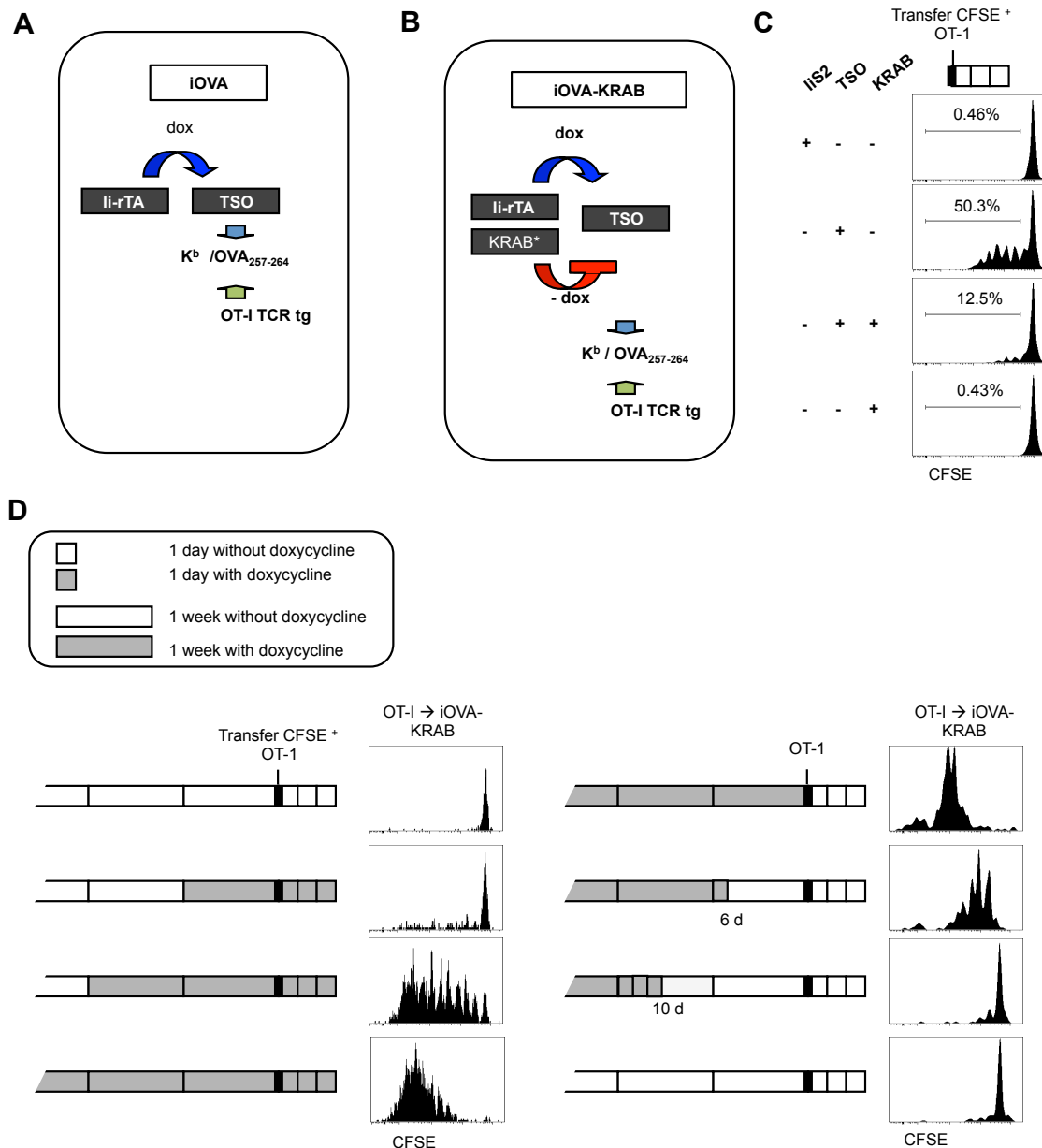


**Figure D6.1: The tet-repressor KRAB improves the performance of TSO expression.**

(A) Scheme of double transgenics for tetracycline-inducible epitope expression. To generate mice with controllable presentation of the H-2K<sup>b</sup>/OVA<sub>257-264</sub> complex, a transcriptional unit consisting of a signal sequence, the epitope, stop codons and a splicing substrate was put under the control of tet-responsive regulatory elements (TSO) and introduced into the germ line of B6 animals. This minigene targets the OVA<sub>257-264</sub> peptide directly to the ER in a proteasome- and TAP- independent fashion and excludes indirect presentation of transferred OVA protein by other APCs. TSO<sup>+</sup> founder animals were bred to the li-rTA line. iOVA offsprings displayed dox-inducible OVA<sub>257-264</sub> presentation in vivo as evidenced by proliferation of CFSE-labeled OT-I TCR transgenic T cells. (B) The repressor KRAB (hPGK-tTRKRAB), which induces DNA methylation and H3K9me3 via KAP1 was crossed into iOVA mice, to diminish a dox-independent expression of OVA<sub>257-264</sub> on H-2K<sup>b</sup> in iOVA mice. (C) 1 × 10<sup>6</sup> CFSE-labeled CD45.1.1<sup>+</sup> OT-I TCR transgenic T cells were transferred into CD45.2.2<sup>+</sup> iOVA recipient mice with genotypes as indicated. Responsiveness of T cells was measured by CFSE-

## D Results

dilution three days post-transfer. (D) Inducibility and leak tightness of the expression of the H-2K<sup>b</sup>/OVA<sub>257-264</sub> complex was tested.  $1 \times 10^6$  naive CFSE-labeled OT-I T cells were transferred into iOVA-KRAB recipient mice treated with 100 µg/mL (gray box) or without (white box) doxycycline at time points and frames as indicated. CFSE dilution was detected by flow cytometry on three days post-transfer.

### 2 Effector T cell generation in iOVA-KRAB mice

We next tested if antigen-presentation in iOVA-KRAB mice is sufficient to induce effector cell development in OT-I T cells. Thus,  $1 \times 10^6$  OT-I T cells were adoptively transferred into iMCC-KRAB mice pre-treated with 40 µg/mL anti-CD40 one day before transfer and tested five days later. The oral exposure of doxycycline to iOVA-KRAB mice started at least 14 days before cell transfer with doxycycline-containing food and was switched to 100 µg/mL doxycycline in the drinking water until the end of the experiment at the day of transfer. As negative control, OT-I T cells were transferred into antigen-free B6 hosts. To test the proliferation of OT-I T cells, cells were labeled with CFSE before transfer. Upon antigen-exposure in iOVA-KRAB mice, OT-I T cells divided approximately six times within five days. IFN $\gamma$  and granzyme B expression was measured in OT-I T cells after restimulation with PMA and ionomycin *in vitro*. The expression of IFN $\gamma$  was around twice as high in comparison to naïve OT-I T cells, the expression of granzyme B was only slightly increased. Furthermore, the killing capacity of OT-I T cells was tested. Splenocytes from B6 mice were pulsed with a high and low dose of Q4H7 peptide and subsequently labeled with different doses of CFSE and transferred into either B6 or iOVA-KRAB mice five days after OT-I T cells were injected. The clearance of antigen-pulsed APCs was analyzed one day later. Antigen-exposed OT-I T cells were able to remove APCs pulsed with high concentrations of antigen (1 µg/mL) nearly completely and approximately one third of APCs pulsed with low doses of antigen were killed. Thus, OT-I T cells are able to develop into cytotoxic effector T cells in doxycycline-treated iOVA-KRAB mice.

## D Results

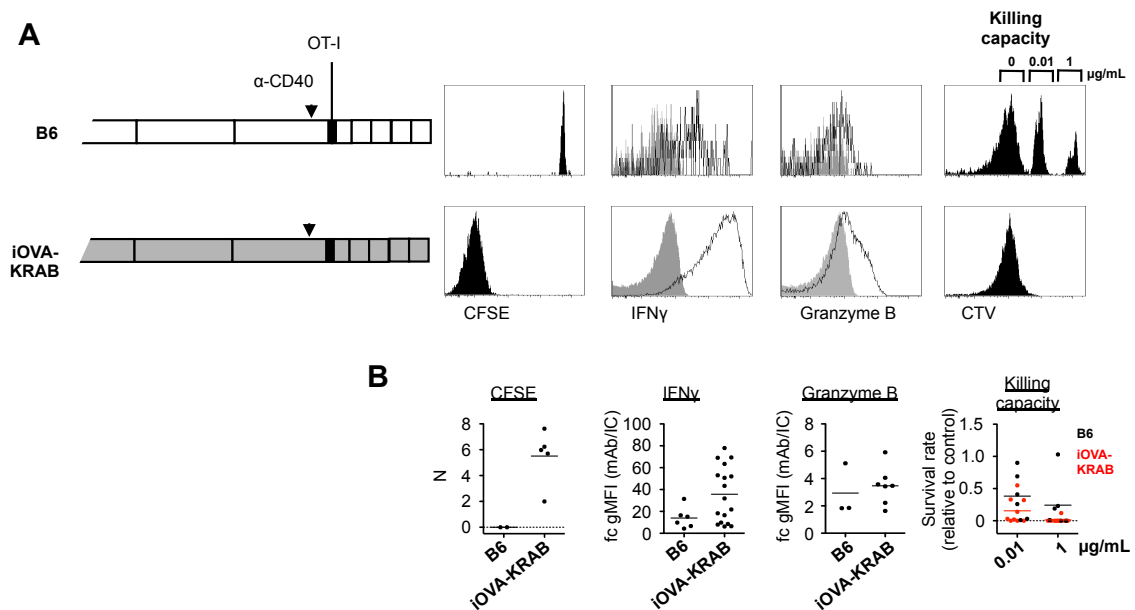


**Figure D6.2: Effector T cell generation in iOVA-KRAB mice.**

(A)  $1 \times 10^6$  CD45.1.1<sup>+</sup> OT-I TCR transgenic T cells were transferred into either CD45.2.2<sup>+</sup> B6 mice or with doxycycline-treated (100  $\mu$ g/mL in drinking water) iOVA-KRAB mice. CFSE dilution, IFN $\gamma$  and granzyme B expression were displayed by flow cytometry five days later. To test killing capacity of OT-I T cells five days post-transfer  $1 \times 10^6$  antigen presenting cells from spleen were pulsed with either 0.1  $\mu$ g/mL, 1  $\mu$ g/mL or none Q4H7 peptide in vitro and labeled with medium, high or no dose of cell trace violet. Same amount of CD45.1.2<sup>+</sup> pulsed cells were transferred into recipient mice. Killing capacity was measured one day after challenge with peptide-pulsed APCs. (B) Average division number of transferred T cells was calculated as  $N = \log_2(\text{gMFI}_{\text{ctrl}}/\text{gMFI}_{\text{sample}})$ . Fold change of the geometrical MFI of cells stained for the specific antigen against isotype control was measured for IFN $\gamma$  and granzyme B. The relative survival rate of peptide pulsed APCs was calculated. APCs transferred into B6 mice are shown in black, those transferred in iOVA-KRAB mice in red. Survival rate was calculated in relation to the abundance of unpulsed APCs.

### 3 Persistent antigen-exposure compromises memory formation in OT-I T cells

To further investigate the effect of transient and persistent antigen exposure to OT-I T cells on memory formation,  $1 \times 10^6$  OT-I T cells were adoptively transferred into recipient mice under three different conditions and analyzed four weeks later. Recipient mice were pre-treated with anti-CD40 (40  $\mu$ g/mouse) one day before transfer. In condition one, OT-I T cells were transferred into antigen-free B6 mice not treated with doxycycline. In condition two, cells were transferred into iOVA-KRAB recipients treated with doxycycline-containing food for at least 14 days before transfer until the day of transfer and in condition 3 iOVA-KRAB recipient mice were additionally exposed to

## D Results

doxycycline in the drinking water (100 µg/mL) until the end of the experiment starting on the day before transfer (Fig. D6.3 A). The surface expression of several activation markers was tested. A differential expression pattern was detected between transiently and persistently antigen-exposed OT-I T cells.

Even though CD44 expression was comparably high in transiently and persistently treated OT-I T cells, the expression of CD62L was significantly reduced six-fold in persistently treated animals. Furthermore, the expression of Ly6C was reduced by half, CXCR3 six-fold and CD127 four-fold on persistently treated OT-I T cells. In addition CD73 expression decreased two- to three-fold. On the other hand persistently treated OT-I T cells monitored a significantly ten-times higher expression of CD69 and an approximately six-fold increased expression of PD-1 (Fig. D6.3 B). Next, cytokine expression was tested after restimulation with PMA and ionomycin *in vitro*. In OT-I T cells persistently exposed to antigen, the expression of IFN $\gamma$  and TNF $\alpha$  were reduced five- and three-times, respectively (Fig. D6.3 C). In contrast to that, killing capacity was even slightly improved in persistently stimulated OT-I T cells (Fig. D6.3 D). Only slight differences in absolute T cell numbers were detected. This indicates, that a persistent antigen-exposure to OT-I T cells under sterile conditions can only partly compromise memory formation.

## D Results

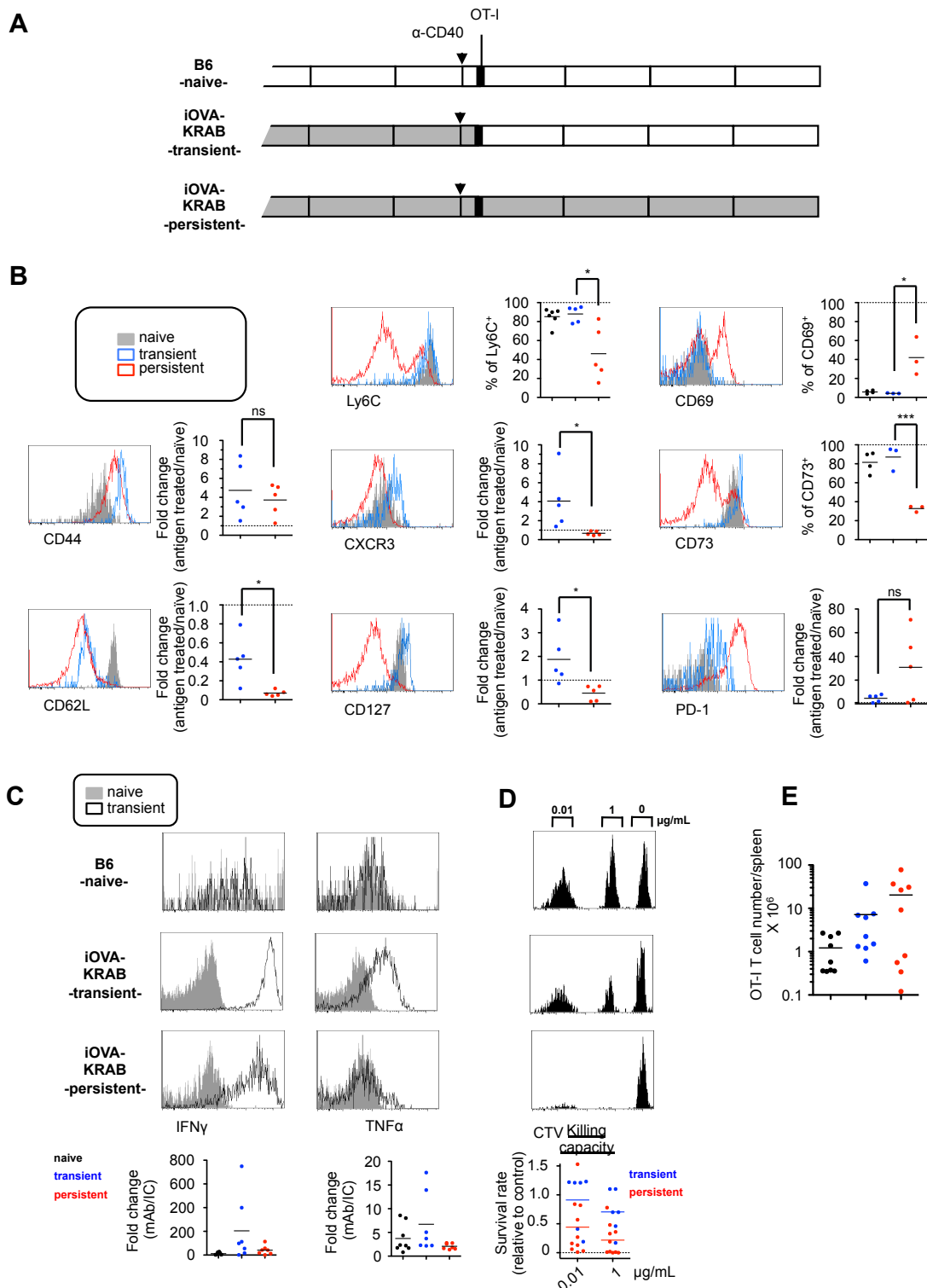


**Figure D6.3 Persistent antigen-exposure to T cells partly compromises memory formation.**

(A)  $1 \times 10^6$  CD45.1.1<sup>+</sup> OT-I TCR transgenic T cells were transferred into either CD45.2.2<sup>+</sup> B6 mice (naïve) or iOVA-KRAB mice treated with doxycycline (100  $\mu\text{g}/\text{mL}$ ) for at least 14 days before transfer (transient) or for at least 14 days post-transfer and beyond (persistent). Recipient mice were injected with 40  $\mu\text{g}$  anti-CD40 i.p. one day

## D Results

before transfer. (B) The expression of surface markers was displayed on day 30 post-transfer in naïve (gray) transiently (blue) and persistently (red) stimulated OT-I T cells by flow cytometry. The fold change of the geometrical MFIs of antigen-treated against naïve OT-I T cells was calculated for CD44, CD62L, CXCR3, CD127 and PD-1 and for markers with a non-homogenous expression, the percentage of positively gated cells was determined (Ly6C, CD69 and CD73). (C) On day 30 post-transfer, OT-I T cells were extracted from spleen and restimulated with PMA (10 ng/mL) and ionomycin (0.5 µg/mL) *in vitro* and subsequently stained for IFN $\gamma$  and TNF $\alpha$  (black) or their respective isotype controls (gray). Fold change was calculated by dividing the geometrical MFIs of the specific antibody to isotype control. (D) To test killing capacity of OT-I T cells 30 days post-transfer  $1 \times 10^6$  antigen presenting cells from spleen were pulsed with either 0.1 µg/mL, 1 µg/mL or none Q4H7 peptide *in vitro* and labeled with medium, high or no dose of cell trace violet. Same amount of CD45.1.2<sup>+</sup> pulsed cells were transferred into recipient mice. Killing capacity was measured one day after challenge with peptide-pulsed APCs. The relative survival rate of peptide pulsed APCs was calculated. APCs transferred into transiently stimulated mice are shown in blue, those transferred in persistently treated mice in red. Survival rate was calculated in relation to the abundance of unpulsed APCs. Statistical analysis was performed using paired Student's t-test with \*:  $p < 0.05$ , \*\*  $p < 0.01$ , \*\*\*  $p < 0.001$

### 4 Establishment of an antigen-inducible latent virus in mice

Gamma herpes viruses such as the Epstein bar virus (EBV) and the Kaposi's sarcoma virus (KSHV) can cause severe infections and are associated with lymphomas in immunocompromised patients. In healthy patients on the other hand these viruses can be found in B cells in a latent state, with having no effect on the host (Ganem, 1997; Schulz, 1998). Since OT-I T cells were only incompletely impaired in iOVA-KRAB mice upon persistent antigen-exposure, MHV-68 was tested with the future perspective of comparing it to iOVA-KRAB mice but under inflammatory conditions. The murine gamma herpes virus 68 (MHV-68) was developed as animal model of gamma herpes virus pathogenesis. Prof. Heiko Adler and colleagues cloned the MHV-68 genome as a bacterial artificial chromosome (BAC) in *E. coli* (Adler *et al.*, 2000). In collaboration with his lab, a version of MHV-68 was developed carrying the sequence for OVA<sub>257-264</sub> under the control of the tet-operator, MHV-68\_OVA. Upon the infection of mice expressing the tet-transactivator, ovalbumin can be expressed on MHC-I of infected cells. R26-rtTA x KRAB mice were tested as hosts under different conditions. In these mice, the reverse tet-transactivator (rtTA<sup>M2</sup>) gene locus is ubiquitously expressed under the Rosa 26 promoter (Hochedlinger *et al.*, 2005). If treated with doxycycline, rtTA<sup>M2</sup> converts into its active form and induced the expression of genes under the control of the tet-operator (Fig. D6.4 A).

In this experimental setup,  $1 \times 10^6$  naïve OT-I T cells were labeled with CFSE and subsequently transferred into R26-rtTA mice, either carrying the Rosa-26-rtTA locus as one (R26<sup>wt/ki</sup>) or two (R26<sup>ki/ki</sup>) alleles or into mice negative for the transgene (R26<sup>wt/wt</sup>).

## D Results

Host mice were infected with  $2 \times 10^5$  PFU MHV-68\_OVA one day later. Proliferation was tested three days after infection. No proliferation of OT-I T cells was detected in uninfected R26<sup>wt/wt</sup> mice. Upon infection, OT-I T cell proliferation was induced independent of the presence of doxycycline. This effect could be reduced by almost half in infected heterozygous R26<sup>wt/ki</sup> mice that additionally expressed the tet-transrepressor KRAB. KRAB alone was not able to reduce the induction in R26<sup>ki/ki</sup> mice to the same extent, indicating that KRAB can only repress the expression of the peptide in the presence of low levels of rtTA<sup>M2</sup>. If treated with 100 µg/mL doxycycline in the drinking water from day 14 before infection on, a proliferation was induced in R26<sup>wt/ki</sup> as well as in R26<sup>ki/ki</sup> mice to an expand of approximately 80%. Thus, OVA<sub>257-264</sub> expression can be controlled by doxycycline in heterozygous R26-rtTA x KRAB mice infected with MHV-68\_OVA, creating an inducible virus mouse model for challenging OT-I T cells, *in vivo* (Fig. D6.4 B). In the future, this virus can be used to study the effect of transient and persistent antigen-presentation on TCR transgenic OT-I T cells under inflammatory conditions side by side. So far this question could only be addressed by using different strains of the same virus such as the chronic and acute LCMV clone 13 and Armstrong in different doses (Wherry *et al.*, 2003; Zajac *et al.*, 1998).

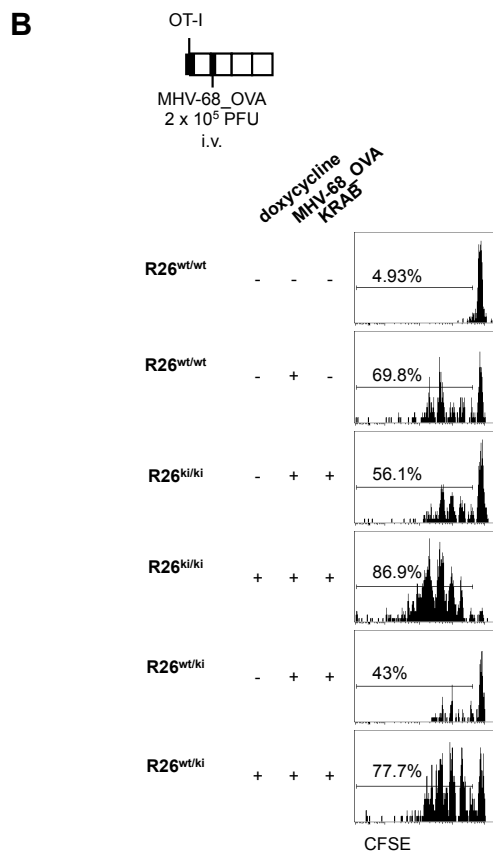
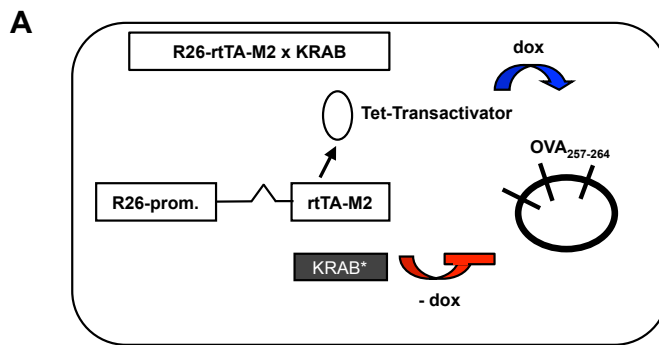


**Figure D6.4 KRAB improves MHV-68\_OVA performance in R26-rtTA-M2 x KRAB mice.**

(A) Scheme of MHV-68\_OVA infected R26-rtTA-M2 x KRAB mice. In the presence of doxycycline, the ubiquitously expressed tet-transactivator can bind to the tet-operator on MHV-68\_OVA and induce the expression of OVA<sub>257-263</sub>. In the absence of doxycycline, the tet-repressor KRAB binds to the tet-operator and inhibits the synthesis of OVA<sub>257-264</sub>. (B) 1 x 10<sup>6</sup> CFSE-labeled OT-I T cells were transferred into R26-rtTA-M2 mice with different copy numbers of the tet-transactivator gene, positive or negative for KRAB. Mice were treated with doxycycline if indicated. One day later, mice were intravenously injected with 2 x 10<sup>5</sup> PFU MHV-68\_OVA. CFSE-dilution of OT-I T cells was measured on day 3 post-infection. Gate was set on proliferating T cells.

## E Discussion

This study has shown a direct correlation between RNA Polymerase I activity and proliferation in T cells in an mTORC1 dependent manner. The upregulation of global and ribosomal RNA as well as proliferation was compromised in mTORC1-deficient T cells. In the course of this work, new techniques as well as *in vitro* and *in vivo* test systems were developed.

### 1 TCR signaling increases mTORC1 activity

The ligation of co-stimulatory receptors besides TCR triggering on a T cell is prerequisite for T cell activation. A lack of such signals results in anergy and thus dysfunction of a T cell (Jenkins, 1992; Schwartz, 2003). In several studies, mTORC1 signaling became known as mediator of secondary signals necessary for productive T cell activation. mTORC1 is activated by the kinase Akt which in turn gets activated by PI3K. The activation of PI3K relies on co-stimulatory signals generated by CD28 and other amplifying signals such as IL-2 receptor signaling (Inoki *et al.*, 2003b; Pollizzi & Powell, 2015; Tee *et al.*, 2003; Zoncu *et al.*, 2011). One of the described targets downstream of mTORC1 is S6 kinase beta-1 (S6K1). When phosphorylated and thus activated by mTORC1, it mediates the phosphorylation of the ribosomal protein S6 (pS6). It has been shown that the stimulation of the TCR with anti-CD3/28 *in vitro* induces the phosphorylation of S6 by S6K1 (Choo *et al.*, 2008). In addition, the induction of mTORC1 signaling in response to weak TCR signals, e.g. in T cells deficient for the TCR signaling molecule Lck, was reduced, which points out that TCR signal strength directly corresponds to mTORC1 signaling (Tan *et al.*, 2017b). Even though the phosphorylation of S6 is not required for T cell development, growth and antigen-dependent proliferation and differentiation, it is a reliable indicator of mTORC1 activity (Salmond *et al.*, 2015).

In agreement with the current literature, our data showed an increased phosphorylation of S6 in T cells two hours after stimulation *in vitro* (Fig. D1.1A). Stimulation with anti-CD3 or anti-CD28 alone was not sufficient to induce the same amount of response as both antibodies did in combination. This indicates two things: First, co-stimulation via CD28 alone is not sufficient to induce mTORC1 signaling and second, CD28 signaling has an amplifying effect on the signaling via the TCR. Yang *et al.* reported similar results: Two hours of stimulation with anti-CD3 alone were sufficient to induce pS6, but CD28 engagement was needed to remain this signal high at later time points such as

## E Discussion

four hours post-stimulation (Yang *et al.*, 2013). Furthermore, the role of co-stimulation on a transcriptional level during T cell activation was investigated in *in vitro* stimulated CD4<sup>+</sup> T cells in the absence or presence of co-stimulatory molecules such as CD28. Also in this study, CD28 signaling had merely an enhancing effect on gene expression in T cells induced by TCR signaling (Wakamatsu *et al.*, 2013). To further investigate the supportive effect of co-stimulation on mTORC1 signaling, experiments with different doses of anti-CD28 together with anti-CD3 at different time points during early T cell activation need to be performed. Multiple receptors signal via mTORC1, among them is the IL-2 receptor (Rollings *et al.*, 2018; Ross & Cantrell, 2018; Waickman & Powell, 2012). If mTORC1 activity is directly regulated by TCR signaling or also indirectly induced by IL-2 needs to be tested in further experiments using blocking antibodies against IL-2, IL-2R or in gene-ablated animals.

In summary, TCR signals, in combination with co-stimulatory signaling via CD28 affects the phosphorylation of targets downstream of mTORC1.

We further tested S6 phosphorylation in mTORC1-deficient T cells. mTORC1 can be activated either directly via PI3K signaling or indirectly by Erk, Tsc1 and Rheb. Stimulation via Erk can be induced by PMA and ionomycin. In response to PMA and ionomycin, T-Raptor<sup>-/-</sup> cells display a reduced signaling (Fig. D1.1C). Nevertheless, the phosphorylation of S6 was not completely erased. Similar results were detected in iNKT cells, thymocytes and T cells by other groups (Shin *et al.*, 2014; Yang *et al.*, 2013). It is likely that other pathways are responsible for the phosphorylation of S6 in Raptor-deficient T cells. Two candidates are the kinases Pim-1 and Pim-2. Both are described to mediate resistance to low-dose rapamycin treatment in T cells *in vitro* (Fox *et al.*, 2005). Furthermore, a rapamycin-resistant S6 phosphorylation at S240/244 induced by serum factors in a cell-cycle dependent manner in fibroblasts was reported (Rosner & Hengstschlager, 2010).

In conclusion, mTORC1 activity, measured by the phosphorylation of S6, is significantly reduced in Raptor-deficient T cells. Residual pS6 could be detected, which is probably due to alternative pathways upstream of S6K1.

### 2 Cell size increase is delayed in T-Raptor<sup>-/-</sup> cells

When a T cell gets stimulated *in vitro*, it starts to increase in size within 24 hours, known as blast formation (Fig D3.4). As potent inhibitor of mTORC1 in mammalian cells, rapamycin is described to impair blast formation of T cells early upon activation

## E Discussion

with anti-CD3/28 or cognate peptide. Similar findings were reported for T cells deficient for Raptor and thus mTORC1 activity and in wing cells of *Drosophila* (Pollizzi *et al.*, 2015; So *et al.*, 2016; Terada *et al.*, 1995; Yang *et al.*, 2013; Zhang *et al.*, 2000).

In this thesis, T cells were activated *in vitro* with anti-CD3/28 for 48 hours and relative cell size was measured by flow cytometry using forward scatter as a surrogate parameter (Tzur *et al.*, 2011). We found that mTORC1-deficient T cells increased their size as mTORC1-sufficient T cells did at this time point (Fig. D1.2 A). Since most of the cell size measurements of other studies were performed 24 hours post-stimulation, and thus 24 hours earlier than done here, it is likely that the increase in cell size is not generally disrupted but delayed in mTORC1-deficient T cells: T-WT and T-Rptor<sup>-/-</sup> cells showed differential FSC-A patterns 16 hours post-transfer in an antigen-dependent GvH response *in vivo* (Fig. D1.2 C). 24 hours later, this difference was undetectable, with T-WT and T-Rptor<sup>-/-</sup> cells showing the same forward scatter. This is consistent with data showing that rapamycin-treatment was responsible for a delayed cell size increase in human T cells, measured by the presence of  $\beta$ -Tubulin and a delayed cyclin A expression, highly expressed in the G<sub>1</sub>/S-phase (Gelfand *et al.*, 1995; Terada *et al.*, 1995). Similar results were also obtained in *S. cerevisiae* (Barbet *et al.*, 1996) and in mouse embryonic fibroblast (MEF) cells deficient for the transcription initiation factor IA (TIF-IA), a downstream target of mTORC1 regulating ribosomal RNA synthesis (Mayer *et al.*, 2004). However, Yang and colleagues detected a lower size of T-Rptor<sup>-/-</sup> cells three days after transfer into mice that have been treated with peptide (Fox *et al.*, 2005; Tan *et al.*, 2017a; Yang *et al.*, 2013). Nevertheless, the dose of peptide injected was not discussed in this study. Thus, lower doses of antigen could potentially lead to a higher delay in cell size increase, which could be overcome with high antigen-doses in T-Rptor<sup>-/-</sup> cells. Further experiments need to be performed testing the kinetic of blast formation in Raptor-deficient T cells. Also other methods to define the size of a cell need to be used to corroborate our results. Besides microscopy, the Coulter Counter is widely used to measure the cell size directly (Tzur *et al.*, 2011). In summary, T cell blast formation was impaired upon T cell stimulation transiently in mTORC1-deficient T cells, indicating that mTORC1 regulates rapid cell size increase of T cells following stimulation.

### 3 Proliferation of T-Rptor<sup>-/-</sup> cells is compromised *in vivo*

Upon T cell activation, T cells must proliferate rapidly. Within this expansion phase, T cells show a high biosynthetic activity in which they have to replicate DNA, produce

## E Discussion

proteins and generate membranes. mTORC1 is a mediator of these highly anabolic processes and thus profoundly associated with the proliferative capacity of T cells (Delgoffe & Powell, 2015)

In this thesis, five different experimental setups were used to explore the role of mTORC1 in T cell proliferation.

First, T-WT and T-Rptor<sup>-/-</sup> cells were adoptively transferred into H2-K<sup>b/bm1</sup> or H2-A<sup>b/bm12</sup> heterozygous recipients to follow T-Rptor<sup>-/-</sup> cells in a graft-versus-host response. Alloreactive mTORC1-deficient T cells were not able to expand to the same degree as T-WT cells and fewer alloreactive (CFSE<sup>low</sup>) cells could be retrieved on day five after transfer. The responsive cells had divided 1.9 to 4.6 times on an average compared to approximately eight divisions of T-WT cells (Fig D2.1). In addition the mutant cells were lost due to apoptosis. These data are in agreement with another study performed with alloresponsive T cells from mice on the H-2<sup>b</sup> background. If transferred into either mice from H-2<sup>d</sup> or H-2<sup>b/d</sup> background, rapamycin treatment led to lower GvHD scores in all organs tested, lower serum cytokine levels and less glycolysis, allowing a correlation between mTORC1 activity and alloresponse but no direct causation. The same was true in Raptor- but not Rictor-deficient T cells (Nguyen *et al.*, 2016). Nevertheless, no proliferation assays such as CFSE-dilutions were performed in this study. A second study addressed rapamycin-induced changes in Treg-mediated suppression of graft rejection. Upon transplantation of human internal mammary artery into immunodeficient BALB/c Rag2<sup>-/-</sup> Il2rg<sup>-/-</sup> mice injected with allogenic human PBMCs together with *ex vivo* expanded Treg cells, it was shown that rapamycin increased a Treg-mediated effect of less graft rejection by alloresponsive T cells (Hester *et al.*, 2012). Similar results have been obtained after inhibition of Akt, which acts upstream of mTORC1 (Herrero-Sanchez *et al.*, 2016). In conclusion, the alloresponse of Raptor-deficient T cells was impaired due to less cell proliferation and accumulation upon activation.

In a second experiment, polyclonal CD8<sup>+</sup> T-WT and T-Rptor<sup>-/-</sup> cells were stimulated *in vitro* for 48 hours and subsequently transferred into antigen-free hosts. It has been reported that a short antigen pulse in a time frame of 48 hours is sufficient to fully activate CD8<sup>+</sup> T cells and to induce proliferation even if antigen presentation does not continue (Rabenstein *et al.*, 2014). In this study, T-Rptor<sup>-/-</sup> cells were not able to induce antigen-independent proliferation in CD8<sup>+</sup> T cells (Fig D2.2, D2.1). This indicates an essential role for mTORC1 in maintaining proliferation in CD8<sup>+</sup> T cells when antigen is cleared.

## E Discussion

Next, antigen-specific proliferation of adoptively transferred AND and OT-I TCR transgenic T cell was tested in mice expressing MCC<sub>93-103</sub> on MHC-II and OVA<sub>257-264</sub> on MHC-I, respectively. Yang and colleagues had suggested that mTORC1 was only needed for leaving quiescence upon TCR stimulation or in other words that mTORC1 activity is only needed for the first but not any further divisions. They tested it by stimulating T cells *in vitro* with anti-CD3/28 and added rapamycin at different time points after stimulation. If added 24 hours or later post-stimulation, cell cycle was not impaired as measured by BrdU incorporation and the DNA dye 7-AAD (Yang *et al.*, 2013). *In vivo* we found, T-Rp<sup>-/-</sup> cells were not only delayed in cell cycle entry, but subsequent rounds of division were slowed down from approximately three to one divisions per day (Fig D2.3, D2.2). Furthermore, cell cycle analysis in activated T cells with the DNA staining dye DAPI and two antibodies binding pRb and H3P, phosphorylated in cells that have entered G<sub>1</sub>- or M-phases, respectively, confirmed this finding (Fig. D5). We detected that T-Rp<sup>-/-</sup> cells are enriched in G<sub>0</sub>-phase and depleted in the S-phase of the cell cycle, whereas the percentage of cells in G<sub>1</sub>-, G<sub>2</sub>- and M-phases remained unchanged. We also found that the RNA Polymerase I inhibitor quarfloxin not only blocks cell cycle entry if added at the beginning of stimulation, but also at later time points, indicating that RNA Polymerase I activity, just like mTORC1, is necessary not only for the first cell division but also later on (Fig. D4). In summary, our data indicate that a constant activity of mTORC1 and its downstream target RNA Polymerase I are necessary for T cell proliferation, *in vivo* and *in vitro*.

We next investigated how mTORC1 sufficient and deficient T cells respond to a viral infection. OT-I TCR transgenic T cells were adoptively transferred into mice that were subsequently infected with a Modified Vaccinia Ankara virus expressing Ovalbumin (MVA-Ova). MVA-OVA preferentially infects dendritic cells with viral life cycle arrest before late gene expression, limiting the presentation of antigen to the turnover of the infected DCs and thus induces a short antigen pulse only (Liu *et al.*, 2008).

The response to MVA-OVA was reduced in mTORC1-deficient T cells, which resulted in lower effector and memory T cell numbers (Fig. D2.4). Thus, an additional cytokine induction by the infected environment could not improve a T cell response to antigen in comparison to antigen-presentation alone. These results are in agreement with data demonstrating that T cells deficient for the mTORC1-activator Rheb proliferated less in response to Vaccinia infection *in vivo* (Delgoffe *et al.*, 2011). Nevertheless, a short

## E Discussion

inhibition of mTORC1 by low-dose rapamycin could improve memory formation in CD8<sup>+</sup> T cells and induce iTreg cell differentiation in CD4<sup>+</sup> T cells, indicating a differential outcome of partial and transient mTORC1 inhibition (Araki *et al.*, 2009; Haxhinasto *et al.*, 2008; Nguyen *et al.*, 2016). In conclusion, mTORC1-deficient T cells expand less in response to MVA-OVA.

We also found that on day 36 post-transfer, T-Rptor<sup>-/-</sup> cells were lost in half of the uninfected recipient mice under steady-state conditions, indicating a defect in homeostatic survival (Fig. D2.4).

To further address homeostatic expansion of mTORC1-deficient T cells, a fifth experimental setup was used. Polyclonal T-WT and T-Rptor<sup>-/-</sup> cells were transferred into lymphopenic RAG1-deficient hosts to monitor lymphopenic proliferation. No proliferation was detected in mTORC1-deficient T cells (Fig D2.5). Similar results were reported on Raptor-deficient cells transferred into lethally irradiated mice (Li *et al.*, 2011; Rathmell *et al.*, 2001; Yang *et al.*, 2013). Whether the signals inducing mTORC1-dependent proliferation in lymphopenic mice and in homeostasis are the same, was not investigated so far. However, it is known that the two cytokines IL-7 and IL-15 are important for homeostatic survival of memory cells under non-inflammatory conditions. Both are reported to induce mTORC1 signaling and thus could be essential for lymphopenic proliferation (Ali *et al.*, 2015; Li *et al.*, 2011; Marzec *et al.*, 2008; Rathmell *et al.*, 2001; Sowell *et al.*, 2017). IL-7 is essential for lymphopenic proliferation of effector cells, as tested in IL-7-deficient OT-I T cells (Schluns *et al.*, 2000). Further experiments in IL-15R or IL-7R deficient T cells need to be performed to test whether these signaling pathways are connected to mTORC1 and thus proliferation.

In summary, proliferation of mTORC1-deficient T cells was impaired in lymphopenic hosts.

Taken together, mTORC1 signaling was found to be essential for T cells to proliferate *in vivo* under five conditions: GvH reactions, responses to transient and persistent TCR stimuli, a viral infection and in lymphopenic hosts.

### 4 RNA Polymerase I-induced rRNA expression can be linked with T cell proliferation

#### 4.1 mTORC1 controls RNA Polymerase I expression

The synthesis of rRNA is likely to put the highest energetic demands on proliferating T cells (Moss *et al.*, 2007; Warner, 2001). mTORC1 is described to regulate the phosphorylation and thus activation of two transcription factors associated with RNA polymerase I, which catalyzes the synthesis of ribosomal DNA (Hannan *et al.*, 2003; Mayer & Grummt, 2006). An analysis of data published by the laboratory of Hongbo Chi revealed an mTORC1-dependent upregulation of RNA Polymerase I subunits on protein level, which are necessary for the transcription of ribosomal RNA upon TCR stimulation (Fig. D3.1 and Tan *et al.*, 2017). The data also show that ribosome biogenesis and translation heavily depend on mTORC1 (Tan *et al.*, 2017a). mTORC1 regulates the activity of RNA Polymerase I but also II and III, which mediate the transcription of mRNA and tRNA, respectively (Iadevaia *et al.*, 2012).

Nevertheless, a direct effect of mTORC1 on RNA Polymerase II subunit expression was not shown so far (Fig. D3.1). Thus, it is more likely that the effect of mTORC1 is mediated via the translation of specialized mRNAs, the so-called 5' TOP mRNAs, encoding ribosome biogenesis genes. Moreover, a disruption of upstream signals of mTORC1 such as glucose uptake, had no effect on RNA Polymerase II recruitment to DNA, indicating that mTORC1 does not regulate RNA Polymerase II activity via the influx of metabolites such as glucose (Finlay *et al.*, 2012). The regulatory effect of mTOR on RNA Polymerase III was only tested in *S. cerevisiae*, worms, flies and tumor cell lines so far (Filer *et al.*, 2017; Kantidakis *et al.*, 2010; Mayer *et al.*, 2006). Mayer and colleagues pointed out in more detail that mTOR regulates TIFIII B, a transcription initiation factor binding to RNA Polymerase III (Mayer & Grummt, 2006; Mayer *et al.*, 2006).

It is described that the regulatory effect of mTORC1 on RNA Polymerase I operates at least via the activation of TIF-IA and upstream binding factor (UBF), two transcription factors associated with the activity of RNA Polymerase I. Furthermore, rapamycin treatment of activated T cells altered the phosphorylation of TIF-IA. The consequences were lower pre-RNA levels but not necessarily 28S RNA, which indicates that RNA processing might not be affected (Claypool *et al.*, 2004; Hannan *et al.*, 2003; Hardwick *et al.*, 1999; Mahajan, 1994; Mayer *et al.*, 2004; Zaragoza *et al.*, 1998). Furthermore, the phosphorylation of the CDK2-Cyclin E complex, which kinase activities induces the

## E Discussion

phosphorylation of TIF-IA at Ser44 during G<sub>1</sub> to S-phase transition, was altered. Thus, it is likely that mTORC1 regulates TIF-IA via this cyclin complex (Mayer *et al.*, 2004).

In summary, mTORC1 signaling is necessary for the upregulation of RNA polymerase I on protein levels as well as proteins associated with ribosomal biogenesis upon stimulation of the TCR, which affects the translational activity in T cells.

### 4.2 mTORC1 is necessary for global RNA upregulation

To further address the question of how mTORC1 shapes total and ribosomal RNA expression, the composition of all RNA species, except tRNA and thus RNA polymerase III activity, in activated T cells was measured by total RNA sequencing. Due to secondary structures formed by tRNAs the accessibility of the linker sequence was blocked, which interfered with cDNA synthesis. In a second approach, global RNA expression was detected on the single cell level by flow cytometry. In combination, both techniques showed a reduced expression of all RNA species in mTORC1-deficient T cells (Fig. D3.2, Fig. D3.5).

Total RNA sequencing revealed that 83-87% of all RNA species of a T cell could be assigned to rRNA, independent of stimulation or mTORC1 activity. Furthermore, mTORC1 deficiency did not cause any changes in the abundance of other RNA species. This indicates high activity of RNA polymerase I on the one hand and mTORC1 as regulator not only of the expression of RNA polymerase I transcribed rRNA but also RNA species expressed by RNA polymerase II on the other hand. Nonetheless, mRNA levels were slightly reduced in mTORC1-deficient activated T cells (Fig. D3.2). The major demand RNA Polymerase I activity puts on T cells can be assessed by the high abundance of its product, the rRNA in comparison to mRNA (4.8%).

We further tested whether mTORC1-disruption affects rRNA synthesis only or also processing or rRNA to functional ribosomes. A previous study showed that different inhibitors of signaling molecules involved in rRNA synthesis can either interrupt rRNA transcription or 47S RNA processing (Burger *et al.*, 2010). For instance actinomycin D, an inhibitor of RNA Polymerase I at low concentrations and II activity at high concentrations, was rather responsible for a reduced rRNA synthesis in human sarcoma cell lines instead of 47S rRNA processing (Bensaude, 2011; Burger *et al.*, 2010). The same effect was reported upon rapamycin treatment (Burger *et al.*, 2010). In this thesis, no differential expression of 28S, 18S and 5.8S rRNA was detected in WT and mTORC1-deficient T cells, indicating that mTORC1 likely regulates the expression of pre-rRNA by RNA Polymerase I instead of inducing its processing (Fig.

## E Discussion

D3.2 E). In addition, direct inhibition of RNA Polymerase I with quarfloxin and actinomycin D interfered with RNA expression and proliferation of activated T cells, pointing towards a direct correlation between RNA Polymerase I activity, rRNA synthesis and T cell expansion. Since pre-rRNA processing was not affected in mTORC1-deficient T cells, formation of fully functional ribosomes should be possible. Further investigation regarding the translation in mTORC1-deficient T cells has to be performed.

Taken together, we found that mTORC1 disruption affects RNA polymerase I and II-dependent transcription, while 47S rRNA processing was not impaired in mTORC1-deficient T cells.

### 4.3 T cell proliferation can be linked to RNA synthesis

The biosynthesis of ribosomes is essential to sustain and duplicate translational activity in a proliferating cell. This highly energy-demanding process is described to be regulated by mTORC1 at least via its downstream targets TIF-IA and Ubf, two transcription factors required to be phosphorylated for the activity of RNA polymerase I and thus rRNA synthesis (Claypool *et al.*, 2004; Hannan *et al.*, 2003; Mayer *et al.*, 2004; Tan *et al.*, 2017a). Furthermore, it is known that mTORC1 signaling is crucial for T cell proliferation (Delgoffe *et al.*, 2009a; Delgoffe *et al.*, 2009b; Delgoffe *et al.*, 2011; He *et al.*, 2011; Tan *et al.*, 2017a; Tan *et al.*, 2017b; Yang *et al.*, 2013; Zeng *et al.*, 2013; Zhang *et al.*, 2011). We found that T-Raptor<sup>-/-</sup> cells proliferate slower and are more prone to die *in vivo* (Fig. D2.2). In addition, inhibitors of RNA Polymerase I were used to document their effect on proliferation and RNA synthesis. We detected that not only the direct inhibitor of mTOR, Torin 1 or the inhibition of glycolysis by 2-DG affected T cell proliferation upon *in vitro* stimulation with anti-CD3/28, but also the inhibition of mRNA and rRNA synthesis by quarfloxin and actinomycin D. We found that an inhibition of RNA polymerase I by quarfloxin and thus rRNA synthesis exclusively was sufficient to block T cell proliferation *in vitro* (Fig. D3.7). In addition, RNA expression levels as well as blast formation and cell cycle entry was impaired to comparable levels as detected in mTORC1-deficient T cells, indicating that RNA polymerase I inhibition could phenocopy the effect of mTORC1-deficiency in these parameters (Fig D3.5, D3.7). An inhibition of mTOR or glycolysis as well as of RNA polymerase I and II showed more drastic effects on cell cycle entry and proliferation than mTORC1-deficiency and inhibition of RNA polymerase I alone (Fig. D3.5, D3.7). This could indicate, that T cell proliferation is not exclusively regulated by mTORC1 and rRNA expression but also other signaling pathways associated with mTOR fuel into potent T

## E Discussion

cell expansion. It is likely that mTORC1 and RNA synthesis regulate the division speed and cell survival in proliferating T cells, not only for quiescence exit but also for ongoing proliferation, as discussed in detail in chapter E 3. If there is a direct correlation between mTORC1 signaling via TIF-IA and UBF, rRNA synthesis and proliferation has not been investigated so far in T cells.

In addition we saw that DNA synthesis was not fully impaired by mTORC1 disruption, indicating that low levels of newly synthesized RNA are enough to induce entry into the cell cycle (Fig. D3.5). Whether a T cell needs to reach a certain threshold of RNA content to start proliferating or if the signal generated by RNA expression is proportional to T cell proliferation is not clear. We found that T-WT cells that have been treated with inhibitors against mTORC1 signaling components show a direct correlation between RNA expression and cell cycle progression, suggesting direct correlation between RNA expression and proliferation (Fig. D3.7). Cao and colleagues have published a similar connection in T cells treated with 2-DG, an inhibitor of glycolysis (Cao *et al.*, 2014). In summary, we found a direct correlation between T cell proliferation and RNA expression.

We next tested whether lower levels of rRNA due to mTORC1-deficiency had not only an effect on T cell proliferation but also translation. It was recently published that the translation of 5' TOP mRNA is enhanced in an mTORC1-dependent manner in T cells (Araki *et al.*, 2017). 5' TOP mRNAs mainly encode for proteins associated with ribosome formation and translational initiation as well as T cell effector function (Thoreen *et al.*, 2012). Furthermore, rapamycin has an impact on overall protein synthesis and specifically the translation of 5' TOP mRNAs is affected by mTORC1 inhibition (Iadevaia *et al.*, 2012; Terada *et al.*, 1995). We found that the translational activity was impaired in mTORC1-deficient CD4<sup>+</sup> T cells 48 hours post-stimulation *in vitro*. Further experiments need to be performed addressing the translation activity in CD8<sup>+</sup> T cells. Data on the kinetics of the translational initiation and activity need to be generated *in vitro* and *in vivo* to provide clear interpretations for the role of mTORC1 on both.

In summary, we have described a direct effect of RNA Polymerase I inhibition on T cell proliferation comparable to observations made in mTORC1-deficient T cells. Consequently, the translational activity in mTORC1-deficient T cells was impaired *in vitro*.

## E Discussion

Ribosomal RNA has additional functions besides translating mRNA into protein. Newly synthesized rRNA is organized in subnuclear structures called nucleoli, providing a niche for several regulatory molecules to bind. This study showed that a persistent synthesis of rRNA is needed to maintain proliferation in T cells, since T cells treated with the RNA polymerase I inhibitor quarfloxin 24 hours post-initial stimulation were not able to enter the cell cycle and start to proliferate (Fig. D4). Impaired mTORC1 activity led to an enrichment of T-Rptor<sup>-/-</sup> cells in G<sub>0</sub> and to fewer cells in S-Phase after 48 hours of *in vitro* stimulation with anti-CD3/28 (Fig. D5). Similar results were reported on TIF-IA-deficient cells, a downstream target of mTORC1, that regulates RNA Polymerase I activity (Yuan *et al.*, 2005). The cell cycle is regulated by the up- and downregulation of different cyclins. TIF-IA depleted cells have decreased levels of cyclin A and E, but not D1 and p27. On the other hand p130, which is highly expressed in quiescent cells and a known inhibitor of RNA polymerase I and p21, an inhibitor of cyclin dependent kinases, is increased (Ciarmatori *et al.*, 2001; Rubbi & Milner, 2003; Yuan *et al.*, 2005). This indicates that T cells impaired in rRNA expression are not able to leave quiescence properly and if so die upon failed transition into S-Phase. A major apoptotic inducer is the tumor suppressor p53. Previous studies demonstrated that TIF-IA inactivation leads to an interaction of MDM2, a negative regulator of p53, with ribosomal proteins such as L11 instead of binding to rRNA in the nucleolus, thus disrupting its inhibitory function. Hence, p53 is stabilized and genes involved in apoptosis could be activated (Yuan *et al.*, 2005). In this study, rRNA expression had a direct effect on the cell cycle of T cells. Several questions still remain to be clarified. It is not clear yet whether RNA Polymerase I has a direct effect on cyclin expression or if they are regulated via the nucleolus exclusively. Furthermore, the relation between RNA and DNA synthesis has to be investigated. In activated T-WT cells, DNA and RNA are synthesized in direct proportion to one another in cells in S-phase and the transition to S-Phase requires RNA Polymerase I release from DNA (Smirnov *et al.*, 2016). Thus, an inhibition of RNA Polymerase I can have different outcomes depending on which cell cycle phase a cell is in.

Taken together, we have found a direct correlation between ongoing RNA Polymerase I activity and thus rRNA synthesis and T cell proliferation after *in vitro* stimulation. This process relies on mTORC1 and has either a direct or indirect effect on the expression of all other RNA species detectable in our experimental setup.

### 5 Differences between CD4<sup>+</sup> and CD8<sup>+</sup> T cells

Even though developed side by side in the thymus, antigen-recognition, diversity and effector functions are very different in CD4<sup>+</sup> and CD8<sup>+</sup> T cells. Our lab has recently shown that besides above-mentioned differences, CD4<sup>+</sup> and CD8<sup>+</sup> T cells depend differently on persistent antigen presentation with CD4<sup>+</sup> T cells only being able to proliferate when antigen is presented continuously (Rabenstein *et al.*, 2014).

In this thesis, we found that CD4<sup>+</sup> and CD8<sup>+</sup> T cells show different kinetics regarding their increase in size, RNA expression and cell cycle entry upon *in vitro* stimulation, whereby CD4<sup>+</sup> T cells appear to be slower in all three points. Among CD8<sup>+</sup> T cells, a peak of RNA expression was reached by 24 hours post-stimulation. In CD4<sup>+</sup> T cells it was delayed to 48 hours post-stimulation. The same was true for blast formation and cell cycle entry (Fig. D3.4). In addition, CD4<sup>+</sup> T cells tend to show a reduced division velocity *in vitro* but not *in vivo* (Fig D3.7; Fig. D2.2). Previously published microarray analysis of *in vitro* stimulated CD4<sup>+</sup> and CD8<sup>+</sup> T cells showed only few differences in their protein-coding RNA, despite their obvious functional differences (Mingueneau *et al.*, 2013; Rabenstein *et al.*, 2014), indicating that rather translation than transcription may be differentially regulated in CD4<sup>+</sup> and CD8<sup>+</sup> T cells. The group of Rafi Ahmed showed that translation is actively regulated in an mTORC1-dependent manner by the content of polysomes and monosomes. They described that effector gene mRNAs and 5' TOP mRNAs are mainly bound by polysomes, during CD8<sup>+</sup> effector T cell differentiation (Araki *et al.*, 2017). Whether CD4<sup>+</sup> and CD8<sup>+</sup> T cells harbor a differential content of monosomes and polysomes needs to be tested in further experiments, in order to clarify differential translational activities in those two cell subsets.

Moreover, in experiments using increasing doses of inhibitors interfering with the mTORC1 signaling pathways we found that CD4<sup>+</sup> T cells are more susceptible to metabolic inhibitors and are more affected regarding their cell cycle entry, increase in size and RNA expression by mTORC1-deficiency, thus indicating a higher dependence on mTORC1 signaling (Fig. D3.7, Fig. D3.5) (Cao *et al.*, 2014). Nevertheless, *in vivo* proliferation assays were not able to support these findings, indicating that the differences found *in vitro* are potentially harder to detect *in vivo*. To overcome this problem, changes in medium as well as the addition of cytokines such as IL-2 need to be tested regarding proliferation and cell survival. This might reveal the influence of signal strength on cell survival in mTORC1-compromised T cells (Fig. D3.5).

Taken together, differences observed between CD4<sup>+</sup> and CD8<sup>+</sup> T cells regarding RNA expression, blast formation, cell cycle entry, proliferation and susceptibility to metabolic

## E Discussion

inhibitors might be induced by suboptimal stimulation conditions *in vitro* and could not corroborate *in vivo*.

### 6 Role of mTORC2 on RNA synthesis, stability and T cell proliferation

The role of mTORC2 in proliferating T cells is not very well established. It was shown that mTORC2 binds to actively translating ribosomes (Oh *et al.*, 2010). If this directly regulates RNA synthesis as well as proliferation is unknown. If anything, *in vitro* stimulated mTORC2-deficient T cells showed a higher expression of global RNA (Fig. D3.5). This could point to a direction that mTORC2 acts as a negative regulator on RNA synthesis and thus proliferation.

### 7 Technical challenges and benefits

#### 7.1 Pyronin Y in flow cytometry

RNA synthesis is a major component of biosynthesis in activated T cells. mTORC1 is described to regulate rRNA synthesis, which makes approximately 83-87% of a T cells RNA. At least in yeast and tumor cell lines, ribosome synthesis has been described as being essential for translational activity and expansion (Claypool *et al.*, 2004; Hannan *et al.*, 2003; Mayer *et al.*, 2004).

Thus, assessing RNA content in T cells is important for studying cell growth and differentiation. In the early eighties Pyronin Y was first used to visualize RNA content by flow cytometry. Plotted against the DNA dye Hoechst it enabled the analysis of mainly the G<sub>0</sub>- and G<sub>1</sub>-phases of the cell cycle (Kim & Sederstrom, 2015; Shapiro, 1981). Since then Pyronin Y was frequently used to study cell cycle in proliferating T cells (Behbehani *et al.*, 2012; Challen *et al.*, 2009; Crissman *et al.*, 1985; Cui *et al.*, 2003; Janumyan *et al.*, 2003; Nakamura-Ishizu *et al.*, 2014; Qiu *et al.*, 2013; Schmid *et al.*, 2000). In more recent studies, Pyronin Y was used to measure total RNA abundance in thymocytes (Mingueneau *et al.*, 2013).

Several challenges had to be overcome regarding the usage of Pyronin Y. Since Pyronin Y intercalates into double stranded nucleic acid it thus not only stains RNA but also DNA. To fully avoid a staining of DNA by Pyronin Y, all DNA binding sites were saturated by previous incubation with the DNA-only binding dye DAPI. In order to avoid technically induced differences between samples, the same amount of cells was stained in the same reaction tube if possible (Fig. D3.3).

## E Discussion

With this technique we found a nine- and twelve-fold increase of global RNA expression in CD4<sup>+</sup> and CD8<sup>+</sup> T-WT cells upon stimulation *in vitro* for 48 hours, respectively, which was two-fold reduced in mTORC1-deficient T cells (Fig. D3.5). A second way to measure RNA concentrations is based on fluorescence, since RNA has an absorption maximum at a wavelength of 260nm. Like RNA measurements based on gel electrophoresis (detecting 28S and 18S rRNA), no evaluation on a single cell level is possible. Both techniques were performed in this thesis. Purified RNA from *in vitro* stimulated T cells was measured with the Qubit RNA HS Assay from thermofisher (fluorescence-based) and Shimadzu MultiNA microchip electrophoresis (electrophoresis-based). With both techniques a higher increase in RNA content upon stimulation was detected in T cells upon stimulation (44-fold in CD4<sup>+</sup> and 26-fold in CD8<sup>+</sup> T cells), which was 2.6-fold reduced in Raptor-deficient T cells (Fig. D3.2). There is a discrepancy in comparison to data generated with Pyronin Y. This can be due to a lower accessibility of RNA to Pyronin Y dye in fixed cells compared to absorption by quantified RNA in a buffer. The reduced amount of RNA in mutant cells was nevertheless detectable.

Pyronin Y allowed the visualization and measurement of relative RNA expression on a single cell level in small, unstimulated versus stimulated T cells. The detected RNA mostly visualized ribosomal RNA, since in T cells, 83-87% of RNA belonged to this species (Fig. D3.2). It allowed studying the effect of drugs interfering with TCR and mTOR signaling on RNA expression in the context of the cell cycle with promising applications in the future.

### 7.2 mTORC1 signaling inhibitors

mTOR was first discovered in yeast as target of the toxin rapamycin an antifungal and antibiotic product by *Streptomyces hygroscopicus*. It was described to block the transition from G<sub>1</sub> to S phase in fungi (Heitman *et al.*, 1991; Singh *et al.*, 1979). Since then, many inhibitors interfering with mTOR signaling have been successfully tested as cancer treatment drugs. Nevertheless, many of them showed low success in the clinic (Saxton & Sabatini, 2017).

In this study, *in vitro* application of the inhibitors 2-DG (target: glycolysis), quarfloxin (CX-5461) (target: RNA Polymerase I), torin 1 (target: mTORC1 and mTORC2), actinomycin D (target: RNA Polymerase I and II) and tigecycline (target: mitochondrial ribosome synthesis) were used to further dissect signaling molecules involved in mTORC1 signaling, that are essential for RNA synthesis and proliferation. By this, the selective RNA polymerase I inhibitor quarfloxin resulted in reduced RNA content and

## E Discussion

impaired cell cycle entry, which was found to resemble the phenotype described in mTORC1-deficient T cells (Fig. D3.7).

Nevertheless, results obtained from *in vitro* drug treatment of stimulated T cells have their limits regarding their comparability to mTORC1-deficiency. One example is the conclusion drawn in several studies regarding the role of mTORC1 in T cell memory development. Results from transiently treated T cells with low-dose rapamycin (mTORC1-inhibitor) *in vitro*, showed a beneficial differentiation to memory T cells (Araki *et al.*, 2009; Pearce *et al.*, 2009; Rao *et al.*, 2010). In this thesis we found that long-term accumulation was impaired in mTORC1-deficient T cells upon viral infections (Fig. D2.4). Similar results were obtained in vaccine-induced CD8<sup>+</sup> T cells treated persistently with high doses of rapamycin (Li *et al.*, 2012).

Since mTOR is a highly conserved molecule in diverse cells of multiple organisms, a treatment with mTORC1 signaling inhibitor drugs has systemic effects on plethora of immune cells (Saxton & Sabatini, 2017). Nevertheless, many inhibitors of the mTORC1 pathway, such as quarfloxin already found usage in clinical studies to impair cancer cell proliferation (Bywater *et al.*, 2012; Cargnello *et al.*, 2015). *In vivo* applications of this inhibitor in mice can be used to study possible side effects in human cancer treatment. Our results raise concerns regarding quarfloxin since adaptive immune responses would be transiently hampered.

Furthermore, *in vitro* experiments using mTORC1-inhibitors in different doses can be used to allow a very broad screening of many targets of the mTORC1 signaling cascade, to give a first insight into key players responsible for physiological changes in T cells. This allows a more efficient selection of interesting targets to study in conditional knock-out mice *in vivo*.

In conclusion, combined studies of mTORC1-deficient T cells and inhibitor-treated WT T cells are necessary to fully reveal the mechanism underlying mTORC1-dependent RNA synthesis and proliferation.

### 8 KRAB in a tet-inducible system

Comparative studies performed in 2014 by Rabenstein et al. used tetracycline-inducible antigen-expression systems to directly compare antigen-dependency in CD4<sup>+</sup> and CD8<sup>+</sup> T cells. One limitation faced was a residual OVA<sub>257-264</sub>-MHC-I expression in iOVA mice: OT-I T cells did not only proliferate in doxycycline-treated recipients but also in untreated mice (Fig. D6.1) (Rabenstein *et al.*, 2014). To overcome “leakiness” in their study, T cell priming was performed *in vitro* before a transfer into either antigen-free or antigen-expressing hosts (Rabenstein *et al.*, 2014). In this thesis, the use of an additional transgenic tetracycline-dependent repressor carrying the Krüppel-associated box (KRAB) in iOVA transgenic mice was investigated to develop a system, which allowed for *in vivo* priming of TCR transgenic OT-I T cells with transient and persistent antigen-presentation. The KRAB zinc finger protein acts as transcriptional repressors. In 1995, a fusion protein consisting of the KRAB domain of human Kox1 and the tet-repressor from Tn10 of *E. coli* was developed (tTR-KRAB). This fusion protein could bind to the tet-operator in the absence of doxycycline and repress gene transcription by inducing histone modifications via the KRAB-associated protein 1 (KAP1). It was shown in HeLa cells that KRAB was released within two days of doxycycline treatment (Deuschle *et al.*, 1995). The same was shown in HEK293T cells transduced with a tTR-KRAB-carrying lentivirus (Barde *et al.*, 2009). The same lentivirus was used to generate mice transgenic for an ubiquitously expressed tTR to transduce KRAB-expression in mice and thus repression of gene expression, but only two conditions were tested in mice up to that point: doxycycline-treatment from the same time point of transduction on or no doxycycline-treatment at all. In this course they showed that doxycycline treatment induced the expression of a reporter gene under the control of the tet-operator (Barde *et al.*, 2009).

In mouse cell lines it was shown that KRAB activity was not reversible if active during embryonic development (Wiznerowicz *et al.*, 2007). We thus wanted to know whether the same is true in iOVA mice. Therefore, iOVA mice were crossed to rTA-KRAB expressing mice generated in Barde et al., 2009 (Barde *et al.*, 2009). Breedings were treated with doxycycline-containing food to avoid irreversible binding of KRAB to the tet-operator controlled expression cassette of OVA<sub>257-264</sub>. This thesis demonstrated that other than in HeLa and HEK293T cells, KRAB release from the tet-operator takes at least two weeks (versus two days in cell lines) of doxycycline treatment in the drinking water. Thus the expression of tet-operator controlled genes is slower in mice than in

## E Discussion

cell lines. Nevertheless, if doxycycline treatment was started at least two weeks before transfer of OT-T cells, T cell priming was successful (Fig. D6.1).

Turning off antigen-expression in iOVA-KRAB mice took at least ten days of treatment with doxycycline-free water and food (Fig. D6.1). In iMCC mice, in which the expression of MCC<sub>93-103</sub> is regulated within the tet-operator and induced via doxycycline treatment, it has been shown that the half-life of doxycycline is around 24 hours. Antigen-expression in this system is blocked within at least 48 hours (Obst *et al.*, 2005). Thus it is likely that not doxycycline availability but rather epigenetic changes mediated by the KRAB domain are the reason for the extended time of reversibility of KRAB inhibition in iOVA-KRAB mice. The reversible activity of KRAB in iOVA mice allowed a comparative analysis of antigen-persistence versus antigen-withdrawal after *in vivo* priming. We found that the introduction of KRAB and thus a transient antigen-exposure to OT-I T cells allowed for the expression of memory-associated surface molecules such as CD127, CXCR3 and Ly6C 30 days post-transfer (Fig D6.3). The expression of these molecules was reduced by persistent antigen-presentation in mice constantly treated with doxycycline (Fig. D6.3). Thus, an introduction of KRAB into iOVA mice could improve the performance of controlled antigen-expression in a doxycycline-dependent manner.

In a second approach an MHV-68 virus variant expressing OVA<sub>257-264</sub> under the control of the tet-operator was developed in collaboration with the group of Prof. Heiko Adler at the Helmholtz Research Center for Environmental Health. MHV-68 is a latent gamma herpes virus infecting mainly B cells in mice. In this study MHV-68\_OVA was tested in R26-rtTA mice, which constitutively and ubiquitously express the reverse tet-transactivator. If treated with doxycycline, rtTA can bind to the tet-operator and induce gene expression of any reporter locus (Hochedlinger *et al.*, 2005). If infected with MHV-68\_OVA, viral antigen-expression was detected by the proliferative response of transferred OT-I T cells independent of the expression of the rtTA or doxycycline. To improve the controllability of this system, the KRAB transgene mentioned before was crossed into the R26-rtTA mouse line. In the presence of KRAB, the “leaky” expression of OVA<sub>257-264</sub> could be reduced by half in mice heterozygous for the R26-rtTA locus. Thus in the course of this thesis a doxycycline-inducible peptide-expressing virus was generated which enables cognate antigen-expression to OT-I mice *in vivo*.

Taken together, the expression of the tetracycline-controllable transrepressor KRAB could enable a controllable expression of OVA<sub>257-264</sub> not only in iOVA mice but also in MHV-68\_OVA and thus improve a doxycycline-dependent antigen expressing system

## E Discussion

in mice and on a recombinant, latent virus. With this approach, it was shown that persistent antigen-presentation compromises memory development in CD8<sup>+</sup> T cells.

## 9 Outlook

This study showed a direct correlation between ribosomal RNA expression and proliferation in activated T cells in an mTORC1-dependent manner.

It is still unclear which signaling molecules downstream of mTORC1 initiate RNA Polymerase I activity. It is likely that the two transcription factors UBF and TIF-IA are inducing RNA Polymerase I activity. Whether S6 and/or 4E-BP1, two targets of mTORC1, are regulators of those transcription factors still needs to be tested. Conditional knockout mice, lacking these four molecules in combination with techniques developed in this thesis, could allow a further insight into their role on RNA expression as well as proliferation.

Additionally, gain-of function experiments with lentiviral vectors expressing RNA Polymerase I subunits, can be used to test if a phenotype of reduced RNA expression and proliferation can be reversed in mTORC1-deficient T cells *in vitro*.

Moreover, pulse-chase experiments could give answer to the question at which phase of the cell cycle mTORC1 is essential. The two nucleotide analogues EdU and BrdU can be used to test this. Both can be integrated into DNA during the S-phase of the cell cycle. Applied at two different time points after *in vitro* stimulation of T cells, the duration of cell cycle progression can be measured in WT and mTORC1-deficient cells (Weber et al., 2014; Clarke et al., 2017).

Since the nucleolus of T cells plays a major role in regulating cell cycle and survival, a visualization of this sub-compartment could give information of differences in size and shape in relation to cell size in WT and mTORC1-deficient T cells. Antibodies against the nucleoli-associated protein fibrillarin could be used to image nucleoli (Quin et al., 2016).

Furthermore, the background expression of OVA<sub>257-264</sub> in iOVA mice as well as on the virus MHV-68\_OVA could be abrogated by the expression KRAB. This approach can be used to further investigate the effect of persistent and transient antigen-expression on memory T cell development under non-inflammatory conditions in direct comparison to viral infections.

### F Abbreviations

---

2-DG	2-deoxy-D-glucose
4E-BP1	Eukaryotic translation initiation factor E4
5' TOP	5' terminal oligopyrimidine tract
AMP	Adenosin monophosphate
AMPK	AMP-activated protein kinase
APC	Antigen presenting cell
ATP	Adenosine triphosphate
BAC	Bacterial artificial chromosome
Bcl6	B-cell lymphoma 6 protein
BrdU	Bromodesoxyuridine
CD	Cluster of differentiation
CDK	Cycline-dependent kinases
CFSE	Carboxyfluorescein succinimidyl ester
CLIP	Class II-associated invariant chain peptide
CMV	Cytomegalovirus
Cre	Causes recombination
cTEC	Cortical thymus epithelial cell
CTL	Cytotoxic T Lymphocyte
CTLA-4	Cytotoxic T-lymphocyte-associated-protein 4
CTV	Cell trace violet
DAPI	4',6-diamidino-2-phenylindole
DC	Dendritic cell
DEPTOR	DEP-domain containing mTOR-interacting protein
DFC	Dense fibrillar centers
DN	Double negative
DNA	Desoxyribonucleic acid
dNTPs	Deoxynucleotide
DP	Double positive
e.g.	Exempli gratia - for example
EBV	Epstein-Barr virus
EDTA	Ethylenediaminetetraacetic acid
EdU	5-ethynyl-2-deoxyuridine
eIF	Elongation initiation factor
ER	Endoplasmatic reticulum
FACS	Fluorescence-activated cell scanning
FAO	Fatty acid oxidation
FC	Fibrillar centers
FCS	Foetal calf serum
FLCN	Folliculin
Flp	Flippase
FNIP	FLCN-interacting protein
FoxP3	Forkhead box P3

## F Abbreviations

Frt	Flippase recognition target
FSC-A	Forward scatter area
FVD	Fixable viable dye
GAP	GTPase-activating protein
GC	Grnular components
GEF	Guanosine triphosphate exchange factor
gMFI	Geometrical mean fluorescence intensity
GTP	Guanosine triphosphate
GTP	Guanosine-5'-triphosphate
GvHD	Graft-versus-Host Disease
H3	Histone 3
HLA	Human leukocyte antigen
IFN	Interferon
Ig	Immunoglobulin
Ii	Invariant chain
IL	Interleukin
ITAM	Immunoreceptor tyrosine based activating motif
KAP1	KRAB-associated protein 1
Kox1	Zinc finger protein 10
KRAB	Kruppel associated box
KSHV	Kaposi's sarcoma-associated herpesvirus
L-HPG	L-Homopropargylglycine
LAG-3	Lymphocyte-activation gene 3
LAT	Linker of Activated T cells
LCK	Lymphocyte-specific protein tyrosine kinase
LCMV	Lymphocytic choriomeningitis virus
loxP	Locus of X-over P1
M-Phase	Mitose phase
mAb	Monoclonal antibody
MAPK	Mitogen activated protein-kinase
MCC	Moth cytochrome c
MEF	Mouse embryonic fibroblasts
MFI	Mean fluorescence intensity
mg	Milligram
MHC	Major Histocompatibility Complex
MHV-68	Murin Gammaherpesvirus 68
mL	Milliliter
mLST8	Mammalian lethal with SEC13 protein 8
mM	Millimolar
MPEC	Memory precursor effector cell
mRNA	messengerRNA
mSin1	Mammalian stress-activated protein kinase [SAPK]-interacting protein
mTEC	Medullar thymus epithelial cell
mTOR	mammalian/mechanistic target of rapamycin

## F Abbreviations

mTORC1	mammalian/mechanistic target of rapamycin complex 1
mTORC2	mammalian/mechanistic target of rapamycin complex 2
MVA	Modified vaccinia ankara
NFAT	Nuclear factor of activated T-cells
NFκB	Nuclear factor kappa-light-chain-enhancer of activated B cells
ng	Nanogram
NK cells	Natural Killer cells
NKT	Natural killer T cell
OVA	Ovalbumin
OXPHOS	Oxidative Phosphorylation
PBS	Phosphate buffered saline
PCR	Polymerase chain reaction
PDCC4	Programmed cell death protein 4
PKD1	Phosphoinositide-dependent kinase-1
PFA	Paraformaldehyd
PI3K	Phosphoinoside 3-kinase
Pim-1/-2	Proto-oncogene serine/threonine-protein kinase
PIP <sub>3</sub>	Phosphatidylinositol (3,4,5)-trisphosphate
PKB	Protein kinase B
pMHC	Peptide bound to MHC
PRAS40	Proline-rich AKT substrate 1
PRR	Pattern recognition receptor
R26	Rosa-26
RAG	Recombination-activating gene
Raptor	Regulatory-associated protein of mTOR
Rb	Retinoblastoma protein
rDNA	Ribosomal DNA
RHEB	Ras homolog enriched in brain
Rictor	Rapamycin-insensitive companion of mammalian target of rapamycin
RNA	Ribonucleic acid
Rory	RAR-related orphan receptor gamma
ROS	Reactive oxygen species
Rn3	RNA polymerase I-specific transcription initiation factor 3
rRNA	Ribosomal RNA
rtTA	Reverse tetracycline-responsive transactivator
rtTA	Reverse tetracycline-controlled transcriptional activation
S-Phase	Synthesis phase
S6K1	p70 S6 kinase 1
SLC38A9	Sodium-coupled neutral amino acid transporter 9
SLEC	Short-lived effector cells
SREBP	Sterol regulatory element-binding protein
T-bet	T-box transcription factor
TAE	Tris-acetate-EDTA
TAP	Transporter associated with antigen processing

## F Abbreviations

TAP	Transporter associated with antigen processing
TCR	T cell receptor
tet	Tetracycline
tetO	Tetracycline operator
tetR	Tetracycline repressor
Texh	Exhausted T cell
TFEB	Transcription factor EB
Tfh	T follicular helper cell
TGF	Tumor Growth Factor
Th cell	T helper cell
Thr	Threonine
TIF-IA	Transcription initiation factor IA
TIFIIIB	Transcription initiation factor IIIB
Tmem	Memory T cell
TNF	Tumor necrosis factor
Treg	Regulatory T cell
TRIS	Tris(hydroxymethyl)aminomethane
tRNA	Transfer-RNA
TSC	Tuberous sclerosis
tTA	Tetracycline-controlled transcriptional activation
UBF	Upstream binding factor
ULK1	Unc-51 like autophagy activating kinase
UV	Ultra violet
Wnt	Wingless/integrated
WT	Wildtype
ZAP70	Zeta-chain-associated protein kinase 70
µg	Microgram
µl	Microliter
µM	Micromolar

---

## G Literature

Abbas, A.K., Murphy, K.M., and Sher, A. (1996). Functional diversity of helper T lymphocytes. *Nature* 383, 787-793.

Adler, H., Messerle, M., Wagner, M., and Koszinowski, U.H. (2000). Cloning and mutagenesis of the murine gammaherpesvirus 68 genome as an infectious bacterial artificial chromosome. *J Virol* 74, 6964-6974.

Aggarwal, S., Ghilardi, N., Xie, M.H., de Sauvage, F.J., and Gurney, A.L. (2003). Interleukin-23 promotes a distinct CD4 T cell activation state characterized by the production of interleukin-17. *J Biol Chem* 278, 1910-1914.

Ali, A.K., Nandagopal, N., and Lee, S.H. (2015). IL-15-PI3K-AKT-mTOR: A Critical Pathway in the Life Journey of Natural Killer Cells. *Front Immunol* 6, 355.

Ananieva, E.A., Patel, C.H., Drake, C.H., Powell, J.D., and Hutson, S.M. (2014). Cytosolic branched chain aminotransferase (BCATc) regulates mTORC1 signaling and glycolytic metabolism in CD4<sup>+</sup> T cells. *J Biol Chem* 289, 18793-18804.

Araki, K., Morita, M., Bederman, A.G., Konieczny, B.T., Kissick, H.T., Sonenberg, N., and Ahmed, R. (2017). Translation is actively regulated during the differentiation of CD8<sup>+</sup> effector T cells. *Nat Immunol* 18, 1046-1057.

Araki, K., Turner, A.P., Shaffer, V.O., Gangappa, S., Keller, S.A., Bachmann, M.F., Larsen, C.P., and Ahmed, R. (2009). mTOR regulates memory CD8 T-cell differentiation. *Nature* 460, 108-112.

Araki, K., Youngblood, B., and Ahmed, R. (2013). Programmed cell death 1-directed immunotherapy for enhancing T-cell function. *Cold Spring Harb Symp Quant Biol* 78, 239-247.

Aylett, C.H., Sauer, E., Imseng, S., Boehringer, D., Hall, M.N., Ban, N., and Maier, T. (2016). Architecture of human mTOR complex 1. *Science* 351, 48-52.

Badovinac, V.P., Porter, B.B., and Harty, J.T. (2002). Programmed contraction of CD8(+) T cells after infection. *Nat Immunol* 3, 619-626.

Bar-Peled, L., Chantranupong, L., Cherniack, A.D., Chen, W.W., Ottina, K.A., Grabiner, B.C., Spear, E.D., Carter, S.L., Meyerson, M., and Sabatini, D.M. (2013). A Tumor suppressor complex with GAP activity for the Rag GTPases that signal amino acid sufficiency to mTORC1. *Science* 340, 1100-1106.

Barbet, N.C., Schneider, U., Helliwell, S.B., Stansfield, I., Tuite, M.F., and Hall, M.N. (1996). TOR controls translation initiation and early G1 progression in yeast. *Mol Biol Cell* 7, 25-42.

## G Literature

Barde, I., Laurenti, E., Verp, S., Groner, A.C., Towne, C., Padrun, V., Aebischer, P., Trumpp, A., and Trono, D. (2009). Regulation of episomal gene expression by KRAB/KAP1-mediated histone modifications. *J Virol* 83, 5574-5580.

Behbehani, G.K., Bendall, S.C., Clutter, M.R., Fantl, W.J., and Nolan, G.P. (2012). Single-cell mass cytometry adapted to measurements of the cell cycle. *Cytometry A* 81, 552-566.

Bell, E.B., Sparshott, S.M., Drayson, M.T., and Ford, W.L. (1987). The stable and permanent expansion of functional T lymphocytes in athymic nude rats after a single injection of mature T cells. *J Immunol* 139, 1379-1384.

Ben-Sahra, I., Hoxhaj, G., Ricoult, S.J.H., Asara, J.M., and Manning, B.D. (2016). mTORC1 induces purine synthesis through control of the mitochondrial tetrahydrofolate cycle. *Science* 351, 728-733.

Bensaude, O. (2011). Inhibiting eukaryotic transcription: Which compound to choose? How to evaluate its activity? *Transcription* 2, 103-108.

Berod, L., Friedrich, C., Nandan, A., Freitag, J., Hagemann, S., Harmrolfs, K., Sandouk, A., Hesse, C., Castro, C.N., Bahre, H., Tschirner, S.K., Gorinski, N., Gohmert, M., Mayer, C.T., Huehn, J., Ponimaskin, E., Abraham, W.R., Muller, R., Lochner, M., and Sparwasser, T. (2014). De novo fatty acid synthesis controls the fate between regulatory T and T helper 17 cells. *Nat Med* 20, 1327-1333.

Bouso, P., and Robey, E. (2003). Dynamics of CD8<sup>+</sup> T cell priming by dendritic cells in intact lymph nodes. *Nat Immunol* 4, 579-585.

Brooks, D.G., Walsh, K.B., Elsaesser, H., and Oldstone, M.B. (2010). IL-10 directly suppresses CD4 but not CD8 T cell effector and memory responses following acute viral infection. *Proc Natl Acad Sci U S A* 107, 3018-3023.

Brown, E.J., Albers, M.W., Shin, T.B., Ichikawa, K., Keith, C.T., Lane, W.S., and Schreiber, S.L. (1994). A mammalian protein targeted by G1-arresting rapamycin-receptor complex. *Nature* 369, 756-758.

Brown, E.J., Beal, P.A., Keith, C.T., Chen, J., Shin, T.B., and Schreiber, S.L. (1995). Control of p70 s6 kinase by kinase activity of FRAP in vivo. *Nature* 377, 441-446.

Brugarolas, J., Lei, K., Hurley, R.L., Manning, B.D., Reiling, J.H., Hafen, E., Witters, L.A., Ellisen, L.W., and Kaelin, W.G., Jr. (2004). Regulation of mTOR function in response to hypoxia by REDD1 and the TSC1/TSC2 tumor suppressor complex. *Genes Dev* 18, 2893-2904.

Brunn, G.J., Hudson, C.C., Sekulic, A., Williams, J.M., Hosoi, H., Houghton, P.J., Lawrence, J.C., Jr., and Abraham, R.T. (1997). Phosphorylation of the translational repressor PHAS-I by the mammalian target of rapamycin. *Science* 277, 99-101.

## G Literature

Bruno, L., von Boehmer, H., and Kirberg, J. (1996). Cell division in the compartment of naive and memory T lymphocytes. *Eur J Immunol* 26, 3179-3184.

Burger, K., Muhl, B., Harasim, T., Rohrmoser, M., Malamoussi, A., Orban, M., Kellner, M., Gruber-Eber, A., Kremmer, E., Holzel, M., and Eick, D. (2010). Chemotherapeutic drugs inhibit ribosome biogenesis at various levels. *J Biol Chem* 285, 12416-12425.

Burnett, P.E., Barrow, R.K., Cohen, N.A., Snyder, S.H., and Sabatini, D.M. (1998). RAFT1 phosphorylation of the translational regulators p70 S6 kinase and 4E-BP1. *Proc Natl Acad Sci U S A* 95, 1432-1437.

Bywater, M.J., Poortinga, G., Sanij, E., Hein, N., Peck, A., Cullinane, C., Wall, M., Cluse, L., Drygin, D., Anderes, K., Huser, N., Proffitt, C., Bliesath, J., Haddach, M., Schwaebe, M.K., Ryckman, D.M., Rice, W.G., Schmitt, C., Lowe, S.W., Johnstone, R.W., Pearson, R.B., McArthur, G.A., and Hannan, R.D. (2012). Inhibition of RNA polymerase I as a therapeutic strategy to promote cancer-specific activation of p53. *Cancer Cell* 22, 51-65.

Cafferkey, R., Young, P.R., McLaughlin, M.M., Bergsma, D.J., Koltin, Y., Sathe, G.M., Faucette, L., Eng, W.K., Johnson, R.K., and Livi, G.P. (1993). Dominant missense mutations in a novel yeast protein related to mammalian phosphatidylinositol 3-kinase and VPS34 abrogate rapamycin cytotoxicity. *Mol Cell Biol* 13, 6012-6023.

Cao, Y., Rathmell, J.C., and Macintyre, A.N. (2014). Metabolic reprogramming towards aerobic glycolysis correlates with greater proliferative ability and resistance to metabolic inhibition in CD8 versus CD4 T cells. *PLoS One* 9, e104104.

Cargnello, M., Tcherkezian, J., and Roux, P.P. (2015). The expanding role of mTOR in cancer cell growth and proliferation. *Mutagenesis* 30, 169-176.

Challen, G.A., Boles, N., Lin, K.K., and Goodell, M.A. (2009). Mouse hematopoietic stem cell identification and analysis. *Cytometry A* 75, 14-24.

Challen, G.A., and Goodell, M.A. (2008). Promiscuous expression of H2B-GFP transgene in hematopoietic stem cells. *PLoS One* 3, e2357.

Cham, C.M., Driessens, G., O'Keefe, J.P., and Gajewski, T.F. (2008). Glucose deprivation inhibits multiple key gene expression events and effector functions in CD8<sup>+</sup> T cells. *Eur J Immunol* 38, 2438-2450.

Chan, J.C., Hannan, K.M., Riddell, K., Ng, P.Y., Peck, A., Lee, R.S., Hung, S., Astle, M.V., Bywater, M., Wall, M., Poortinga, G., Jastrzebski, K., Sheppard, K.E., Hemmings, B.A., Hall, M.N., Johnstone, R.W., McArthur, G.A., Hannan, R.D., and Pearson, R.B. (2011). AKT promotes rRNA synthesis and cooperates with c-MYC to stimulate ribosome biogenesis in cancer. *Sci Signal* 4, ra56.

Chantranupong, L., Wolfson, R.L., Orozco, J.M., Saxton, R.A., Scaria, S.M., Bar-Peled, L., Spooner, E., Isasa, M., Gygi, S.P., and Sabatini, D.M. (2014). The Sestrins interact

## G Literature

with GATOR2 to negatively regulate the amino-acid-sensing pathway upstream of mTORC1. *Cell Rep* 9, 1-8.

Choo, A.Y., Yoon, S.O., Kim, S.G., Roux, P.P., and Blenis, J. (2008). Rapamycin differentially inhibits S6Ks and 4E-BP1 to mediate cell-type-specific repression of mRNA translation. *Proc Natl Acad Sci U S A* 105, 17414-17419.

Ciarmatori, S., Scott, P.H., Sutcliffe, J.E., McLees, A., Alzuherri, H.M., Dannenberg, J.H., te Riele, H., Grummt, I., Voit, R., and White, R.J. (2001). Overlapping functions of the pRb family in the regulation of rRNA synthesis. *Mol Cell Biol* 21, 5806-5814.

Claypool, J.A., French, S.L., Johzuka, K., Eliason, K., Vu, L., Dodd, J.A., Beyer, A.L., and Nomura, M. (2004). Tor pathway regulates Rrn3p-dependent recruitment of yeast RNA polymerase I to the promoter but does not participate in alteration of the number of active genes. *Mol Biol Cell* 15, 946-956.

Corbin, G.A., and Harty, J.T. (2004). Duration of infection and antigen display have minimal influence on the kinetics of the CD4<sup>+</sup> T cell response to *Listeria monocytogenes* infection. *J Immunol* 173, 5679-5687.

Crawford, A., Angelosanto, J.M., Kao, C., Doering, T.A., Odorizzi, P.M., Barnett, B.E., and Wherry, E.J. (2014). Molecular and transcriptional basis of CD4<sup>+</sup> T cell dysfunction during chronic infection. *Immunity* 40, 289-302.

Crissman, H.A., Darzynkiewicz, Z., Tobey, R.A., and Steinkamp, J.A. (1985). Correlated measurements of DNA, RNA, and protein in individual cells by flow cytometry. *Science* 228, 1321-1324.

Crotty, S. (2014). T follicular helper cell differentiation, function, and roles in disease. *Immunity* 41, 529-542.

Cruz-Guilloty, F., Pipkin, M.E., Djuretic, I.M., Levanon, D., Lotem, J., Lichtenheld, M.G., Groner, Y., and Rao, A. (2009). Runx3 and T-box proteins cooperate to establish the transcriptional program of effector CTLs. *J Exp Med* 206, 51-59.

Cui, H.H., Valdez, J.G., Steinkamp, J.A., and Crissman, H.A. (2003). Fluorescence lifetime-based discrimination and quantification of cellular DNA and RNA with phase-sensitive flow cytometry. *Cytometry A* 52, 46-55.

Darzynkiewicz, Z., Juan, G., and Srouf, E.F. (2004). Differential staining of DNA and RNA. *Curr Protoc Cytom Chapter 7, Unit 7 3*.

Darzynkiewicz, Z., Traganos, F., and Melamed, M.R. (1980). New cell cycle compartments identified by multiparameter flow cytometry. *Cytometry* 1, 98-108.

Delgoffe, G.M., Kole, T.P., Cotter, R.J., and Powell, J.D. (2009a). Enhanced interaction between Hsp90 and raptor regulates mTOR signaling upon T cell activation. *Mol Immunol* 46, 2694-2698.

## G Literature

Delgoffe, G.M., Kole, T.P., Zheng, Y., Zarek, P.E., Matthews, K.L., Xiao, B., Worley, P.F., Kozma, S.C., and Powell, J.D. (2009b). The mTOR kinase differentially regulates effector and regulatory T cell lineage commitment. *Immunity* 30, 832-844.

Delgoffe, G.M., Pollizzi, K.N., Waickman, A.T., Heikamp, E., Meyers, D.J., Horton, M.R., Xiao, B., Worley, P.F., and Powell, J.D. (2011). The kinase mTOR regulates the differentiation of helper T cells through the selective activation of signaling by mTORC1 and mTORC2. *Nat Immunol* 12, 295-303.

Delgoffe, G.M., and Powell, J.D. (2015). Feeding an army: The metabolism of T cells in activation, anergy, and exhaustion. *Mol Immunol* 68, 492-496.

Derenzini, M., Trere, D., Pession, A., Montanaro, L., Sirri, V., and Ochs, R.L. (1998). Nucleolar function and size in cancer cells. *Am J Pathol* 152, 1291-1297.

Deuschle, U., Meyer, W.K., and Thiesen, H.J. (1995). Tetracycline-reversible silencing of eukaryotic promoters. *Mol Cell Biol* 15, 1907-1914.

Doering, T.A., Crawford, A., Angelosanto, J.M., Paley, M.A., Ziegler, C.G., and Wherry, E.J. (2012). Network analysis reveals centrally connected genes and pathways involved in CD8<sup>+</sup> T cell exhaustion versus memory. *Immunity* 37, 1130-1144.

Dorrello, N.V., Peschiaroli, A., Guardavaccaro, D., Colburn, N.H., Sherman, N.E., and Pagano, M. (2006). S6K1- and betaTRCP-mediated degradation of PDCD4 promotes protein translation and cell growth. *Science* 314, 467-471.

Dowling, M.R., Kan, A., Heinzl, S., Zhou, J.H., Marchingo, J.M., Wellard, C.J., Markham, J.F., and Hodgkin, P.D. (2014). Stretched cell cycle model for proliferating lymphocytes. *Proc Natl Acad Sci U S A* 111, 6377-6382.

Drygin, D., Lin, A., Bliesath, J., Ho, C.B., O'Brien, S.E., Proffitt, C., Omori, M., Haddach, M., Schwaebe, M.K., Siddiqui-Jain, A., Streiner, N., Quin, J.E., Sanij, E., Bywater, M.J., Hannan, R.D., Ryckman, D., Anderes, K., and Rice, W.G. (2011). Targeting RNA polymerase I with an oral small molecule CX-5461 inhibits ribosomal RNA synthesis and solid tumor growth. *Cancer Res* 71, 1418-1430.

Duvel, K., Yecies, J.L., Menon, S., Raman, P., Lipovsky, A.I., Souza, A.L., Triantafellow, E., Ma, Q., Gorski, R., Cleaver, S., Vander Heiden, M.G., MacKeigan, J.P., Finan, P.M., Clish, C.B., Murphy, L.O., and Manning, B.D. (2010). Activation of a metabolic gene regulatory network downstream of mTOR complex 1. *Mol Cell* 39, 171-183.

Efeyan, A., Zoncu, R., Chang, S., Gumper, I., Snitkin, H., Wolfson, R.L., Kirak, O., Sabatini, D.D., and Sabatini, D.M. (2013). Regulation of mTORC1 by the Rag GTPases is necessary for neonatal autophagy and survival. *Nature* 493, 679-683.

Feng, Z., Hu, W., de Stanchina, E., Teresky, A.K., Jin, S., Lowe, S., and Levine, A.J. (2007). The regulation of AMPK beta1, TSC2, and PTEN expression by p53: stress,

## G Literature

cell and tissue specificity, and the role of these gene products in modulating the IGF-1-AKT-mTOR pathways. *Cancer Res* 67, 3043-3053.

Filer, D., Thompson, M.A., Takhaveev, V., Dobson, A.J., Kotronaki, I., Green, J.W.M., Heinemann, M., Tullet, J.M.A., and Alic, N. (2017). RNA polymerase III limits longevity downstream of TORC1. *Nature* 552, 263-267.

Finlay, D.K., Rosenzweig, E., Sinclair, L.V., Feijoo-Carnero, C., Hukelmann, J.L., Rolf, J., Panteleyev, A.A., Okkenhaug, K., and Cantrell, D.A. (2012). PDK1 regulation of mTOR and hypoxia-inducible factor 1 integrate metabolism and migration of CD8<sup>+</sup> T cells. *J Exp Med* 209, 2441-2453.

Fox, C.J., Hammerman, P.S., and Thompson, C.B. (2005). The Pim kinases control rapamycin-resistant T cell survival and activation. *J Exp Med* 201, 259-266.

Frauwirth, K.A., Riley, J.L., Harris, M.H., Parry, R.V., Rathmell, J.C., Plas, D.R., Elstrom, R.L., June, C.H., and Thompson, C.B. (2002). The CD28 signaling pathway regulates glucose metabolism. *Immunity* 16, 769-777.

Frauwirth, K.A., and Thompson, C.B. (2002). Activation and inhibition of lymphocytes by costimulation. *J Clin Invest* 109, 295-299.

Frauwirth, K.A., and Thompson, C.B. (2004). Regulation of T lymphocyte metabolism. *J Immunol* 172, 4661-4665.

Gallimore, A., Glithero, A., Godkin, A., Tissot, A.C., Pluckthun, A., Elliott, T., Hengartner, H., and Zinkernagel, R. (1998). Induction and exhaustion of lymphocytic choriomeningitis virus-specific cytotoxic T lymphocytes visualized using soluble tetrameric major histocompatibility complex class I-peptide complexes. *J Exp Med* 187, 1383-1393.

Ganem, D. (1997). KSHV and Kaposi's sarcoma: the end of the beginning? *Cell* 91, 157-160.

Garami, A., Zwartkruis, F.J., Nobukuni, T., Joaquin, M., Rocco, M., Stocker, H., Kozma, S.C., Hafen, E., Bos, J.L., and Thomas, G. (2003). Insulin activation of Rheb, a mediator of mTOR/S6K/4E-BP signaling, is inhibited by TSC1 and 2. *Mol Cell* 11, 1457-1466.

Gaud, G., Lesourne, R., and Love, P.E. (2018). Regulatory mechanisms in T cell receptor signalling. *Nat Rev Immunol* 18, 485-497.

Gebrane-Younes, J., Fomproix, N., and Hernandez-Verdun, D. (1997). When rDNA transcription is arrested during mitosis, UBF is still associated with non-condensed rDNA. *J Cell Sci* 110 ( Pt 19), 2429-2440.

## G Literature

Gelfand, E.W., Weinberg, K., Mazer, B.D., Kadlecsek, T.A., and Weiss, A. (1995). Absence of ZAP-70 prevents signaling through the antigen receptor on peripheral blood T cells but not on thymocytes. *J Exp Med* 182, 1057-1065.

Geltink, R.I.K., Kyle, R.L., and Pearce, E.L. (2018). Unraveling the Complex Interplay Between T Cell Metabolism and Function. *Annu Rev Immunol* 36, 461-488.

Gerriets, V.A., and Rathmell, J.C. (2012). Metabolic pathways in T cell fate and function. *Trends Immunol* 33, 168-173.

Gingras, A.C., Raught, B., and Sonenberg, N. (1999). eIF4 initiation factors: effectors of mRNA recruitment to ribosomes and regulators of translation. *Annu Rev Biochem* 68, 913-963.

Grogan, J.L., Mohrs, M., Harmon, B., Lacy, D.A., Sedat, J.W., and Locksley, R.M. (2001). Early transcription and silencing of cytokine genes underlie polarization of T helper cell subsets. *Immunity* 14, 205-215.

Groner, A.C., Meylan, S., Ciuffi, A., Zangger, N., Ambrosini, G., Denervaud, N., Bucher, P., and Trono, D. (2010). KRAB-zinc finger proteins and KAP1 can mediate long-range transcriptional repression through heterochromatin spreading. *PLoS Genet* 6, e1000869.

Grummt, I., and Langst, G. (2013). Epigenetic control of RNA polymerase I transcription in mammalian cells. *Biochim Biophys Acta* 1829, 393-404.

Gwinn, D.M., Shackelford, D.B., Egan, D.F., Mihaylova, M.M., Mery, A., Vasquez, D.S., Turk, B.E., and Shaw, R.J. (2008). AMPK phosphorylation of raptor mediates a metabolic checkpoint. *Mol Cell* 30, 214-226.

Han, S., Asoyan, A., Rabenstein, H., Nakano, N., and Obst, R. (2010). Role of antigen persistence and dose for CD4<sup>+</sup> T-cell exhaustion and recovery. *Proc Natl Acad Sci U S A* 107, 20453-20458.

Hannan, K.M., Brandenburger, Y., Jenkins, A., Sharkey, K., Cavanaugh, A., Rothblum, L., Moss, T., Poortinga, G., McArthur, G.A., Pearson, R.B., and Hannan, R.D. (2003). mTOR-dependent regulation of ribosomal gene transcription requires S6K1 and is mediated by phosphorylation of the carboxy-terminal activation domain of the nucleolar transcription factor UBF. *Mol Cell Biol* 23, 8862-8877.

Hannan, R.D., Hempel, W.M., Cavanaugh, A., Arino, T., Dimitrov, S.I., Moss, T., and Rothblum, L. (1998). Affinity purification of mammalian RNA polymerase I. Identification of an associated kinase. *J Biol Chem* 273, 1257-1267.

Hara, K., Maruki, Y., Long, X., Yoshino, K., Oshiro, N., Hidayat, S., Tokunaga, C., Avruch, J., and Yonezawa, K. (2002). Raptor, a binding partner of target of rapamycin (TOR), mediates TOR action. *Cell* 110, 177-189.

## G Literature

Hardwick, J.S., Kuruvilla, F.G., Tong, J.K., Shamji, A.F., and Schreiber, S.L. (1999). Rapamycin-modulated transcription defines the subset of nutrient-sensitive signaling pathways directly controlled by the Tor proteins. *Proc Natl Acad Sci U S A* 96, 14866-14870.

Hashimoto, M., Kamphorst, A.O., Im, S.J., Kissick, H.T., Pillai, R.N., Ramalingam, S.S., Araki, K., and Ahmed, R. (2018). CD8 T Cell Exhaustion in Chronic Infection and Cancer: Opportunities for Interventions. *Annu Rev Med* 69, 301-318.

Haxhinasto, S., Mathis, D., and Benoist, C. (2008). The AKT-mTOR axis regulates de novo differentiation of CD4<sup>+</sup>Foxp3<sup>+</sup> cells. *J Exp Med* 205, 565-574.

He, Q., Gao, Z., Yin, J., Zhang, J., Yun, Z., and Ye, J. (2011). Regulation of HIF-1{alpha} activity in adipose tissue by obesity-associated factors: adipogenesis, insulin, and hypoxia. *Am J Physiol Endocrinol Metab* 300, E877-885.

Heitman, J., Movva, N.R., and Hall, M.N. (1991). Targets for cell cycle arrest by the immunosuppressant rapamycin in yeast. *Science* 253, 905-909.

Helliwell, S.B., Wagner, P., Kunz, J., Deuter-Reinhard, M., Henriquez, R., and Hall, M.N. (1994). TOR1 and TOR2 are structurally and functionally similar but not identical phosphatidylinositol kinase homologues in yeast. *Mol Biol Cell* 5, 105-118.

Hernandez-Verdun, D., Roussel, P., and Gebrane-Younes, J. (2002). Emerging concepts of nucleolar assembly. *J Cell Sci* 115, 2265-2270.

Herrero-Sanchez, M.C., Rodriguez-Serrano, C., Almeida, J., San Segundo, L., Inoges, S., Santos-Briz, A., Garcia-Brinon, J., Corchete, L.A., San Miguel, J.F., Del Canizo, C., and Blanco, B. (2016). Targeting of PI3K/AKT/mTOR pathway to inhibit T cell activation and prevent graft-versus-host disease development. *J Hematol Oncol* 9, 113.

Hester, J., Schiopu, A., Nadig, S.N., and Wood, K.J. (2012). Low-dose rapamycin treatment increases the ability of human regulatory T cells to inhibit transplant arteriosclerosis in vivo. *Am J Transplant* 12, 2008-2016.

Hochedlinger, K., Yamada, Y., Beard, C., and Jaenisch, R. (2005). Ectopic expression of Oct-4 blocks progenitor-cell differentiation and causes dysplasia in epithelial tissues. *Cell* 121, 465-477.

Hogquist, K.A., Jameson, S.C., Heath, W.R., Howard, J.L., Bevan, M.J., and Carbone, F.R. (1994). T cell receptor antagonist peptides induce positive selection. *Cell* 76, 17-27.

Holz, M.K., Ballif, B.A., Gygi, S.P., and Blenis, J. (2005). mTOR and S6K1 mediate assembly of the translation preinitiation complex through dynamic protein interchange and ordered phosphorylation events. *Cell* 123, 569-580.

## G Literature

Hukelmann, J.L., Anderson, K.E., Sinclair, L.V., Grzes, K.M., Murillo, A.B., Hawkins, P.T., Stephens, L.R., Lamond, A.I., and Cantrell, D.A. (2016). The cytotoxic T cell proteome and its shaping by the kinase mTOR. *Nat Immunol* 17, 104-112.

Hutten, S., Prescott, A., James, J., Riesenber, S., Boulon, S., Lam, Y.W., and Lamond, A.I. (2011). An intranucleolar body associated with rDNA. *Chromosoma* 120, 481-499.

Iadevaia, V., Zhang, Z., Jan, E., and Proud, C.G. (2012). mTOR signaling regulates the processing of pre-rRNA in human cells. *Nucleic Acids Res* 40, 2527-2539.

Im, S.J., Hashimoto, M., Gerner, M.Y., Lee, J., Kissick, H.T., Burger, M.C., Shan, Q., Hale, J.S., Lee, J., Nasti, T.H., Sharpe, A.H., Freeman, G.J., Germain, R.N., Nakaya, H.I., Xue, H.H., and Ahmed, R. (2016). Defining CD8<sup>+</sup> T cells that provide the proliferative burst after PD-1 therapy. *Nature* 537, 417-421.

Inoki, K., Li, Y., Xu, T., and Guan, K.L. (2003a). Rheb GTPase is a direct target of TSC2 GAP activity and regulates mTOR signaling. *Genes Dev* 17, 1829-1834.

Inoki, K., Zhu, T., and Guan, K.L. (2003b). TSC2 mediates cellular energy response to control cell growth and survival. *Cell* 115, 577-590.

Jameson, J., Ugarte, K., Chen, N., Yachi, P., Fuchs, E., Boismenu, R., and Havran, W.L. (2002). A role for skin gammadelta T cells in wound repair. *Science* 296, 747-749.

Jameson, S.C. (2002). Maintaining the norm: T-cell homeostasis. *Nat Rev Immunol* 2, 547-556.

Janumyan, Y.M., Sansam, C.G., Chattopadhyay, A., Cheng, N., Soucie, E.L., Penn, L.Z., Andrews, D., Knudson, C.M., and Yang, E. (2003). Bcl-xL/Bcl-2 coordinately regulates apoptosis, cell cycle arrest and cell cycle entry. *EMBO J* 22, 5459-5470.

Jenkins, M.K. (1992). The role of cell division in the induction of clonal anergy. *Immunol Today* 13, 69-73.

Jenkins, M.K., and Moon, J.J. (2012). The role of naive T cell precursor frequency and recruitment in dictating immune response magnitude. *J Immunol* 188, 4135-4140.

Jones, R.G., and Thompson, C.B. (2007). Revving the engine: signal transduction fuels T cell activation. *Immunity* 27, 173-178.

Josefowicz, S.Z., and Rudensky, A. (2009). Control of regulatory T cell lineage commitment and maintenance. *Immunity* 30, 616-625.

Joshi, N.S., Cui, W., Chandele, A., Lee, H.K., Urso, D.R., Hagman, J., Gapin, L., and Kaech, S.M. (2007). Inflammation directs memory precursor and short-lived effector

## G Literature

CD8<sup>+</sup> T cell fates via the graded expression of T-bet transcription factor. *Immunity* 27, 281-295.

Kaech, S.M., and Cui, W. (2012). Transcriptional control of effector and memory CD8<sup>+</sup> T cell differentiation. *Nat Rev Immunol* 12, 749-761.

Kalender, A., Selvaraj, A., Kim, S.Y., Gulati, P., Brule, S., Viollet, B., Kemp, B.E., Bardeesy, N., Dennis, P., Schlager, J.J., Marette, A., Kozma, S.C., and Thomas, G. (2010). Metformin, independent of AMPK, inhibits mTORC1 in a rag GTPase-dependent manner. *Cell Metab* 11, 390-401.

Kantidakis, T., Ramsbottom, B.A., Birch, J.L., Dowding, S.N., and White, R.J. (2010). mTOR associates with TFIIC, is found at tRNA and 5S rRNA genes, and targets their repressor Maf1. *Proc Natl Acad Sci U S A* 107, 11823-11828.

Kaye, J., Hsu, M.L., Sauron, M.E., Jameson, S.C., Gascoigne, N.R., and Hedrick, S.M. (1989). Selective development of CD4<sup>+</sup> T cells in transgenic mice expressing a class II MHC-restricted antigen receptor. *Nature* 341, 746-749.

Kieper, W.C., Pric, M., Schmidt, C.S., Mescher, M.F., and Jameson, S.C. (2001). IL-12 enhances CD8 T cell homeostatic expansion. *J Immunol* 166, 5515-5521.

Kim, D.H., Sarbassov, D.D., Ali, S.M., King, J.E., Latek, R.R., Erdjument-Bromage, H., Tempst, P., and Sabatini, D.M. (2002). mTOR interacts with raptor to form a nutrient-sensitive complex that signals to the cell growth machinery. *Cell* 110, 163-175.

Kim, J., Kundu, M., Viollet, B., and Guan, K.L. (2011). AMPK and mTOR regulate autophagy through direct phosphorylation of Ulk1. *Nat Cell Biol* 13, 132-141.

Kim, K.H., and Sederstrom, J.M. (2015). Assaying Cell Cycle Status Using Flow Cytometry. *Curr Protoc Mol Biol* 111, 28 26 21-11.

Koltin, Y., Faucette, L., Bergsma, D.J., Levy, M.A., Cafferkey, R., Koser, P.L., Johnson, R.K., and Livi, G.P. (1991). Rapamycin sensitivity in *Saccharomyces cerevisiae* is mediated by a peptidyl-prolyl cis-trans isomerase related to human FK506-binding protein. *Mol Cell Biol* 11, 1718-1723.

Kunz, J., Henriquez, R., Schneider, U., Deuter-Reinhard, M., Movva, N.R., and Hall, M.N. (1993). Target of rapamycin in yeast, TOR2, is an essential phosphatidylinositol kinase homolog required for G1 progression. *Cell* 73, 585-596.

Laplante, M., and Sabatini, D.M. (2012). mTOR signaling in growth control and disease. *Cell* 149, 274-293.

Lawrence, C.W., and Braciale, T.J. (2004). Activation, differentiation, and migration of naive virus-specific CD8<sup>+</sup> T cells during pulmonary influenza virus infection. *J Immunol* 173, 1209-1218.

## G Literature

Lee, K., Gudapati, P., Dragovic, S., Spencer, C., Joyce, S., Killeen, N., Magnuson, M.A., and Boothby, M. (2010). Mammalian target of rapamycin protein complex 2 regulates differentiation of Th1 and Th2 cell subsets via distinct signaling pathways. *Immunity* 32, 743-753.

Lee, P.P., Fitzpatrick, D.R., Beard, C., Jessup, H.K., Lehar, S., Makar, K.W., Perez-Melgosa, M., Sweetser, M.T., Schlissel, M.S., Nguyen, S., Cherry, S.R., Tsai, J.H., Tucker, S.M., Weaver, W.M., Kelso, A., Jaenisch, R., and Wilson, C.B. (2001). A critical role for Dnmt1 and DNA methylation in T cell development, function, and survival. *Immunity* 15, 763-774.

Lee, Y.K., Mukasa, R., Hatton, R.D., and Weaver, C.T. (2009). Developmental plasticity of Th17 and Treg cells. *Curr Opin Immunol* 21, 274-280.

Li, Q., Rao, R., Vazzana, J., Goedegebuure, P., Odunsi, K., Gillanders, W., and Shrikant, P.A. (2012). Regulating mammalian target of rapamycin to tune vaccination-induced CD8<sup>+</sup> T cell responses for tumor immunity. *J Immunol* 188, 3080-3087.

Li, Q., Rao, R.R., Araki, K., Pollizzi, K., Odunsi, K., Powell, J.D., and Shrikant, P.A. (2011). A central role for mTOR kinase in homeostatic proliferation induced CD8<sup>+</sup> T cell memory and tumor immunity. *Immunity* 34, 541-553.

Liu, L., Chavan, R., and Feinberg, M.B. (2008). Dendritic cells are preferentially targeted among hematolymphocytes by Modified Vaccinia Virus Ankara and play a key role in the induction of virus-specific T cell responses in vivo. *BMC Immunol* 9, 15.

Liu, Q., Kang, S.A., Thoreen, C.C., Hur, W., Wang, J., Chang, J.W., Markhard, A., Zhang, J., Sim, T., Sabatini, D.M., and Gray, N.S. (2012). Development of ATP-competitive mTOR inhibitors. *Methods Mol Biol* 821, 447-460.

Loewith, R., Jacinto, E., Wullschleger, S., Lorberg, A., Cresspo, J.L., Bonenfant, D., Oppliger, W., Jenoe, P., and Hall, M.N. (2002). Two TOR complexes, only one of which is rapamycin sensitive, have distinct roles in cell growth control. *Mol Cell* 10, 457-468.

Long, X., Lin, Y., Ortiz-Vega, S., Yonezawa, K., and Avruch, J. (2005). Rheb binds and regulates the mTOR kinase. *Curr Biol* 15, 702-713.

Macintyre, A.N., Gerriets, V.A., Nichols, A.G., Michalek, R.D., Rudolph, M.C., Deoliveira, D., Anderson, S.M., Abel, E.D., Chen, B.J., Hale, L.P., and Rathmell, J.C. (2014). The glucose transporter Glut1 is selectively essential for CD4 T cell activation and effector function. *Cell Metab* 20, 61-72.

MacIver, N.J., Michalek, R.D., and Rathmell, J.C. (2013). Metabolic regulation of T lymphocytes. *Annu Rev Immunol* 31, 259-283.

Mahajan, P.B. (1994). Modulation of transcription of rRNA genes by rapamycin. *Int J Immunopharmacol* 16, 711-721.

## G Literature

Manning, B.D., Tee, A.R., Logsdon, M.N., Blenis, J., and Cantley, L.C. (2002). Identification of the tuberous sclerosis complex-2 tumor suppressor gene product tuberin as a target of the phosphoinositide 3-kinase/akt pathway. *Mol Cell* *10*, 151-162.

Margolin, J.F., Friedman, J.R., Meyer, W.K., Vissing, H., Thiesen, H.J., and Rauscher, F.J., 3rd (1994). Kruppel-associated boxes are potent transcriptional repression domains. *Proc Natl Acad Sci U S A* *91*, 4509-4513.

Martina, J.A., Chen, Y., Gucek, M., and Puertollano, R. (2012). mTORC1 functions as a transcriptional regulator of autophagy by preventing nuclear transport of TFEB. *Autophagy* *8*, 903-914.

Marzec, M., Liu, X., Kasprzycka, M., Witkiewicz, A., Raghunath, P.N., El-Salem, M., Robertson, E., Odum, N., and Wasik, M.A. (2008). IL-2- and IL-15-induced activation of the rapamycin-sensitive mTORC1 pathway in malignant CD4<sup>+</sup> T lymphocytes. *Blood* *111*, 2181-2189.

Masopust, D., and Schenkel, J.M. (2013). The integration of T cell migration, differentiation and function. *Nat Rev Immunol* *13*, 309-320.

Matloubian, M., Concepcion, R.J., and Ahmed, R. (1994). CD4<sup>+</sup> T cells are required to sustain CD8<sup>+</sup> cytotoxic T-cell responses during chronic viral infection. *J Virol* *68*, 8056-8063.

Mayer, C., and Grummt, I. (2006). Ribosome biogenesis and cell growth: mTOR coordinates transcription by all three classes of nuclear RNA polymerases. *Oncogene* *25*, 6384-6391.

Mayer, C., Schmitz, K.M., Li, J., Grummt, I., and Santoro, R. (2006). Intergenic transcripts regulate the epigenetic state of rRNA genes. *Mol Cell* *22*, 351-361.

Mayer, C., Zhao, J., Yuan, X., and Grummt, I. (2004). mTOR-dependent activation of the transcription factor TIF-IA links rRNA synthesis to nutrient availability. *Genes Dev* *18*, 423-434.

Mayya, V., and Dustin, M.L. (2016). What Scales the T Cell Response? *Trends Immunol* *37*, 513-522.

McDonagh, M., and Bell, E.B. (1995). The survival and turnover of mature and immature CD8 T cells. *Immunology* *84*, 514-520.

McKenzie, I.F., Morgan, G.M., Blanden, R.V., Melvold, R., and Kohn, H. (1977). Studies of H-2 mutations in C57BL/6 and BALB/c mice. *Transplant Proc* *9*, 551-553.

McKenzie, I.F., Morgan, G.M., Sandrin, M.S., Michaelides, M.M., Melvold, R.W., and Kohn, H.I. (1979). B6.C-H-2bm12. A new H-2 mutation in the I region in the mouse. *J Exp Med* *150*, 1323-1338.

## G Literature

McKinstry, K.K., Strutt, T.M., Kuang, Y., Brown, D.M., Sell, S., Dutton, R.W., and Swain, S.L. (2012). Memory CD4+ T cells protect against influenza through multiple synergizing mechanisms. *J Clin Invest* 122, 2847-2856.

Mempel, T.R., Henrickson, S.E., and Von Andrian, U.H. (2004). T-cell priming by dendritic cells in lymph nodes occurs in three distinct phases. *Nature* 427, 154-159.

Menon, S., Dibble, C.C., Talbott, G., Hoxhaj, G., Valvezan, A.J., Takahashi, H., Cantley, L.C., and Manning, B.D. (2014). Spatial control of the TSC complex integrates insulin and nutrient regulation of mTORC1 at the lysosome. *Cell* 156, 771-785.

Mingueneau, M., Kreslavsky, T., Gray, D., Heng, T., Cruse, R., Ericson, J., Bendall, S., Spitzer, M.H., Nolan, G.P., Kobayashi, K., von Boehmer, H., Mathis, D., Benoist, C., Immunological Genome, C., Best, A.J., Knell, J., Goldrath, A., Joic, V., Koller, D., Shay, T., Regev, A., Cohen, N., Brennan, P., Brenner, M., Kim, F., Nageswara Rao, T., Wagers, A., Heng, T., Ericson, J., Rothamel, K., Ortiz-Lopez, A., Mathis, D., Benoist, C., Bezman, N.A., Sun, J.C., Min-Oo, G., Kim, C.C., Lanier, L.L., Miller, J., Brown, B., Merad, M., Gautier, E.L., Jakubzick, C., Randolph, G.J., Monach, P., Blair, D.A., Dustin, M.L., Shinton, S.A., Hardy, R.R., Laidlaw, D., Collins, J., Gazit, R., Rossi, D.J., Malhotra, N., Sylvania, K., Kang, J., Kreslavsky, T., Fletcher, A., Elpek, K., Bellemare-Pelletier, A., Malhotra, D., and Turley, S. (2013). The transcriptional landscape of alphabeta T cell differentiation. *Nat Immunol* 14, 619-632.

Miossec, P., Korn, T., and Kuchroo, V.K. (2009). Interleukin-17 and type 17 helper T cells. *N Engl J Med* 361, 888-898.

Mombaerts, P., Iacomini, J., Johnson, R.S., Herrup, K., Tonegawa, S., and Papaioannou, V.E. (1992). RAG-1-deficient mice have no mature B and T lymphocytes. *Cell* 68, 869-877.

Moran, A.E., Holzapfel, K.L., Xing, Y., Cunningham, N.R., Maltzman, J.S., Punt, J., and Hogquist, K.A. (2011). T cell receptor signal strength in Treg and iNKT cell development demonstrated by a novel fluorescent reporter mouse. *J Exp Med* 208, 1279-1289.

Mosmann, T.R., and Coffman, R.L. (1989). TH1 and TH2 cells: different patterns of lymphokine secretion lead to different functional properties. *Annu Rev Immunol* 7, 145-173.

Moss, T., Langlois, F., Gagnon-Kugler, T., and Stefanovsky, V. (2007). A housekeeper with power of attorney: the rRNA genes in ribosome biogenesis. *Cell Mol Life Sci* 64, 29-49.

Moss, T., and Stefanovsky, V.Y. (2002). At the center of eukaryotic life. *Cell* 109, 545-548.

Nakamura-Ishizu, A., Takizawa, H., and Suda, T. (2014). The analysis, roles and regulation of quiescence in hematopoietic stem cells. *Development* 141, 4656-4666.

## G Literature

Nelson, R.W., Beisang, D., Tubo, N.J., Dileepan, T., Wiesner, D.L., Nielsen, K., Wuthrich, M., Klein, B.S., Kotov, D.I., Spanier, J.A., Fife, B.T., Moon, J.J., and Jenkins, M.K. (2015). T cell receptor cross-reactivity between similar foreign and self peptides influences naive cell population size and autoimmunity. *Immunity* 42, 95-107.

Nemeth, A., and Grummt, I. (2018). Dynamic regulation of nucleolar architecture. *Curr Opin Cell Biol* 52, 105-111.

Nguyen, H.D., Chatterjee, S., Haarberg, K.M., Wu, Y., Bastian, D., Heinrichs, J., Fu, J., Daenthanasamak, A., Schutt, S., Shrestha, S., Liu, C., Wang, H., Chi, H., Mehrotra, S., and Yu, X.Z. (2016). Metabolic reprogramming of alloantigen-activated T cells after hematopoietic cell transplantation. *J Clin Invest* 126, 1337-1352.

Nurse, P. (2000). A long twentieth century of the cell cycle and beyond. *Cell* 100, 71-78.

O'Shea, J.J., and Paul, W.E. (2010). Mechanisms underlying lineage commitment and plasticity of helper CD4<sup>+</sup> T cells. *Science* 327, 1098-1102.

Obst, R. (2015). The Timing of T Cell Priming and Cycling. *Front Immunol* 6, 563.

Obst, R., van Santen, H.M., Mathis, D., and Benoist, C. (2005). Antigen persistence is required throughout the expansion phase of a CD4<sup>+</sup> T cell response. *J Exp Med* 201, 1555-1565.

Odorizzi, P.M., and Wherry, E.J. (2012). Inhibitory receptors on lymphocytes: insights from infections. *J Immunol* 188, 2957-2965.

Oh, W.J., Wu, C.C., Kim, S.J., Facchinetti, V., Julien, L.A., Finlan, M., Roux, P.P., Su, B., and Jacinto, E. (2010). mTORC2 can associate with ribosomes to promote cotranslational phosphorylation and stability of nascent Akt polypeptide. *EMBO J* 29, 3939-3951.

Paley, M.A., Kroy, D.C., Odorizzi, P.M., Johnnidis, J.B., Dolfi, D.V., Barnett, B.E., Bikoff, E.K., Robertson, E.J., Lauer, G.M., Reiner, S.L., and Wherry, E.J. (2012). Progenitor and terminal subsets of CD8<sup>+</sup> T cells cooperate to contain chronic viral infection. *Science* 338, 1220-1225.

Pardee, A.B. (1989). G1 events and regulation of cell proliferation. *Science* 246, 603-608.

Passegue, E., Wagers, A.J., Giuriato, S., Anderson, W.C., and Weissman, I.L. (2005). Global analysis of proliferation and cell cycle gene expression in the regulation of hematopoietic stem and progenitor cell fates. *J Exp Med* 202, 1599-1611.

Pearce, E.L., Walsh, M.C., Cejas, P.J., Harms, G.M., Shen, H., Wang, L.S., Jones, R.G., and Choi, Y. (2009). Enhancing CD8 T-cell memory by modulating fatty acid metabolism. *Nature* 460, 103-107.

## G Literature

Pederson, T. (2010). "Compact" nuclear domains: reconsidering the nucleolus. *Nucleus* 1, 444-445.

Pereira, P., and Rocha, B. (1991). Post-thymic in vivo expansion of mature alpha beta T cells. *Int Immunol* 3, 1077-1080.

Perry, R.P., and Kelley, D.E. (1970). Inhibition of RNA synthesis by actinomycin D: characteristic dose-response of different RNA species. *J Cell Physiol* 76, 127-139.

Peterson, T.R., Laplante, M., Thoreen, C.C., Sancak, Y., Kang, S.A., Kuehl, W.M., Gray, N.S., and Sabatini, D.M. (2009). DEPTOR is an mTOR inhibitor frequently overexpressed in multiple myeloma cells and required for their survival. *Cell* 137, 873-886.

Pipkin, M.E., Sacks, J.A., Cruz-Guilloty, F., Lichtenheld, M.G., Bevan, M.J., and Rao, A. (2010). Interleukin-2 and inflammation induce distinct transcriptional programs that promote the differentiation of effector cytolytic T cells. *Immunity* 32, 79-90.

Pollizzi, K.N., and Powell, J.D. (2015). Regulation of T cells by mTOR: the known knowns and the known unknowns. *Trends Immunol* 36, 13-20.

Pollizzi, K.N., Waickman, A.T., Patel, C.H., Sun, I.H., and Powell, J.D. (2015). Cellular size as a means of tracking mTOR activity and cell fate of CD4<sup>+</sup> T cells upon antigen recognition. *PLoS One* 10, e0121710.

Porstmann, T., Santos, C.R., Griffiths, B., Cully, M., Wu, M., Leever, S., Griffiths, J.R., Chung, Y.L., and Schulze, A. (2008). SREBP activity is regulated by mTORC1 and contributes to Akt-dependent cell growth. *Cell Metab* 8, 224-236.

Powderly, K.M., Clarke, S.M., Amsler, M., Wolverson, C., Malliakas, C.D., Meng, Y., Jacobsen, S.D., and Freedman, D.E. (2017). High-pressure discovery of beta-NiBi. *Chem Commun (Camb)* 53, 11241-11244.

Powell, J.D., Lerner, C.G., and Schwartz, R.H. (1999). Inhibition of cell cycle progression by rapamycin induces T cell clonal anergy even in the presence of costimulation. *J Immunol* 162, 2775-2784.

Powell, J.D., Pollizzi, K.N., Heikamp, E.B., and Horton, M.R. (2012). Regulation of immune responses by mTOR. *Annu Rev Immunol* 30, 39-68.

Qiu, L., Liu, M., and Pan, K. (2013). A triple staining method for accurate cell cycle analysis using multiparameter flow cytometry. *Molecules* 18, 15412-15421.

Rabenstein, H., Behrendt, A.C., Ellwart, J.W., Naumann, R., Horsch, M., Beckers, J., and Obst, R. (2014). Differential kinetics of antigen dependency of CD4<sup>+</sup> and CD8<sup>+</sup> T cells. *J Immunol* 192, 3507-3517.

## G Literature

Rao, R.R., Li, Q., Odunsi, K., and Shrikant, P.A. (2010). The mTOR kinase determines effector versus memory CD8<sup>+</sup> T cell fate by regulating the expression of transcription factors T-bet and Eomesodermin. *Immunity* 32, 67-78.

Rathmell, J.C., Farkash, E.A., Gao, W., and Thompson, C.B. (2001). IL-7 enhances the survival and maintains the size of naive T cells. *J Immunol* 167, 6869-6876.

Robitaille, A.M., Christen, S., Shimobayashi, M., Cornu, M., Fava, L.L., Moes, S., Prescianotto-Baschong, C., Sauer, U., Jenoe, P., and Hall, M.N. (2013). Quantitative phosphoproteomics reveal mTORC1 activates de novo pyrimidine synthesis. *Science* 339, 1320-1323.

Rocha, B., Dautigny, N., and Pereira, P. (1989). Peripheral T lymphocytes: expansion potential and homeostatic regulation of pool sizes and CD4/CD8 ratios in vivo. *Eur J Immunol* 19, 905-911.

Roczniak-Ferguson, A., Petit, C.S., Froehlich, F., Qian, S., Ky, J., Angarola, B., Walther, T.C., and Ferguson, S.M. (2012). The transcription factor TFEB links mTORC1 signaling to transcriptional control of lysosome homeostasis. *Sci Signal* 5, ra42.

Rollings, C.M., Sinclair, L.V., Brady, H.J.M., Cantrell, D.A., and Ross, S.H. (2018). Interleukin-2 shapes the cytotoxic T cell proteome and immune environment-sensing programs. *Sci Signal* 11.

Rosner, M., and Hengstschlager, M. (2010). Evidence for cell cycle-dependent, rapamycin-resistant phosphorylation of ribosomal protein S6 at S240/244. *Amino Acids* 39, 1487-1492.

Ross, S.H., and Cantrell, D.A. (2018). Signaling and Function of Interleukin-2 in T Lymphocytes. *Annu Rev Immunol* 36, 411-433.

Rousseau, A., and Bertolotti, A. (2016). An evolutionarily conserved pathway controls proteasome homeostasis. *Nature* 536, 184-189.

Rubbi, C.P., and Milner, J. (2003). Disruption of the nucleolus mediates stabilization of p53 in response to DNA damage and other stresses. *EMBO J* 22, 6068-6077.

Sabatini, D.M., Erdjument-Bromage, H., Lui, M., Tempst, P., and Snyder, S.H. (1994). RAFT1: a mammalian protein that binds to FKBP12 in a rapamycin-dependent fashion and is homologous to yeast TORs. *Cell* 78, 35-43.

Sabers, C.J., Martin, M.M., Brunn, G.J., Williams, J.M., Dumont, F.J., Wiederrecht, G., and Abraham, R.T. (1995). Isolation of a protein target of the FKBP12-rapamycin complex in mammalian cells. *J Biol Chem* 270, 815-822.

## G Literature

Sage, J., Mulligan, G.J., Attardi, L.D., Miller, A., Chen, S., Williams, B., Theodorou, E., and Jacks, T. (2000). Targeted disruption of the three Rb-related genes leads to loss of G(1) control and immortalization. *Genes Dev* 14, 3037-3050.

Sakaguchi, S. (2000). Regulatory T cells: key controllers of immunologic self-tolerance. *Cell* 101, 455-458.

Sakaguchi, S., Yamaguchi, T., Nomura, T., and Ono, M. (2008). Regulatory T cells and immune tolerance. *Cell* 133, 775-787.

Salmond, R.J., Brownlie, R.J., Meyuhas, O., and Zamoyska, R. (2015). Mechanistic Target of Rapamycin Complex 1/S6 Kinase 1 Signals Influence T Cell Activation Independently of Ribosomal Protein S6 Phosphorylation. *J Immunol* 195, 4615-4622.

Sancak, Y., Bar-Peled, L., Zoncu, R., Markhard, A.L., Nada, S., and Sabatini, D.M. (2010). Ragulator-Rag complex targets mTORC1 to the lysosomal surface and is necessary for its activation by amino acids. *Cell* 141, 290-303.

Sancak, Y., Peterson, T.R., Shaul, Y.D., Lindquist, R.A., Thoreen, C.C., Bar-Peled, L., and Sabatini, D.M. (2008). The Rag GTPases bind raptor and mediate amino acid signaling to mTORC1. *Science* 320, 1496-1501.

Sancak, Y., Thoreen, C.C., Peterson, T.R., Lindquist, R.A., Kang, S.A., Spooner, E., Carr, S.A., and Sabatini, D.M. (2007). PRAS40 is an insulin-regulated inhibitor of the mTORC1 protein kinase. *Mol Cell* 25, 903-915.

Sarbassov, D.D., Ali, S.M., Kim, D.H., Guertin, D.A., Latek, R.R., Erdjument-Bromage, H., Tempst, P., and Sabatini, D.M. (2004). Rictor, a novel binding partner of mTOR, defines a rapamycin-insensitive and raptor-independent pathway that regulates the cytoskeleton. *Curr Biol* 14, 1296-1302.

Saxton, R.A., Knockenbauer, K.E., Wolfson, R.L., Chantranupong, L., Pacold, M.E., Wang, T., Schwartz, T.U., and Sabatini, D.M. (2016). Structural basis for leucine sensing by the Sestrin2-mTORC1 pathway. *Science* 351, 53-58.

Saxton, R.A., and Sabatini, D.M. (2017). mTOR Signaling in Growth, Metabolism, and Disease. *Cell* 169, 361-371.

Scheer, U., and Hock, R. (1999). Structure and function of the nucleolus. *Curr Opin Cell Biol* 11, 385-390.

Schietinger, A., and Greenberg, P.D. (2014). Tolerance and exhaustion: defining mechanisms of T cell dysfunction. *Trends Immunol* 35, 51-60.

Schluns, K.S., Kieper, W.C., Jameson, S.C., and Lefrancois, L. (2000). Interleukin-7 mediates the homeostasis of naive and memory CD8 T cells in vivo. *Nat Immunol* 1, 426-432.

## G Literature

Schmid, I., Cole, S.W., Korin, Y.D., Zack, J.A., and Giorgi, J.V. (2000). Detection of cell cycle subcompartments by flow cytometric estimation of DNA-RNA content in combination with dual-color immunofluorescence. *Cytometry* 39, 108-116.

Schorl, C., and Sedivy, J.M. (2003). Loss of protooncogene c-Myc function impedes G1 phase progression both before and after the restriction point. *Mol Biol Cell* 14, 823-835.

Schroder, K., Hertzog, P.J., Ravasi, T., and Hume, D.A. (2004). Interferon-gamma: an overview of signals, mechanisms and functions. *J Leukoc Biol* 75, 163-189.

Schulz, T.F. (1998). Kaposi's sarcoma-associated herpesvirus (human herpesvirus-8). *J Gen Virol* 79 ( Pt 7), 1573-1591.

Schwartz, R.H. (2003). T cell anergy. *Annu Rev Immunol* 21, 305-334.

Sengupta, S., Peterson, T.R., Laplante, M., Oh, S., and Sabatini, D.M. (2010). mTORC1 controls fasting-induced ketogenesis and its modulation by ageing. *Nature* 468, 1100-1104.

Settembre, C., Di Malta, C., Polito, V.A., Garcia Arencibia, M., Vetrini, F., Erdin, S., Erdin, S.U., Huynh, T., Medina, D., Colella, P., Sardiello, M., Rubinsztein, D.C., and Ballabio, A. (2011). TFEB links autophagy to lysosomal biogenesis. *Science* 332, 1429-1433.

Settembre, C., Zoncu, R., Medina, D.L., Vetrini, F., Erdin, S., Erdin, S., Huynh, T., Ferron, M., Karsenty, G., Vellard, M.C., Facchinetti, V., Sabatini, D.M., and Ballabio, A. (2012). A lysosome-to-nucleus signalling mechanism senses and regulates the lysosome via mTOR and TFEB. *EMBO J* 31, 1095-1108.

Shapiro, H.M. (1981). Flow cytometric estimation of DNA and RNA content in intact cells stained with Hoechst 33342 and pyronin Y. *Cytometry* 2, 143-150.

Sharpe, A.H., Wherry, E.J., Ahmed, R., and Freeman, G.J. (2007). The function of programmed cell death 1 and its ligands in regulating autoimmunity and infection. *Nat Immunol* 8, 239-245.

Shaw, R.J., Bardeesy, N., Manning, B.D., Lopez, L., Kosmatka, M., DePinho, R.A., and Cantley, L.C. (2004). The LKB1 tumor suppressor negatively regulates mTOR signaling. *Cancer Cell* 6, 91-99.

Shin, H., Blackburn, S.D., Blattman, J.N., and Wherry, E.J. (2007). Viral antigen and extensive division maintain virus-specific CD8 T cells during chronic infection. *J Exp Med* 204, 941-949.

Shin, J., Wang, S., Deng, W., Wu, J., Gao, J., and Zhong, X.P. (2014). Mechanistic target of rapamycin complex 1 is critical for invariant natural killer T-cell development and effector function. *Proc Natl Acad Sci U S A* 111, E776-783.

## G Literature

Singh, K., Sun, S., and Vezina, C. (1979). Rapamycin (AY-22,989), a new antifungal antibiotic. IV. Mechanism of action. *J Antibiot (Tokyo)* 32, 630-645.

Sirri, V., Roussel, P., and Hernandez-Verdun, D. (1999). The mitotically phosphorylated form of the transcription termination factor TTF-1 is associated with the repressed rDNA transcription machinery. *J Cell Sci* 112 ( Pt 19), 3259-3268.

Skrtic, M., Sriskanthadevan, S., Jhas, B., Gebbia, M., Wang, X., Wang, Z., Hurren, R., Jitkova, Y., Gronda, M., Maclean, N., Lai, C.K., Eberhard, Y., Bartoszko, J., Spagnuolo, P., Rutledge, A.C., Datti, A., Ketela, T., Moffat, J., Robinson, B.H., Cameron, J.H., Wrana, J., Eaves, C.J., Minden, M.D., Wang, J.C., Dick, J.E., Humphries, K., Nislow, C., Giaever, G., and Schimmer, A.D. (2011). Inhibition of mitochondrial translation as a therapeutic strategy for human acute myeloid leukemia. *Cancer Cell* 20, 674-688.

Smirnov, E., Cmarko, D., Mazel, T., Hornacek, M., and Raska, I. (2016). Nucleolar DNA: the host and the guests. *Histochem Cell Biol* 145, 359-372.

So, L., Lee, J., Palafox, M., Mallya, S., Woxland, C.G., Arguello, M., Truitt, M.L., Sonenberg, N., Ruggero, D., and Fruman, D.A. (2016). The 4E-BP-eIF4E axis promotes rapamycin-sensitive growth and proliferation in lymphocytes. *Sci Signal* 9, ra57.

Sowell, R.T., Goldufsky, J.W., Rogozinska, M., Quiles, Z., Cao, Y., Castillo, E.F., Finnegan, A., and Marzo, A.L. (2017). IL-15 Complexes Induce Migration of Resting Memory CD8 T Cells into Mucosal Tissues. *J Immunol* 199, 2536-2546.

Sprent, J., Schaefer, M., Hurd, M., Surh, C.D., and Ron, Y. (1991). Mature murine B and T cells transferred to SCID mice can survive indefinitely and many maintain a virgin phenotype. *J Exp Med* 174, 717-728.

Starr, T.K., Jameson, S.C., and Hogquist, K.A. (2003). Positive and negative selection of T cells. *Annu Rev Immunol* 21, 139-176.

Stimpfling, J.H., and Richardson, A. (1965). Recombination within the Histocompatibility Locus of the Mouse. *Genetics* 51, 831-846.

Tan, H., Yang, K., Li, Y., Shaw, T.I., Wang, Y., Blanco, D.B., Wang, X., Cho, J.H., Wang, H., Rankin, S., Guy, C., Peng, J., and Chi, H. (2017a). Integrative Proteomics and Phosphoproteomics Profiling Reveals Dynamic Signaling Networks and Bioenergetics Pathways Underlying T Cell Activation. *Immunity* 46, 488-503.

Tan, T.C.J., Knight, J., Sbarato, T., Dudek, K., Willis, A.E., and Zamoyska, R. (2017b). Suboptimal T-cell receptor signaling compromises protein translation, ribosome biogenesis, and proliferation of mouse CD8 T cells. *Proc Natl Acad Sci U S A* 114, E6117-E6126.

Tang, F., Wu, Q., Ikenoue, T., Guan, K.L., Liu, Y., and Zheng, P. (2012). A critical role for Rictor in T lymphopoiesis. *J Immunol* 189, 1850-1857.

## G Literature

Tee, A.R., Manning, B.D., Roux, P.P., Cantley, L.C., and Blenis, J. (2003). Tuberous sclerosis complex gene products, Tuberin and Hamartin, control mTOR signaling by acting as a GTPase-activating protein complex toward Rheb. *Curr Biol* 13, 1259-1268.

Terada, N., Takase, K., Papst, P., Nairn, A.C., and Gelfand, E.W. (1995). Rapamycin inhibits ribosomal protein synthesis and induces G1 prolongation in mitogen-activated T lymphocytes. *J Immunol* 155, 3418-3426.

Thiry, M., Lamaye, F., and Lafontaine, D.L. (2011). The nucleolus: when 2 became 3. *Nucleus* 2, 289-293.

Thoreen, C.C., Chantranupong, L., Keys, H.R., Wang, T., Gray, N.S., and Sabatini, D.M. (2012). A unifying model for mTORC1-mediated regulation of mRNA translation. *Nature* 485, 109-113.

Tzur, A., Moore, J.K., Jorgensen, P., Shapiro, H.M., and Kirschner, M.W. (2011). Optimizing optical flow cytometry for cell volume-based sorting and analysis. *PLoS One* 6, e16053.

Urlinger, S., Baron, U., Thellmann, M., Hasan, M.T., Bujard, H., and Hillen, W. (2000). Exploring the sequence space for tetracycline-dependent transcriptional activators: novel mutations yield expanded range and sensitivity. *Proc Natl Acad Sci U S A* 97, 7963-7968.

Utzschneider, D.T., Charmoy, M., Chennupati, V., Pousse, L., Ferreira, D.P., Calderon-Copete, S., Danilo, M., Alfei, F., Hofmann, M., Wieland, D., Pradervand, S., Thimme, R., Zehn, D., and Held, W. (2016). T Cell Factor 1-Expressing Memory-like CD8<sup>+</sup> T Cells Sustain the Immune Response to Chronic Viral Infections. *Immunity* 45, 415-427.

van der Windt, G.J., and Pearce, E.L. (2012). Metabolic switching and fuel choice during T-cell differentiation and memory development. *Immunol Rev* 249, 27-42.

van Santen, H.M., Benoist, C., and Mathis, D. (2004). Number of T reg cells that differentiate does not increase upon encounter of agonist ligand on thymic epithelial cells. *J Exp Med* 200, 1221-1230.

Vander Heiden, M.G., Cantley, L.C., and Thompson, C.B. (2009). Understanding the Warburg effect: the metabolic requirements of cell proliferation. *Science* 324, 1029-1033.

Veiga-Parga, T., Sehrawat, S., and Rouse, B.T. (2013). Role of regulatory T cells during virus infection. *Immunol Rev* 255, 182-196.

Via, C.S. (2010). Advances in lupus stemming from the parent-into-F1 model. *Trends Immunol* 31, 236-245.

Vinuesa, C.G., Linterman, M.A., Yu, D., and MacLennan, I.C. (2016). Follicular Helper T Cells. *Annu Rev Immunol* 34, 335-368.

## G Literature

Voit, R., Hoffmann, M., and Grummt, I. (1999). Phosphorylation by G1-specific cdk-cyclin complexes activates the nucleolar transcription factor UBF. *EMBO J* 18, 1891-1899.

von Boehmer, H. (2005). Mechanisms of suppression by suppressor T cells. *Nat Immunol* 6, 338-344.

Waickman, A.T., and Powell, J.D. (2012). Mammalian target of rapamycin integrates diverse inputs to guide the outcome of antigen recognition in T cells. *J Immunol* 188, 4721-4729.

Wakamatsu, E., Mathis, D., and Benoist, C. (2013). Convergent and divergent effects of costimulatory molecules in conventional and regulatory CD4<sup>+</sup> T cells. *Proc Natl Acad Sci U S A* 110, 1023-1028.

Wang, S., Tsun, Z.Y., Wolfson, R.L., Shen, K., Wyant, G.A., Plovanich, M.E., Yuan, E.D., Jones, T.D., Chantranupong, L., Comb, W., Wang, T., Bar-Peled, L., Zoncu, R., Straub, C., Kim, C., Park, J., Sabatini, B.L., and Sabatini, D.M. (2015). Metabolism. Lysosomal amino acid transporter SLC38A9 signals arginine sufficiency to mTORC1. *Science* 347, 188-194.

Warner, J.R. (2001). Nascent ribosomes. *Cell* 107, 133-136.

Weinberg, R.A. (1995). The retinoblastoma protein and cell cycle control. *Cell* 81, 323-330.

Westermann, A.J., Forstner, K.U., Amman, F., Barquist, L., Chao, Y., Schulte, L.N., Muller, L., Reinhardt, R., Stadler, P.F., and Vogel, J. (2016). Dual RNA-seq unveils noncoding RNA functions in host-pathogen interactions. *Nature* 529, 496-501.

Wherry, E.J. (2011). T cell exhaustion. *Nat Immunol* 12, 492-499.

Wherry, E.J., Blattman, J.N., Murali-Krishna, K., van der Most, R., and Ahmed, R. (2003). Viral persistence alters CD8 T-cell immunodominance and tissue distribution and results in distinct stages of functional impairment. *J Virol* 77, 4911-4927.

Wherry, E.J., Ha, S.J., Kaech, S.M., Haining, W.N., Sarkar, S., Kalia, V., Subramaniam, S., Blattman, J.N., Barber, D.L., and Ahmed, R. (2007). Molecular signature of CD8<sup>+</sup> T cell exhaustion during chronic viral infection. *Immunity* 27, 670-684.

Wherry, E.J., and Kurachi, M. (2015). Molecular and cellular insights into T cell exhaustion. *Nat Rev Immunol* 15, 486-499.

Wieczorek, M., Abualrous, E.T., Sticht, J., Alvaro-Benito, M., Stolzenberg, S., Noe, F., and Freund, C. (2017). Major Histocompatibility Complex (MHC) Class I and MHC Class II Proteins: Conformational Plasticity in Antigen Presentation. *Front Immunol* 8, 292.

## G Literature

Williams, M.A., and Bevan, M.J. (2004). Shortening the infectious period does not alter expansion of CD8 T cells but diminishes their capacity to differentiate into memory cells. *J Immunol* 173, 6694-6702.

Wiznerowicz, M., Jakobsson, J., Szulc, J., Liao, S., Quazzola, A., Beermann, F., Aebischer, P., and Trono, D. (2007). The Kruppel-associated box repressor domain can trigger de novo promoter methylation during mouse early embryogenesis. *J Biol Chem* 282, 34535-34541.

Wolchok, J.D., Kluger, H., Callahan, M.K., Postow, M.A., Rizvi, N.A., Lesokhin, A.M., Segal, N.H., Ariyan, C.E., Gordon, R.A., Reed, K., Burke, M.M., Caldwell, A., Kronenberg, S.A., Agunwamba, B.U., Zhang, X., Lowy, I., Inzunza, H.D., Feely, W., Horak, C.E., Hong, Q., Korman, A.J., Wigginton, J.M., Gupta, A., and Sznol, M. (2013). Nivolumab plus ipilimumab in advanced melanoma. *N Engl J Med* 369, 122-133.

Wolfson, R.L., Chantranupong, L., Saxton, R.A., Shen, K., Scaria, S.M., Cantor, J.R., and Sabatini, D.M. (2016). Sestrin2 is a leucine sensor for the mTORC1 pathway. *Science* 351, 43-48.

Wolfson, R.L., Chantranupong, L., Wyant, G.A., Gu, X., Orozco, J.M., Shen, K., Condon, K.J., Petri, S., Kedir, J., Scaria, S.M., Abu-Remaileh, M., Frankel, W.N., and Sabatini, D.M. (2017). KICSTOR recruits GATOR1 to the lysosome and is necessary for nutrients to regulate mTORC1. *Nature* 543, 438-442.

Wu, T., Ji, Y., Moseman, E.A., Xu, H.C., Manghani, M., Kirby, M., Anderson, S.M., Handon, R., Kenyon, E., Elkahoun, A., Wu, W., Lang, P.A., Gattinoni, L., McGavern, D.B., and Schwartzberg, P.L. (2016). The TCF1-Bcl6 axis counteracts type I interferon to repress exhaustion and maintain T cell stemness. *Sci Immunol* 1.

Yang, K., and Chi, H. (2013). Tuning mTOR activity for immune balance. *J Clin Invest* 123, 5001-5004.

Yang, K., Shrestha, S., Zeng, H., Karmaus, P.W., Neale, G., Vogel, P., Guertin, D.A., Lamb, R.F., and Chi, H. (2013). T cell exit from quiescence and differentiation into Th2 cells depend on Raptor-mTORC1-mediated metabolic reprogramming. *Immunity* 39, 1043-1056.

Yoon, H., Kim, T.S., and Braciale, T.J. (2010). The cell cycle time of CD8<sup>+</sup> T cells responding in vivo is controlled by the type of antigenic stimulus. *PLoS One* 5, e15423.

Yoon, H., Legge, K.L., Sung, S.S., and Braciale, T.J. (2007). Sequential activation of CD8<sup>+</sup> T cells in the draining lymph nodes in response to pulmonary virus infection. *J Immunol* 179, 391-399.

Youngblood, B., Oestreich, K.J., Ha, S.J., Duraiswamy, J., Akondy, R.S., West, E.E., Wei, Z., Lu, P., Austin, J.W., Riley, J.L., Boss, J.M., and Ahmed, R. (2011). Chronic virus infection enforces demethylation of the locus that encodes PD-1 in antigen-specific CD8<sup>+</sup> T cells. *Immunity* 35, 400-412.

## G Literature

Yuan, X., Zhou, Y., Casanova, E., Chai, M., Kiss, E., Grone, H.J., Schutz, G., and Grummt, I. (2005). Genetic inactivation of the transcription factor TIF-IA leads to nucleolar disruption, cell cycle arrest, and p53-mediated apoptosis. *Mol Cell* *19*, 77-87.

Zajac, A.J., Blattman, J.N., Murali-Krishna, K., Sourdive, D.J., Suresh, M., Altman, J.D., and Ahmed, R. (1998). Viral immune evasion due to persistence of activated T cells without effector function. *J Exp Med* *188*, 2205-2213.

Zaragoza, D., Ghavidel, A., Heitman, J., and Schultz, M.C. (1998). Rapamycin induces the G0 program of transcriptional repression in yeast by interfering with the TOR signaling pathway. *Mol Cell Biol* *18*, 4463-4470.

Zeng, H., Yang, K., Cloer, C., Neale, G., Vogel, P., and Chi, H. (2013). mTORC1 couples immune signals and metabolic programming to establish T(reg)-cell function. *Nature* *499*, 485-490.

Zhang, F., Zhou, X., DiSpirito, J.R., Wang, C., Wang, Y., and Shen, H. (2014a). Epigenetic manipulation restores functions of defective CD8<sup>+</sup> T cells from chronic viral infection. *Mol Ther* *22*, 1698-1706.

Zhang, H., Stallock, J.P., Ng, J.C., Reinhard, C., and Neufeld, T.P. (2000). Regulation of cellular growth by the Drosophila target of rapamycin dTOR. *Genes Dev* *14*, 2712-2724.

Zhang, S., Readinger, J.A., DuBois, W., Janka-Junttila, M., Robinson, R., Pruitt, M., Bliskovsky, V., Wu, J.Z., Sakakibara, K., Patel, J., Parent, C.A., Tessarollo, L., Schwartzberg, P.L., and Mock, B.A. (2011). Constitutive reductions in mTOR alter cell size, immune cell development, and antibody production. *Blood* *117*, 1228-1238.

Zhang, Y., Nicholatos, J., Dreier, J.R., Ricoult, S.J., Widenmaier, S.B., Hotamisligil, G.S., Kwiatkowski, D.J., and Manning, B.D. (2014b). Coordinated regulation of protein synthesis and degradation by mTORC1. *Nature* *513*, 440-443.

Zhao, J., Zhai, B., Gygi, S.P., and Goldberg, A.L. (2015). mTOR inhibition activates overall protein degradation by the ubiquitin proteasome system as well as by autophagy. *Proc Natl Acad Sci U S A* *112*, 15790-15797.

Zheng, Y., Collins, S.L., Lutz, M.A., Allen, A.N., Kole, T.P., Zarek, P.E., and Powell, J.D. (2007). A role for mammalian target of rapamycin in regulating T cell activation versus anergy. *J Immunol* *178*, 2163-2170.

Zoncu, R., Efeyan, A., and Sabatini, D.M. (2011). mTOR: from growth signal integration to cancer, diabetes and ageing. *Nat Rev Mol Cell Biol* *12*, 21-35.

## H Acknowledgments

### H Acknowledgments

I want to thank PD Dr. Reinhard Obst for supervision and discussion of this work and Prof. Thomas Brocker for the opportunity to work at the Institute for Immunology.

I further want to thank the SFB 1054 for providing a platform presenting and discussing my data on a regular basis and outstanding professional training possibilities.

I like to thank my collaborators, Dr. Henning Lauterbach and Dr. Hubertus Hochrein from Bavarian Nordic GmbH for kindly providing MVA-OVA, Prof. Dr. Axel Imhof from the BMC for analyzing proteomics data generated in the lab of Hongbo Chi and Dr. Tobias Straub for analyzing RNA sequencing data generated in this thesis.

I further like to thank Dr. Jan Kranich for kindly providing MFG8-GFP, Lisa Richter for guiding me through cell sorting, Prof. Thomas Brocker for providing RAG1-deficient and OT-I TCR transgenic mice, Dr. Veit Bucholz for providing Bm1 mice and Prof. Vigo Heissmeyer for providing R26-rtTA-M2 mice.

I thank Simone Pentz and Anna Kollar for managing mouse lines and genotyping as well as the animal care takers from Goethestraße for animal husbandry.

I thank Dr. Holger Winkels for reading my manuscript and his kind suggestions helping me to improve this thesis.

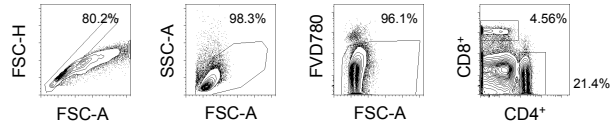
Furthermore, I want to thank the group members of AG Obst for their support, data discussions, lunch and coffee breaks, all non-scientific discussions and the great working atmosphere. I am also thankful to all other co-workers of the Institute for Immunology, especially Janina Ruf, Dr. Markus Zwick and Dr. Andrea Musumeci. Without you working would have been less fun that it was!

Finally, I would like to thank Domi for his constant support, encouragement, trying to understand my project, food provision and numerous climbing sessions, reminding me that life goes on.

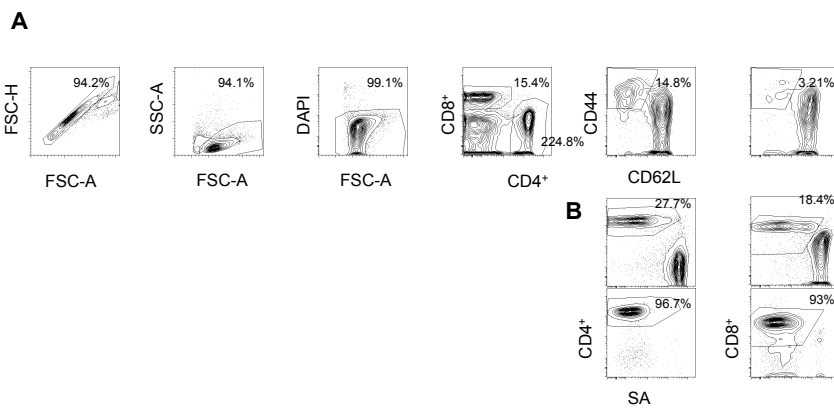
This work is dedicated to my grandfather, Heinz Lindner, who made me understand that knowledge and education are the only things that cannot be taken from me.

# I Appendix

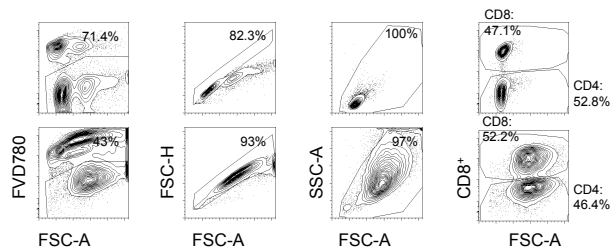
## I Gating strategies



Supplementary figure 1: Gating Strategie Figure D1.1

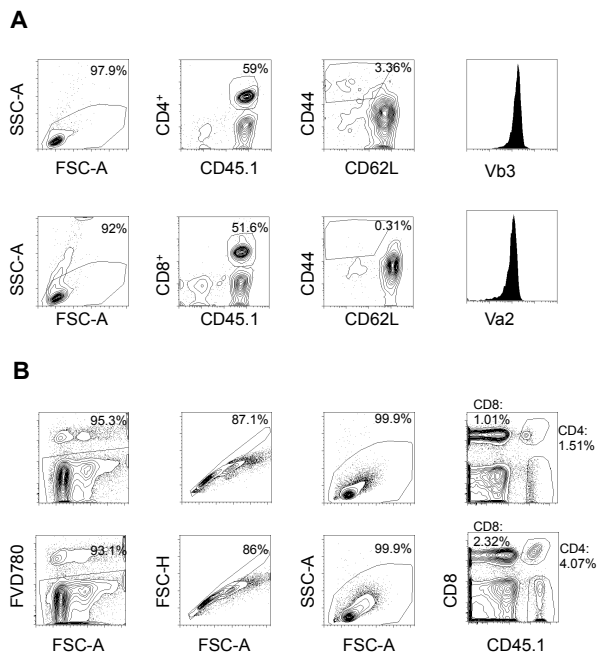


Supplementary figure 2: Gating strategy Figure D1.1, D1.2, D3.2, D3.3A, D3.4, D3.5, D3.6, D3.7, D4, D5  
Pre-stimulation with anti-CD3/28 (A) Activity. (B) MACS purity

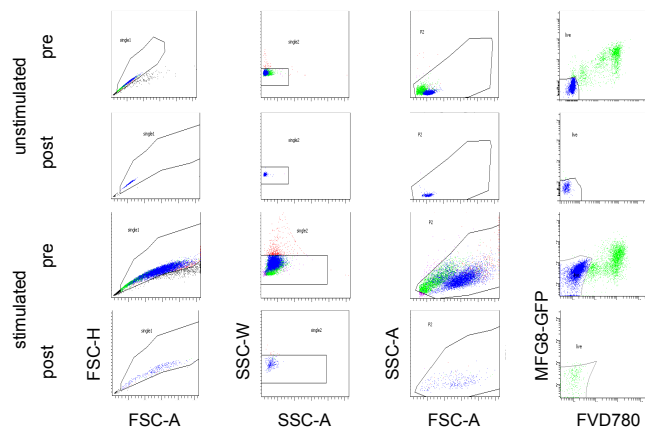


Supplementary figure 3: Gating strategy Figure D1.1, D1.2, D3.3A, D3.4, D3.5, D3.6, D3.7, D4, D5  
Post-stimulation with anti-CD3/28

# I Appendix

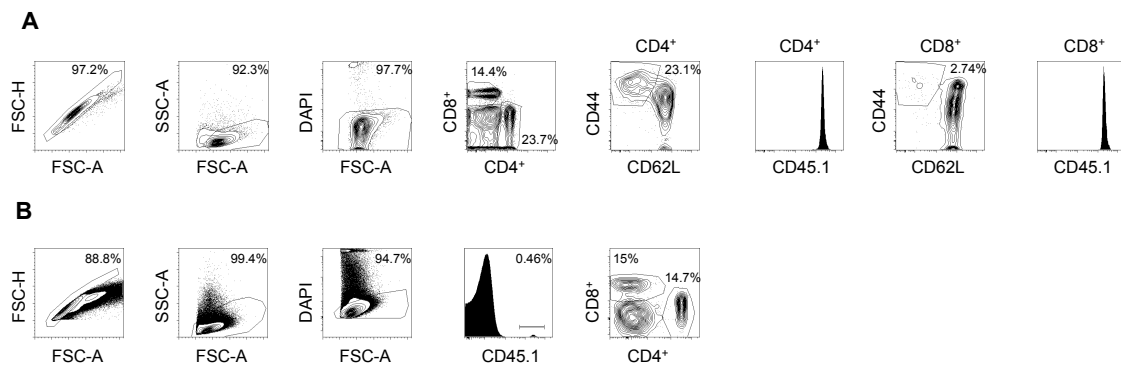


**Supplementary figure 4: Gating Strategy Figure D3.3B**  
 Pyronin Y staining ex vivo (A) pre-transfer Day 0 (B) post-transfer and MACS purification Day 2

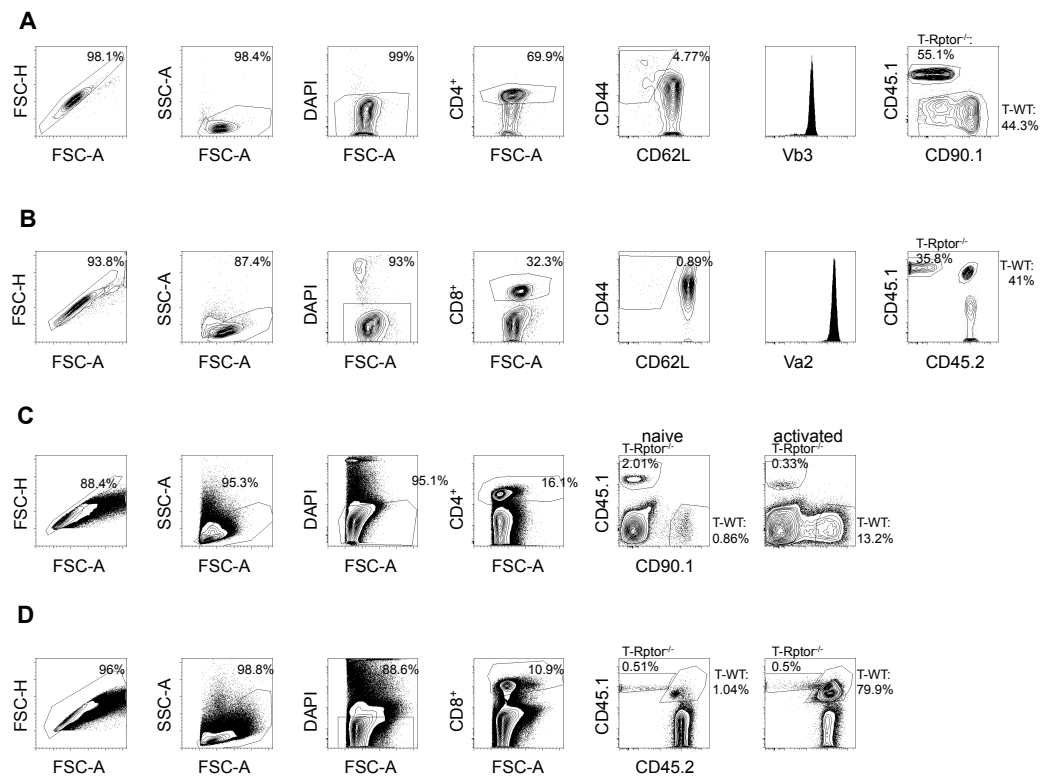


**Supplementary figure 5: Gating Strategy Cell Sort Figure D3.2.**

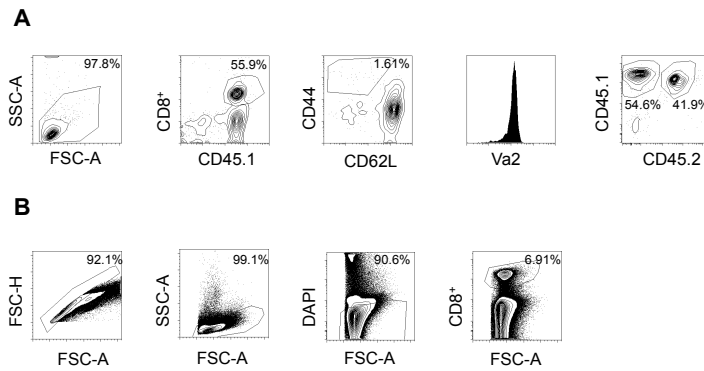
# I Appendix



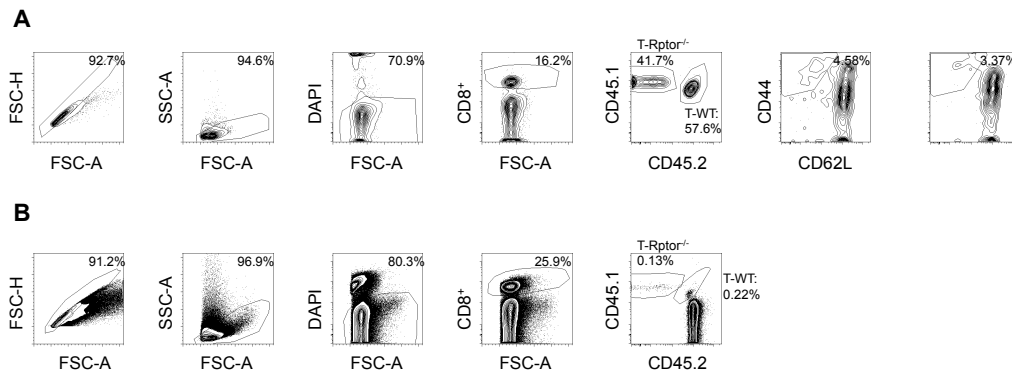
**Supplementary figure 6: Gating Strategie Figure D2.1**  
 (A) Pre-transfer; (B) Day 5 post-transfer



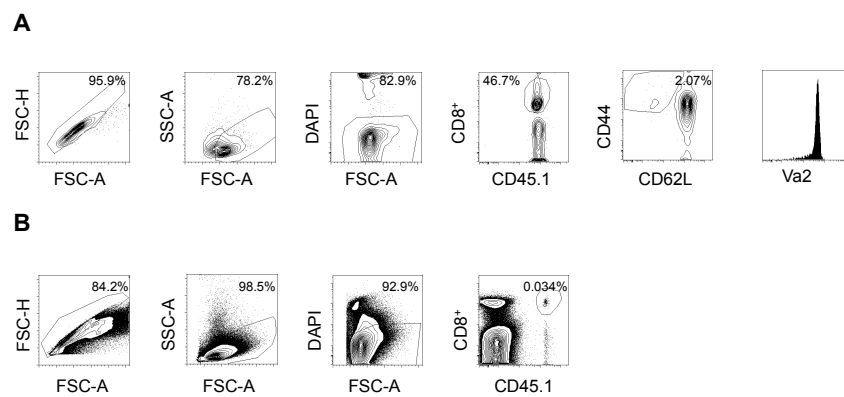
**Supplementary figure 7: Gating strategy Figure D2.2.**  
 Pre-transfer activity and TCR (A) AND; (B) OTI  
 Day 5 post-transfer (C) AND; (D) OTI



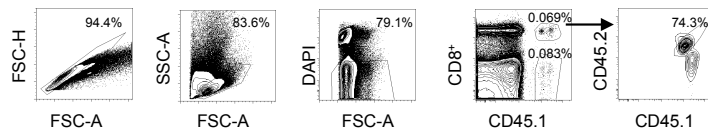
**Supplementary figure 8: Gating strategy Figure D2.3.**  
 (A) Pre-transfer; activity and TCR (B) Day 8/36 post-transfer



**Supplementary figure 9: Gating strategy Figure D2.4.**  
 (A) Pre-transfer activity; (B) Day 5 post-transfer

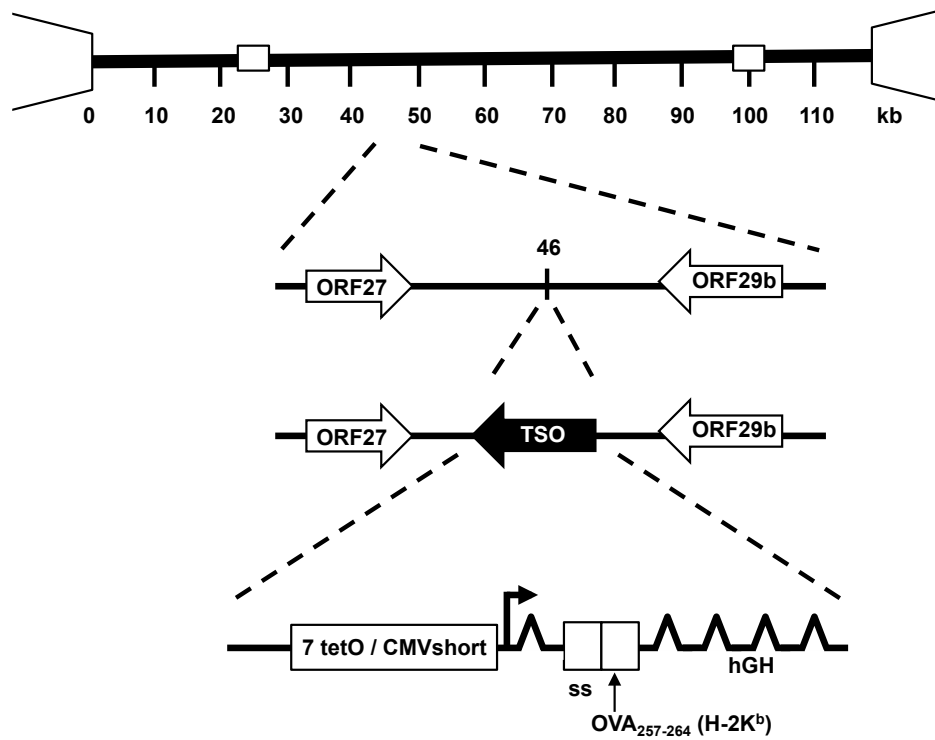


**Supplementary figure 10: Gating Strategie Figure D6.1, D6.2, D6.3, D6.4**  
 (A) Pre-transfer; (B) Post-transfer



**Supplementary figure 11: Gating Strategie Figure D6.2, D6.3 Killing assay**

## II MHV-68\_OVA

**Supplementary figure 12: MHV-68\_OVA.**

Schematic map of the MHV-68\_OVA genome with TSO expression cassette inserted at 46 kb between ORF27 and ORF29b. TSO encodes a minigene combination of OVA<sub>257-264</sub> and the signal sequence of H2-K<sup>b</sup>, which mediates a translation into the endoplasmatic reticulum. This fusion is followed by two stop codons and the human growth hormone splice substrate, required for efficient expression. The expression of OVA<sub>257-264</sub> is under the control of an improved tetracycline response element, which allows the transactivator molecule to bind on opposite sites of the DNA.